Nuclear Magnetic Resonance Spectroscopy

Tuning into the Music of Atoms and Molecules

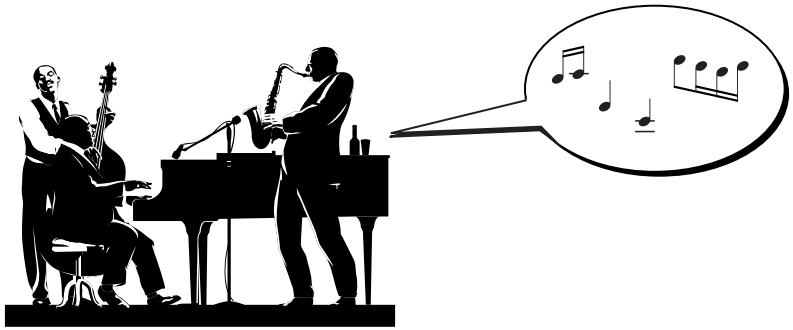

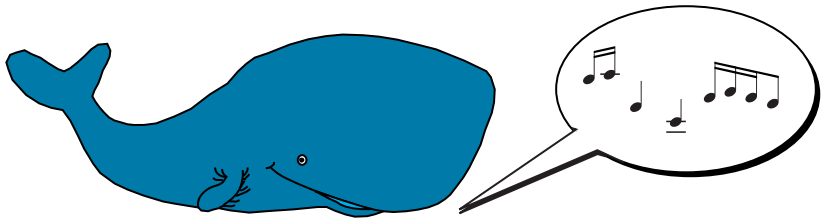

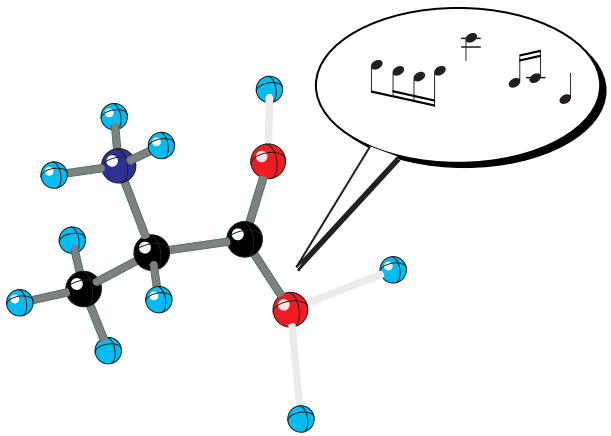

31ST ROCKY MOUNTAIN CONFERENCE ON SOLID-STATE NMR

An International Solid-State Nuclear Magnetic Resonance Spectroscopy Conference

Focusing on Methods and Applications
Breckenridge, Colorado, July 27th to July 31st, 2008

Invited Lectures

Clare Grey (Stony Brook), Vaughan Lecturer

Bernhard Blümich (Aachen)
Paul Callaghan (Wellington)
Hellmut Eckert (Münster)
Gillian Goward (McMaster)
Robert Griffin (MIT)
Jürgen Haase (Leipzig)
Yoshitaka Ishii (Illinois, Chicago)
Chris Jaroniec (Ohio State)
Ann McDermott (Columbia)
Stanley Opella (UC, San Diego)
Jeff Reimer (UC, Berkeley)
Kay Saalwächter (Halle)
Klaus Schmidt-Rohr (Iowa State)
Mark Smith (Warwick)
Jonathan Stebbins (Stanford)
Dieter Suter (Dortmund)
Robert Tycko (NIH)
Rod Wasylishen (Alberta)
Kurt Zilm (Yale)
Josef Zwanziger (Dalhousie)

Scientific Committee

Gordon Kennedy (Exxon Mobil), Chair
Philip Grandinetti (Ohio State), co-Chair
Sarah Larsen (Iowa), past-Chair
Zhehong Gan (NHMFL, Tallahassee)
Gerard Harbison (Nebraska)
Mei Hong (Iowa State)
Ulrich Scheler (IPF, Dresden)
Rob Schurko (Windsor)

Registration and Abstract Deadline: April 15, 2008

Information: www.ssnmr.org

A symposium in the 50th Rocky Mountain Conference on Analytical Chemistry

Spinning Tops Precessing in a Field

Spinning Top has Angular Momentum & Precesses in a Gravitational Field

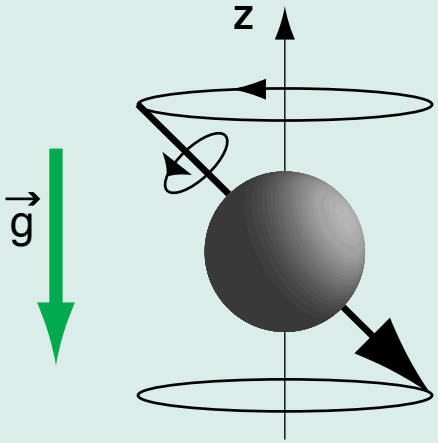

precession frequency increases linearly with gravitational field strength

Magnetic Spinning Top has Angular momentum & Precesses in a Magnetic Field

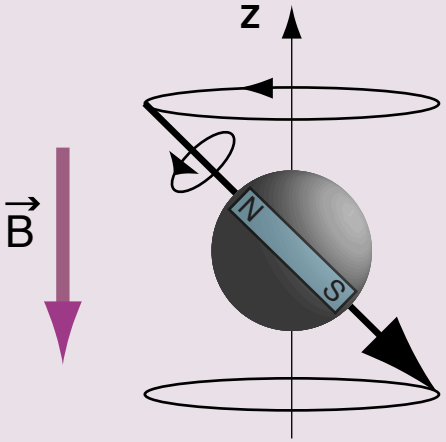

precession frequency increases linearly with magnetic field strength

magnetic field strength

$$\omega = -\gamma B$$

gyromagnetic ratio

Atomic Nuclei with non-zero Angular Momentum will have Magnetic Dipole Moments

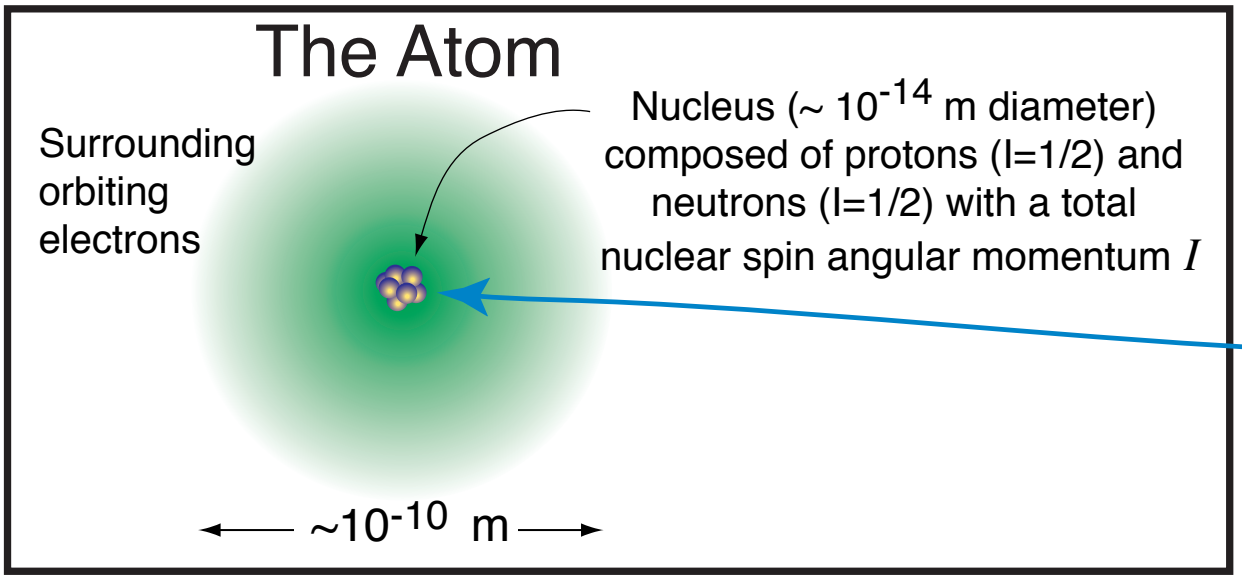

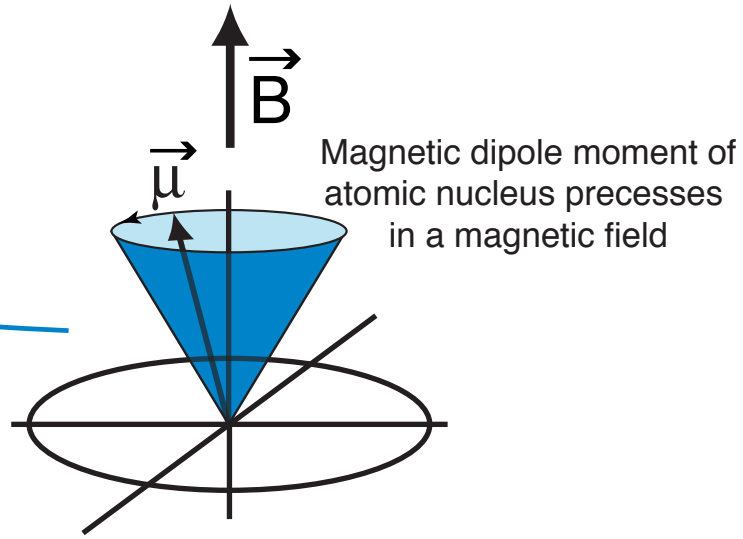

Allowed Nuclear Multipole Moments as a function of Nuclear Spin I

Nuclear Spin	$l=0$ monopole	$l=1$ dipole	$l=2$ quadrupole	$l=3$ octapole	$l=4$ hexadecapole
$I=0$	electric	0	0	0	0
$I=\frac{1}{2}$	electric	magnetic	0	0	0
$I=1$	electric	magnetic	electric	0	0
$I=\frac{3}{2}$	electric	magnetic	electric	magnetic	0
$I=2$	electric	magnetic	electric	magnetic	electric

All Nuclei with Spin I ≥ 1/2 will Precess in a Magnetic Field

Ensemble of I ≥ 1/2 Nuclei Will have small Contribution to Net Sample Magnetization

At Equilibrium I ≥ 1/2 Nuclei have Random Precession Phases and Nearly Random Precession Angles

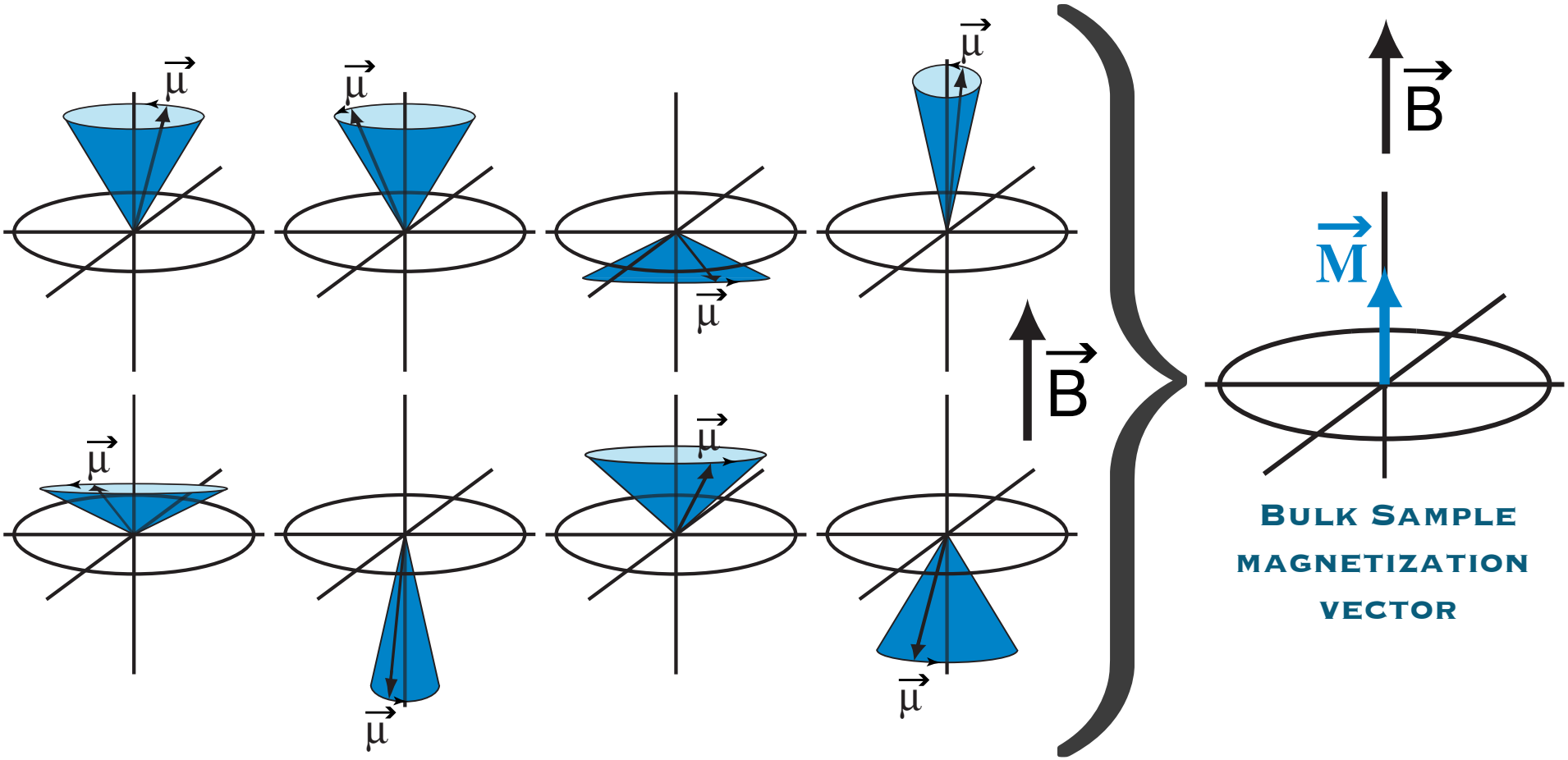

At equilibrium, (PPM) more precession cones along +z than -z, or, if you change the sign of the gyromagnetic ratio, more precession cones along -z than +z.

Magnetic Resonance Approach for Rotating magnetization Vector

Apply Small oscillating magnetic field perpendicular to Bo

If oscillation frequency matches Precession Frequency (resonance)

then Magnetization is rotated.

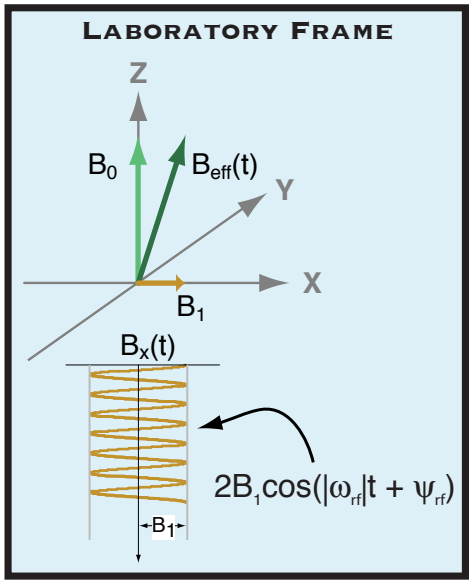

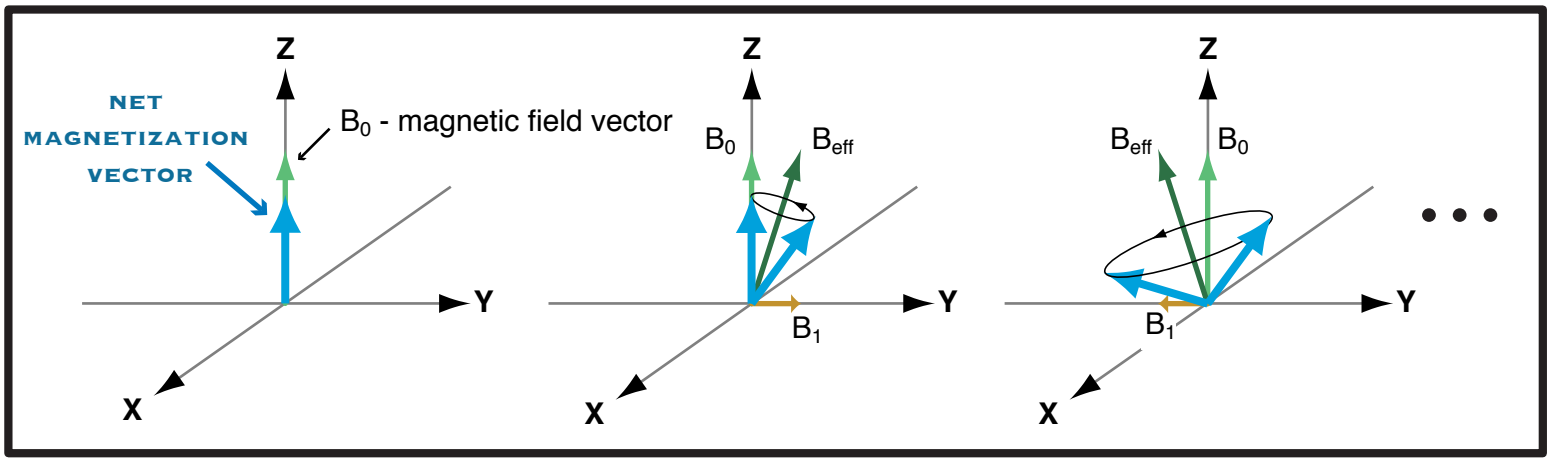

Resonant Frequencies are in the Radio Frequency Region

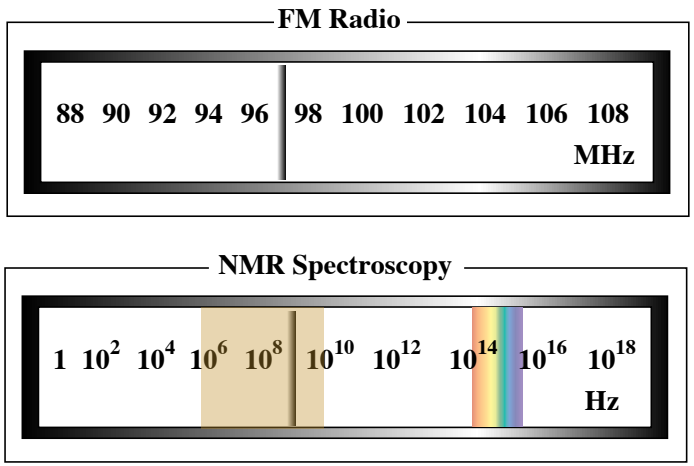

Effect of "90 degree" Pulse of resonant Radio waves

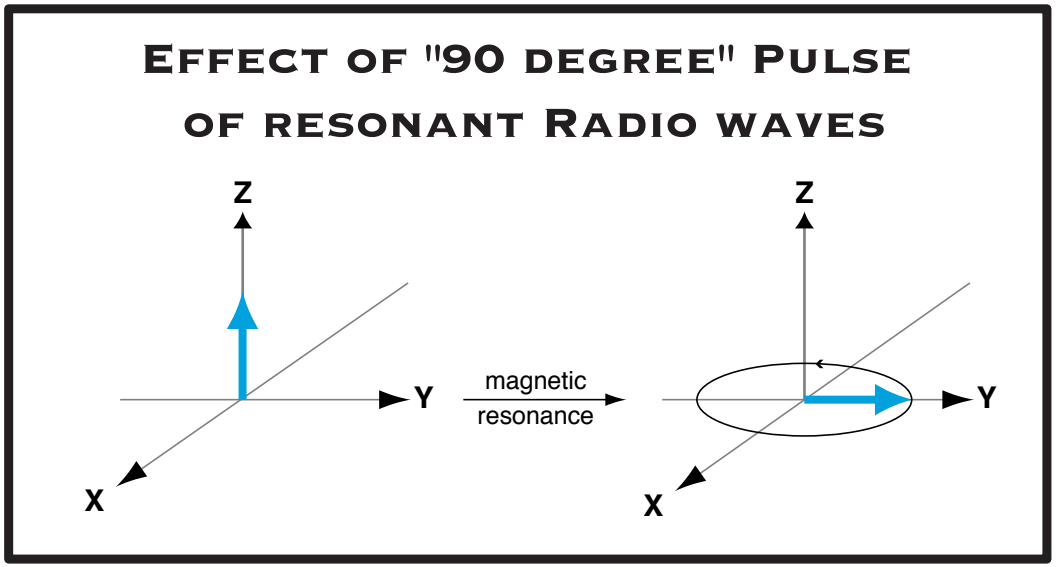

Precessing Magnetization is Detected using a Coil of wire

The Faraday Detector

Just a Coil wrapped around sample

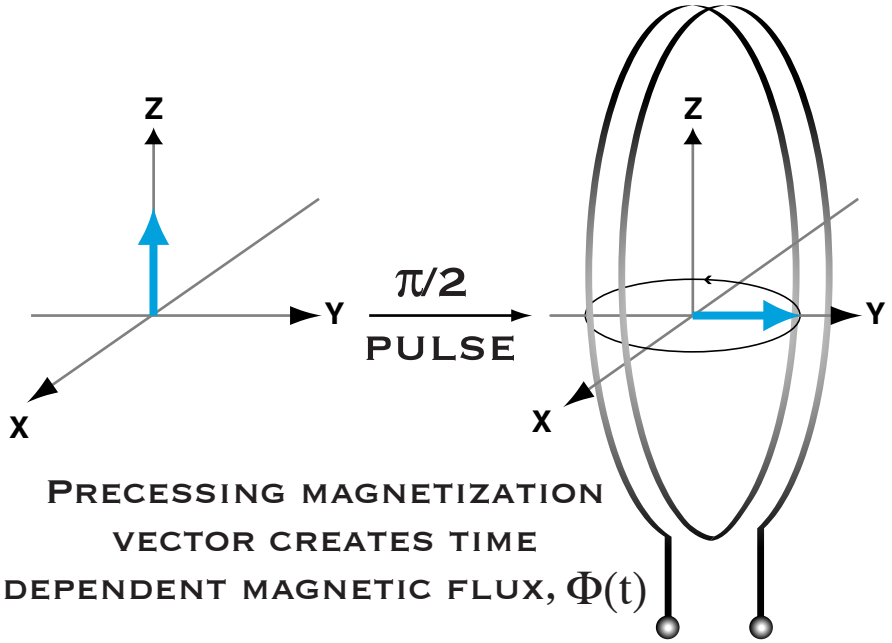

Precessing magnetization vector creates time dependent magnetic flux, $\Phi(t)$

$$S(t) = - d\Phi(t)/dt$$

Signal Detected in Coil is time derivative of Time dependent magnetic flux.

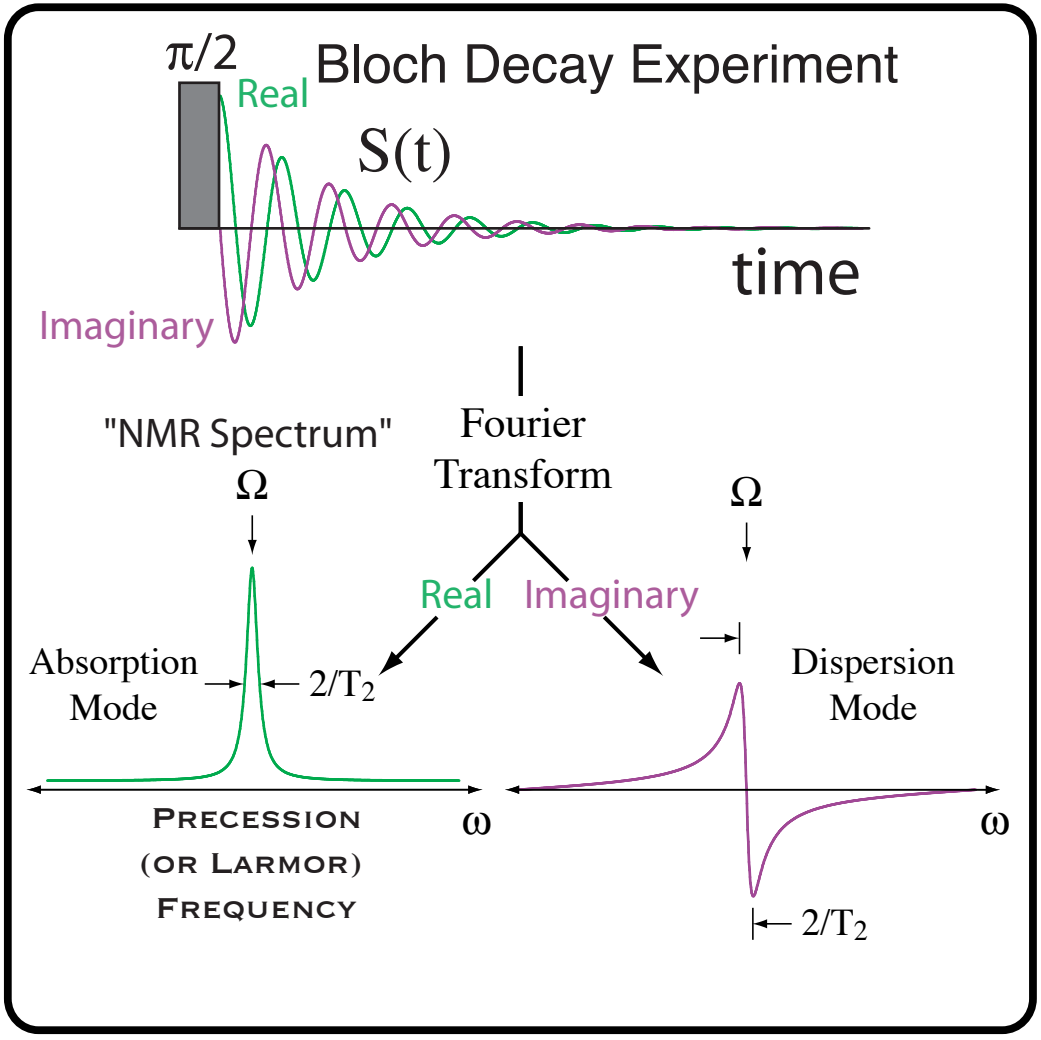

Primitive NMR Spectrometer

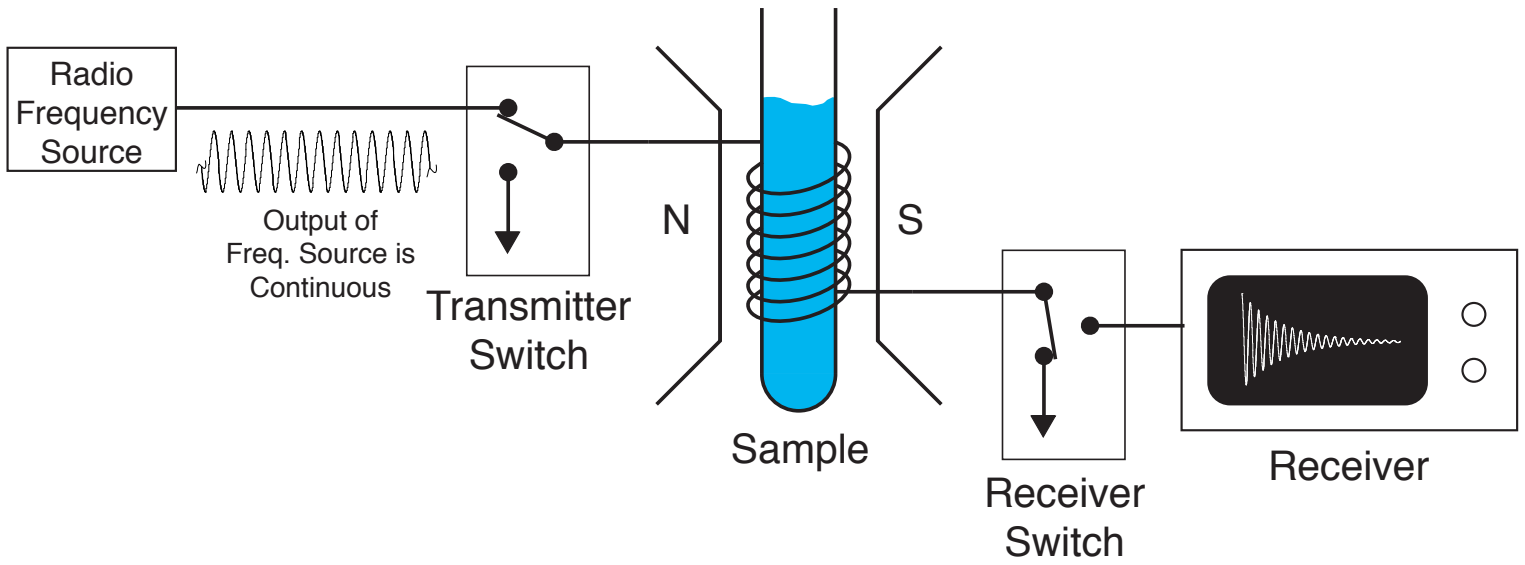

Pulse Program

Step	Transmitter switch state	Receiver switch state	Duration
1	OFF	OFF	10 seconds
2	ON	OFF	4 microseconds
3	OFF	ON	100 milliseconds

Different NMR Active Isotopes have different NMR Frequencies

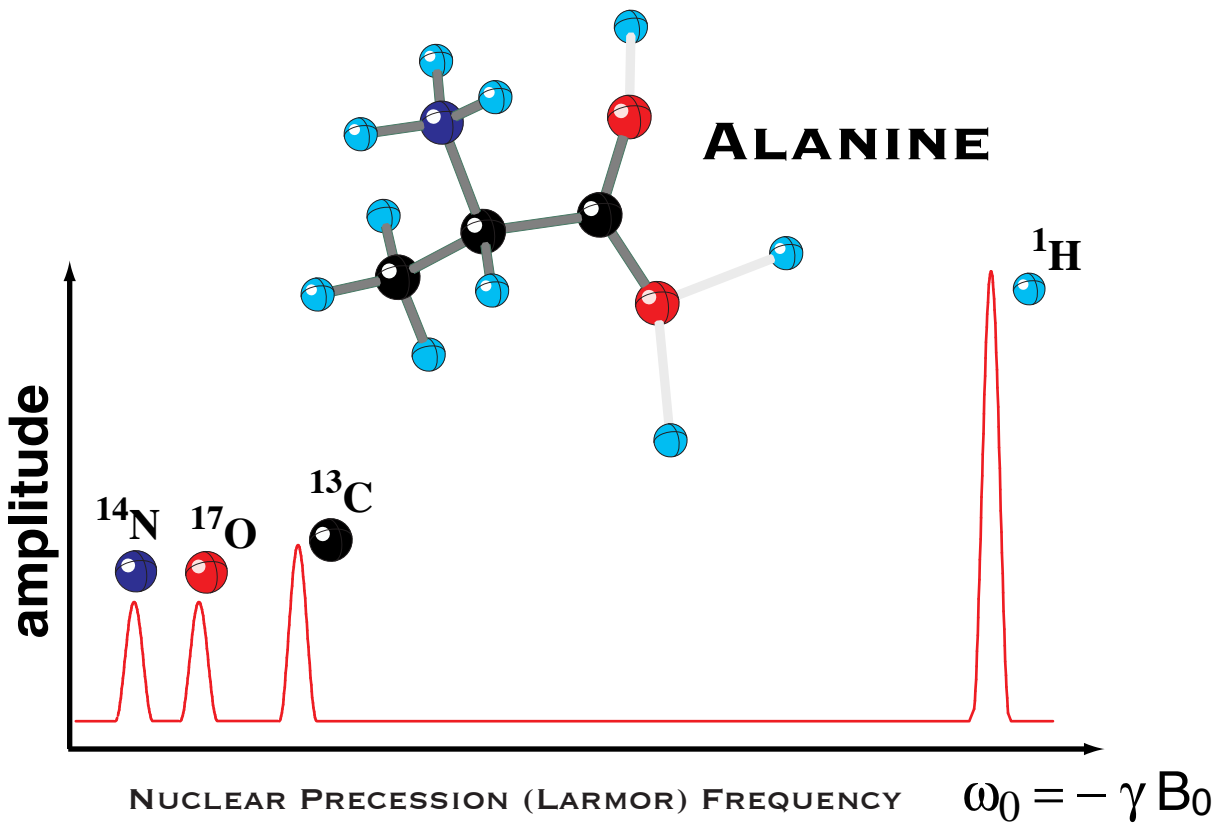

Nucleus	Spin	gyromagnetic ratio γ (10^7 rad/T-s)	Frequency at $B_0 = 2.35$ Tesla $\omega_0/2\pi$ (MHz)
^{1}H	1/2	26.7519	100
^{13}C	1/2	6.7283	25.145004
^{14}N	1	1.9337792	7.226329
^{17}O	5/2	-3.6279	13.561

Identical NMR Active Isotopes in Different Bonding environments have different NMR Frequencies

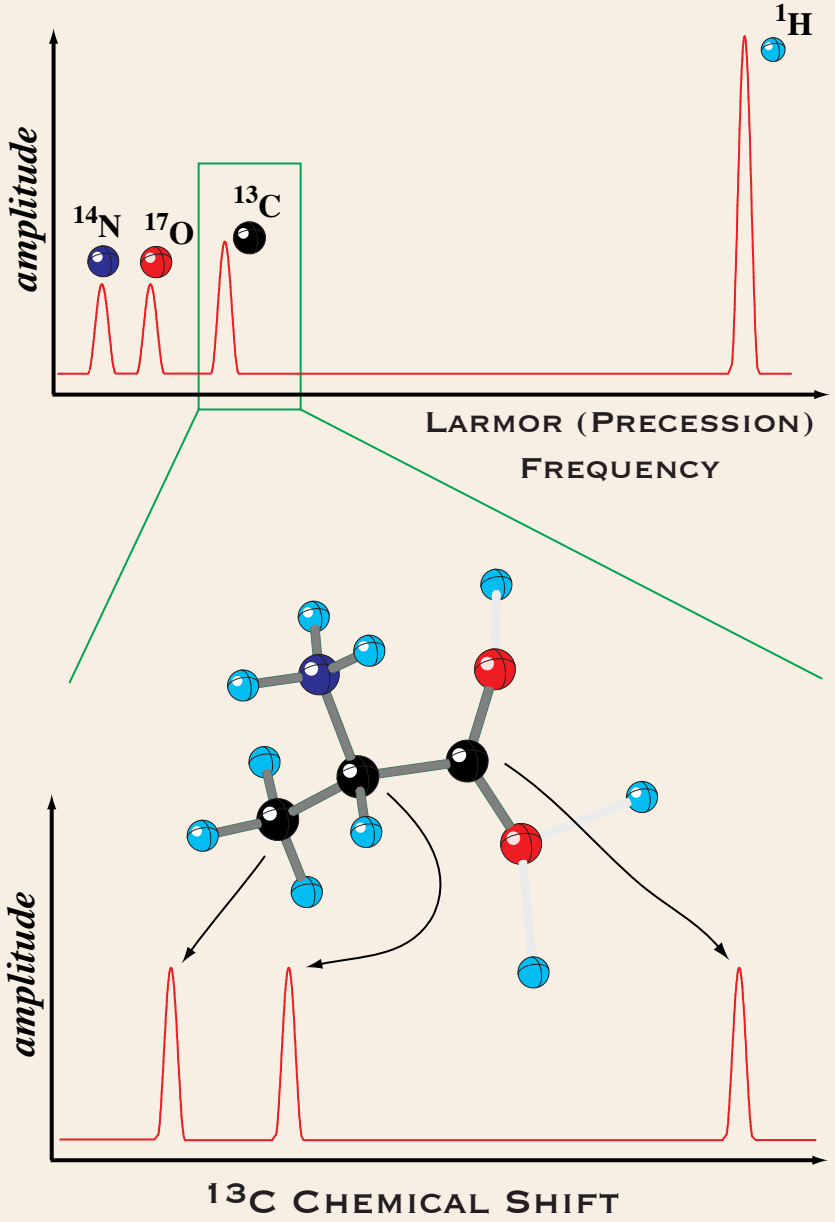

Nuclear Shielding

Surrounding electrons slightly shield the nucleus from the full strength of the external magnetic field, reducing the precession (Larmor) frequency.

$$\omega = -\gamma(1-\sigma)B_0$$

typically on the order of 10^{-6}.

Nuclear shieldings depends on a number of factors, and often increases with increasing local electron density around a nucleus.

Chemical Shift

Defined by Chemists to avoid complications of bulk magnetic susceptibilities. Defined as difference in ppm Between the NMR frequency of a resonance in a reference compound and the NMR a given resonance:

$$\delta = 10^6(\sigma_{ref} - \sigma)$$

Magnetic Dipole Couplings between nuclei split Resonances

Indirect electron mediated magnetic Dipole-Dipole Interaction

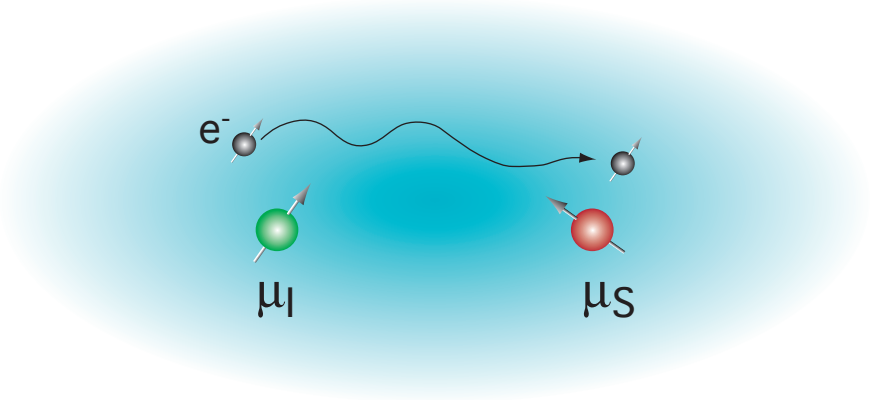

$$E = \left(\frac{2\pi J}{\hbar\gamma_I\gamma_S}\right)\boldsymbol{\mu}_I \cdot \boldsymbol{\mu}_S$$

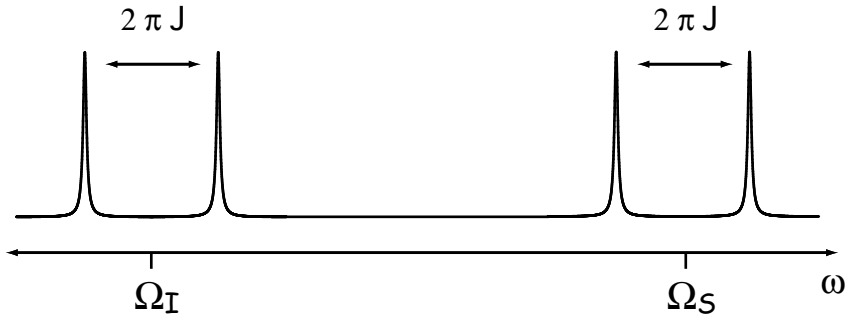

Used to Establish Through Bond Connectivities

Direct Through Space magnetic Dipole-Dipole Interaction

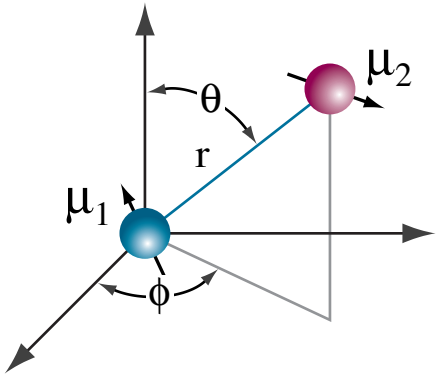

$$E = \frac{\boldsymbol{\mu}_I \cdot \boldsymbol{\mu}_S}{r^3} - \frac{3(\boldsymbol{\mu}_I \cdot \mathbf{r})(\boldsymbol{\mu}_S \cdot \mathbf{r})}{r^5}$$

Averages to Zero in liquid samples,
Not directly Observed in liquid spectrum
Observed indirectly through relaxation

Splitting is directly observable
in Spectra of Solid Samples

Used to Establish Through Space Distances

Atomic Nuclei with spin I ≥ 1 will have an Electric Quadrupole Moment

The nuclear electric quadrupole moment interacts with surrounding electric field gradients. These electric field gradients are generated by orbiting electrons as well as neighboring nuclei.

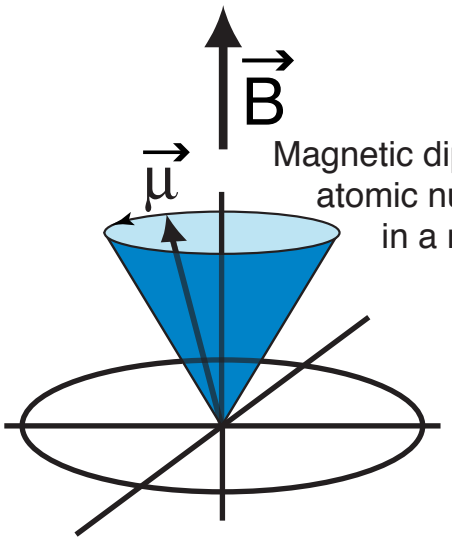

Magnetic dipole moment causes atomic nucleus to precess in a magnetic field

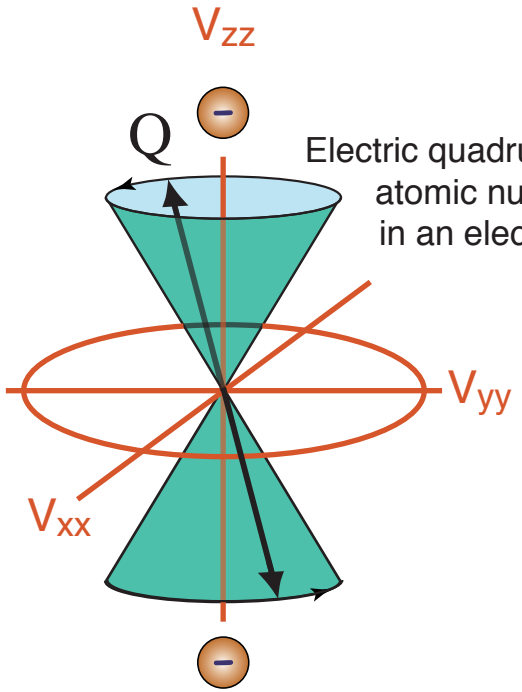

Electric quadrupole moment causes atomic nucleus to precess in an electric field gradient

Like Dipolar Coupling, Quadrupolar couplings Average to Zero in liquid samples, Not directly Observed in liquid spectrum Observed indirectly through relaxation Results in directly observable Splitting in Spectra of Solid Samples

Used to Establish local geometry and bonding around atom

NMR in Solid Samples:
How is it different from Liquid samples?

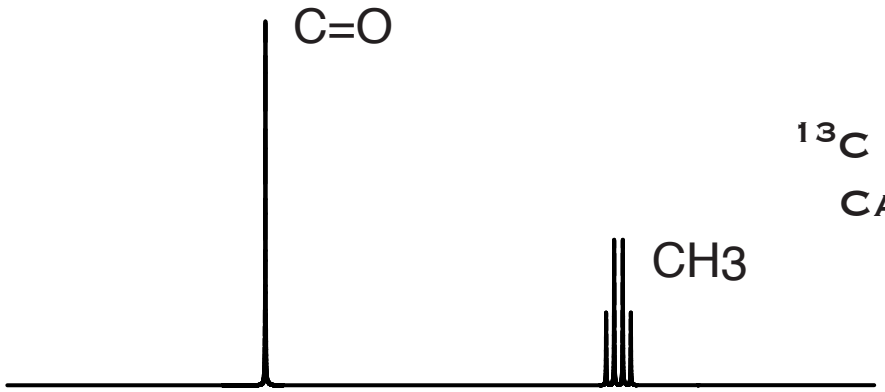

^{13}C liquid state NMR spectrum of
Calcium Acetate hemihydrate
$2\ Ca(CH_3CO_2)_2 \cdot H_20$

^{13}C solid state NMR spectrum of Polycrystalline
Calcium Acetate hemihydrate
$2\ Ca(CH_3CO_2)_2 \cdot H_20$

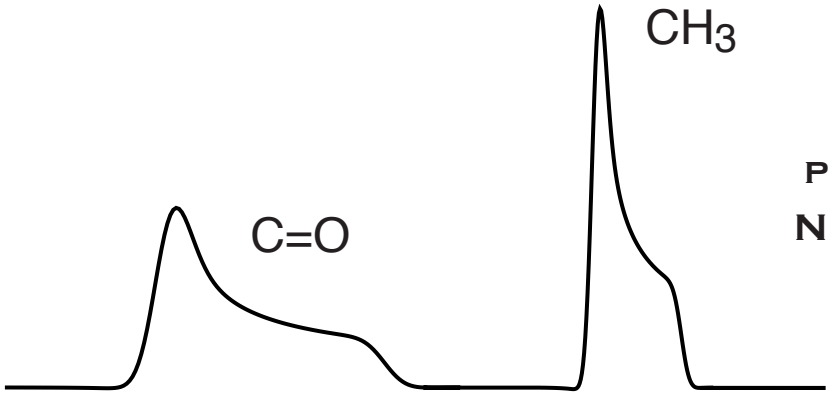

proton decoupled ^{13}C solid state
NMR spectrum of Polycrystalline
Calcium Acetate hemihydrate
$2\ Ca(CH_3CO_2)_2 \cdot H_20$

Solid-State Spectra of polycrystalline samples have lower resolution than Liquids because frequency anisotropies are not averaged away.

Classical Energy For Dipole Coupled Spin Pair

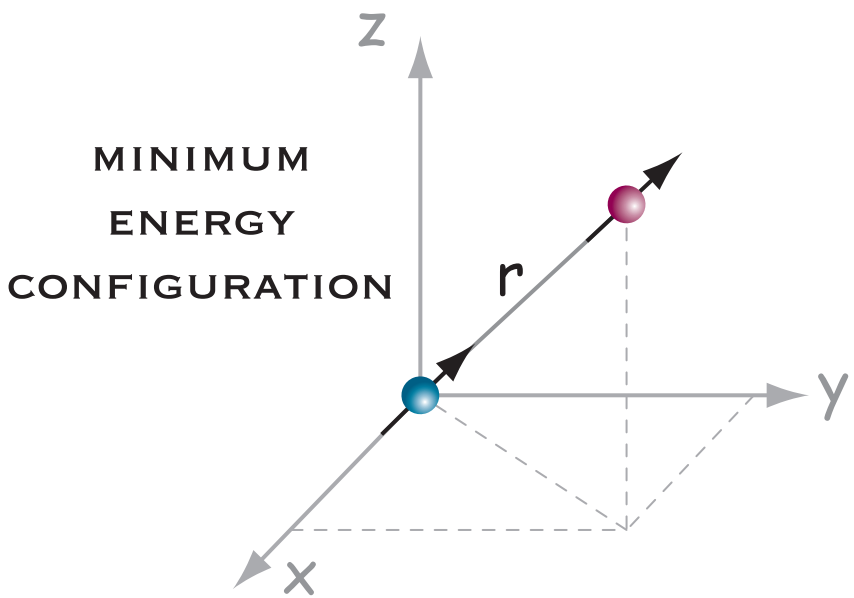

$$E = \frac{\boldsymbol{\mu}_I \cdot \boldsymbol{\mu}_S}{r^3} - \frac{3(\boldsymbol{\mu}_I \cdot \mathbf{r})(\boldsymbol{\mu}_S \cdot \mathbf{r})}{r^5}$$

Tumbling Spin Pair in Gas Phase in the absence of external magnetic field

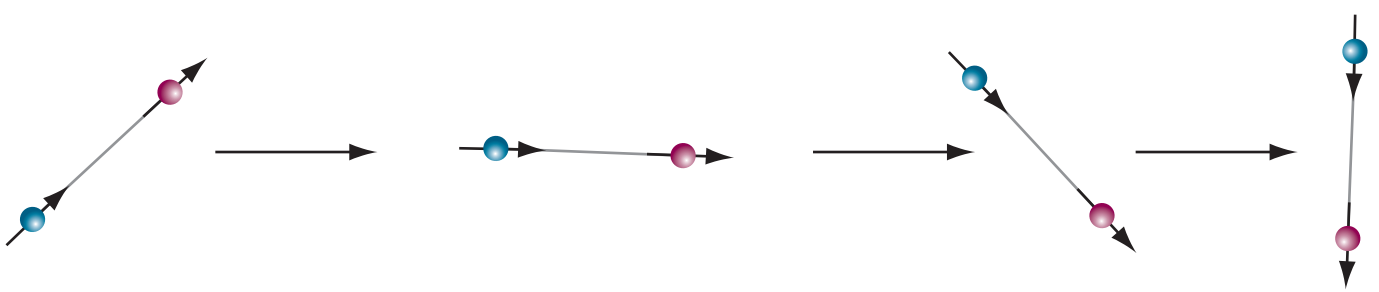

Classical Energy For Dipole Coupled Spin Pair in a Magnetic Field

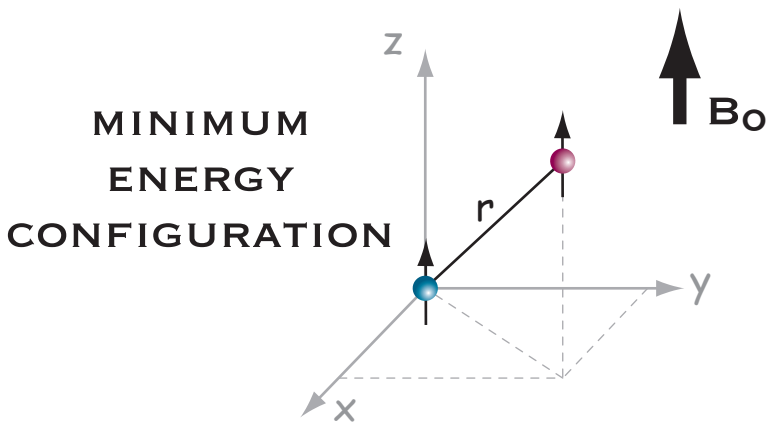

$$E = \boldsymbol{\mu}_I \cdot \mathbf{B}_0 + \boldsymbol{\mu}_S \cdot \mathbf{B}_0 + \frac{\boldsymbol{\mu}_I \cdot \boldsymbol{\mu}_S}{r^3} - \frac{3(\boldsymbol{\mu}_I \cdot \mathbf{r})(\boldsymbol{\mu}_S \cdot \mathbf{r})}{r^5}$$

Tumbling Spin Pair in Gas Phase in the presence of external magnetic field

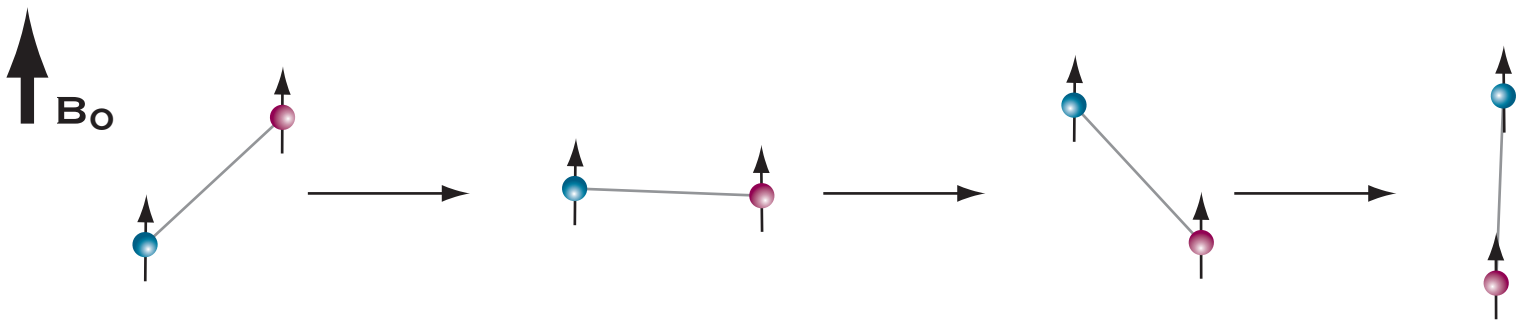

Single Crystal (and Goniometer Probe) Available?

Vosegaard, Skibsted, Bildsøe, and Jakobsen, *J. Magn. Reson. A*, **122**, 111-119(1996)

Single Crystal ^{87}Rb NMR of $RbClO_4$

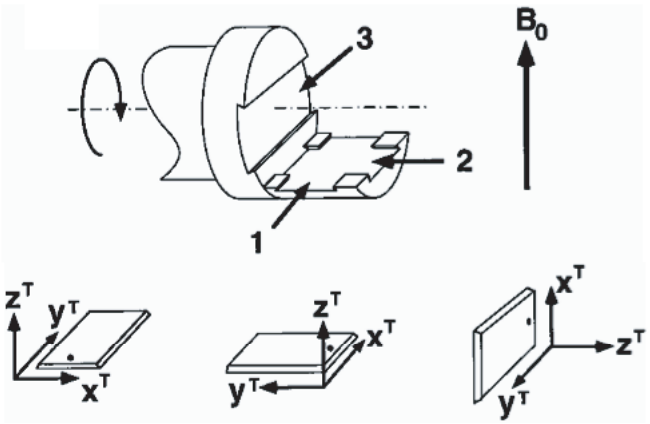

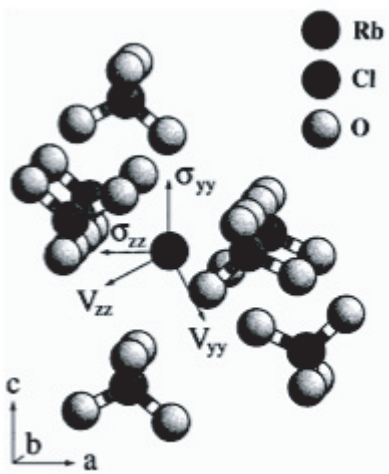

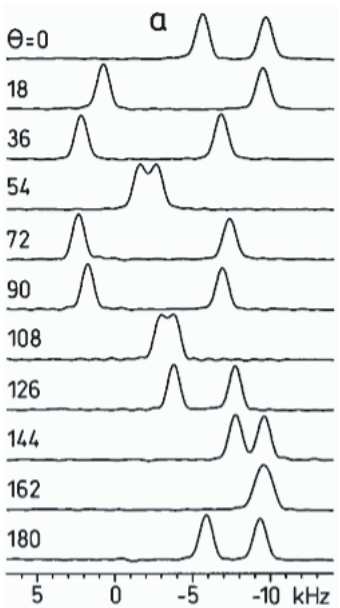

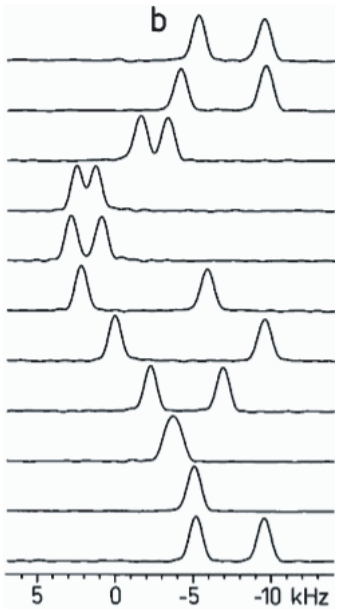

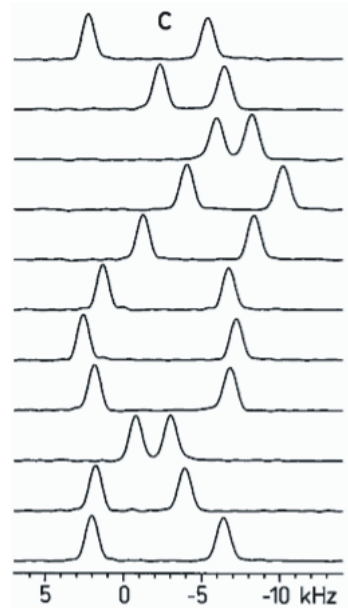

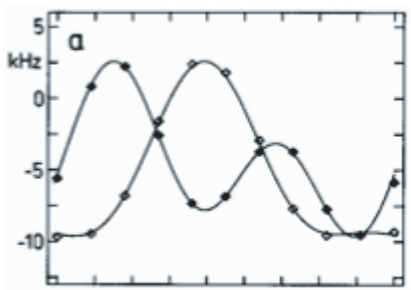

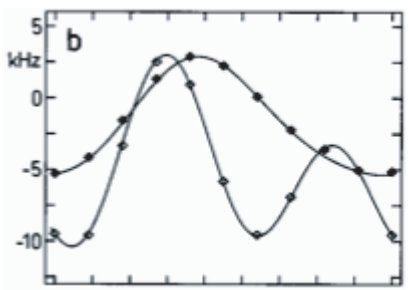

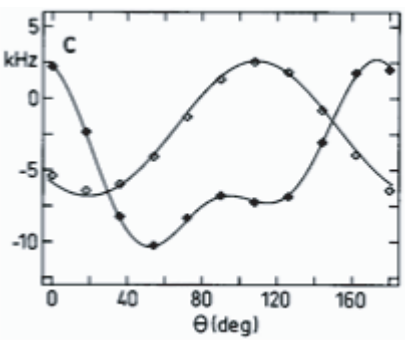

Crystal	Site	Method	C_Q (MHz)	η_Q	δ_σ (ppm)	η_σ	δ_{iso} (ppm)[a]	ψ (degree)	χ (degree)	ξ (degree)	Reference
$RbClO_4$	—	Single-crystal	3.30 ± 0.04	0.21 ± 0.03	13.8 ± 1.5[b]	0.61 ± 0.24[b]	−13.7 ± 0.6[b]	94 ± 14	28 ± 4	87 ± 5	This work
		MAS	3.29 ± 0.05	0.20 ± 0.03	13.5 ± 1.0	0.32 ± 0.20	−13.1 ± 0.3	98 ± 15	34 ± 5	69 ± 20	(7)
		Static	3.24 ± 0.06	0.19 ± 0.06	14 ± 2	0.5 ± 0.3	−14.3 ± 1.8	112 ± 6[c]	28.8 ± 1.5[c]	16 ± 4[c]	(3)

Orientation Dependence of the NMR Transition Frequency

Single X-tal

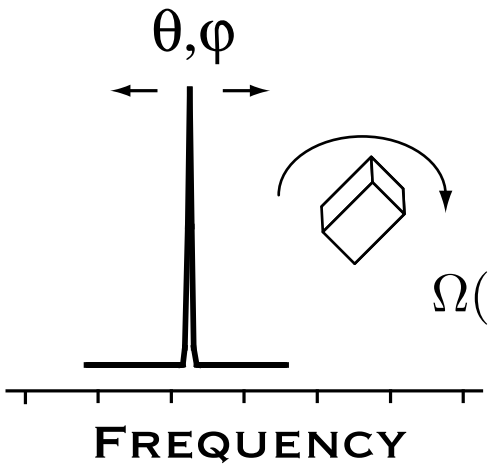

$$\Omega(\theta,\phi) = \Omega_{iso} + \sum_m c_{2,m} Y_{2,m}(\theta,\phi)$$

Polycrystalline sample

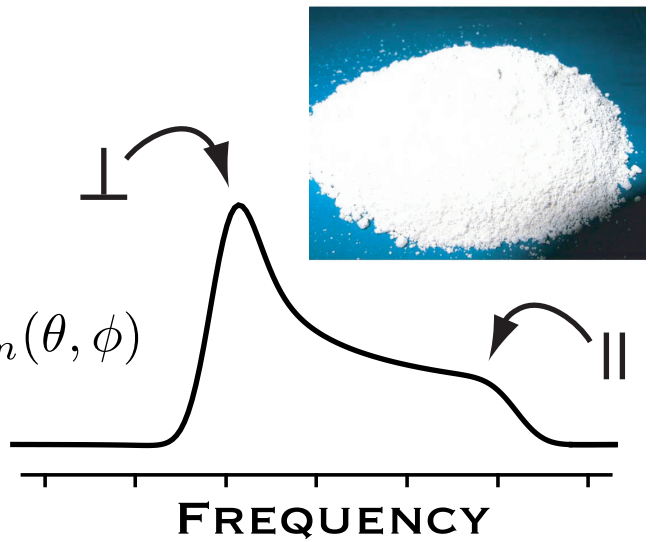

	Chemical Shift	Dipolar (heteronuclear)	Quadrupolar
$\Omega_{iso}^{(1)}$	$\sigma\gamma B_0(m_f - m_i)$	0	0
$c_{2,0}^{(1)}$	$\sqrt{\frac{4\pi}{5}}\,\gamma B_0 \delta^{(cs)}(m_f - m_i)$	$\sqrt{\frac{4\pi}{5}}\,2\,\omega_d(m_{I,f}\,m_{S,f} - m_{I,i}\,m_{S,i})$	$\sqrt{\frac{9}{5}}\,\frac{\pi^{3/2}C_q}{I(2I-1)}(m_f^2 - m_i^2)$
$c_{2,\pm 2}^{(1)}$	$\sqrt{\frac{2\pi}{15}}\,\gamma B_0 \eta_{cs}\delta_{cs}(m_f - m_i)$	0	$\sqrt{\frac{3}{10}}\,\frac{\pi^{3/2}C_q\,\eta_q}{I(2I-1)}(m_f^2 - m_i^2)$

Isotropic frequency shifts and spherical harmonic coefficients for the $m_i \rightarrow m_f$ transition of spin I from first-order perturbation theory for chemical shift, heteronuclear dipolar and quadrupolar interactions. All coefficients with $m =$ odd are zero.

Measuring Order Parameters of Membrane Acyl Chains

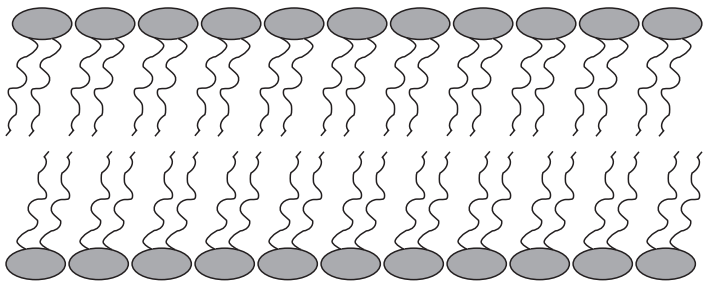

Membrane Bilayer

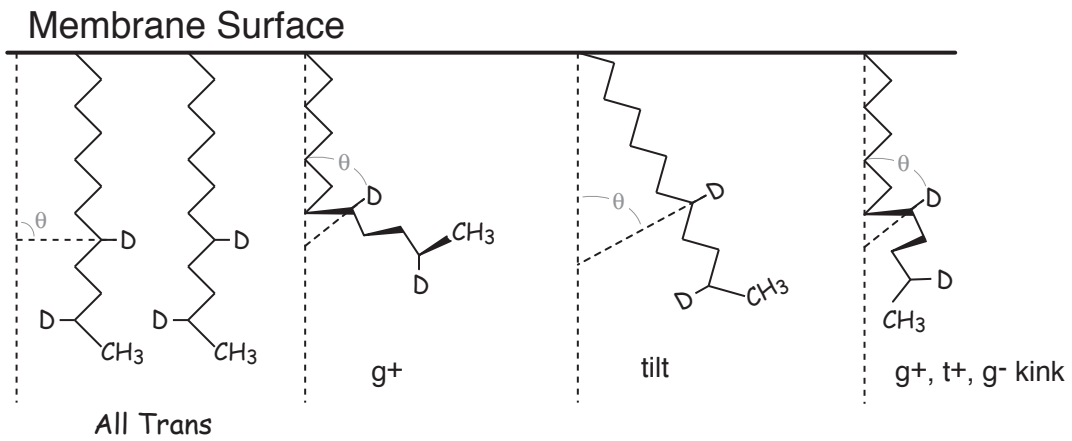

$$S_{CD} = \left\langle \frac{3\cos^2\theta - 1}{2} \right\rangle \propto \langle Y_{2,0}(\theta,\phi) \rangle$$

^{2}D Solid State NMR

Orientation Dependence of the ^{2}D Quadrupolar Coupling for a ^{2}D in a C-D bond on an sp^3 carbon

$$\Omega(\theta,\phi) = c_{2,0} Y_{2,0}(\theta,\phi)$$

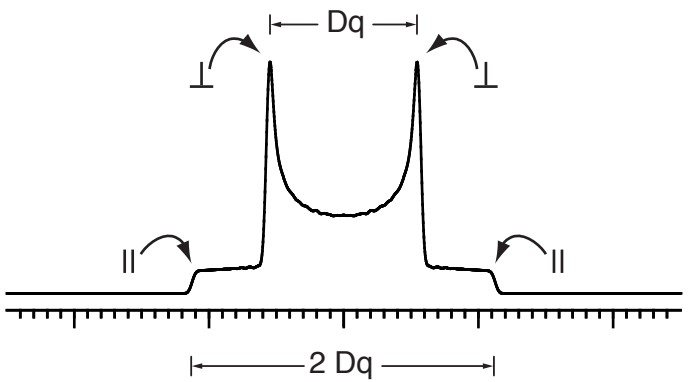

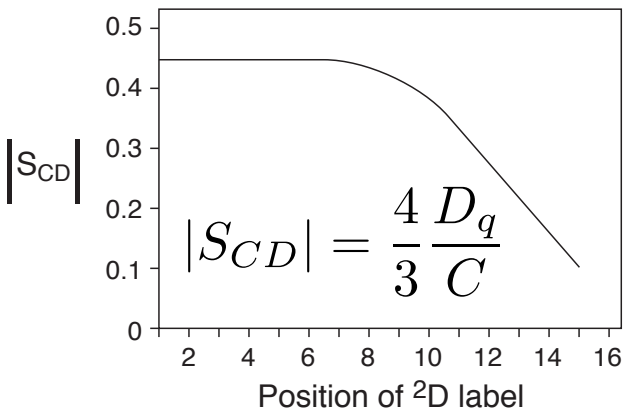

$$|S_{CD}| = \frac{4}{3}\frac{D_q}{C}$$

High Resolution Spectra For Spin 1/2 nuclei in Solids : Magic-Angle Spinning (MAS)

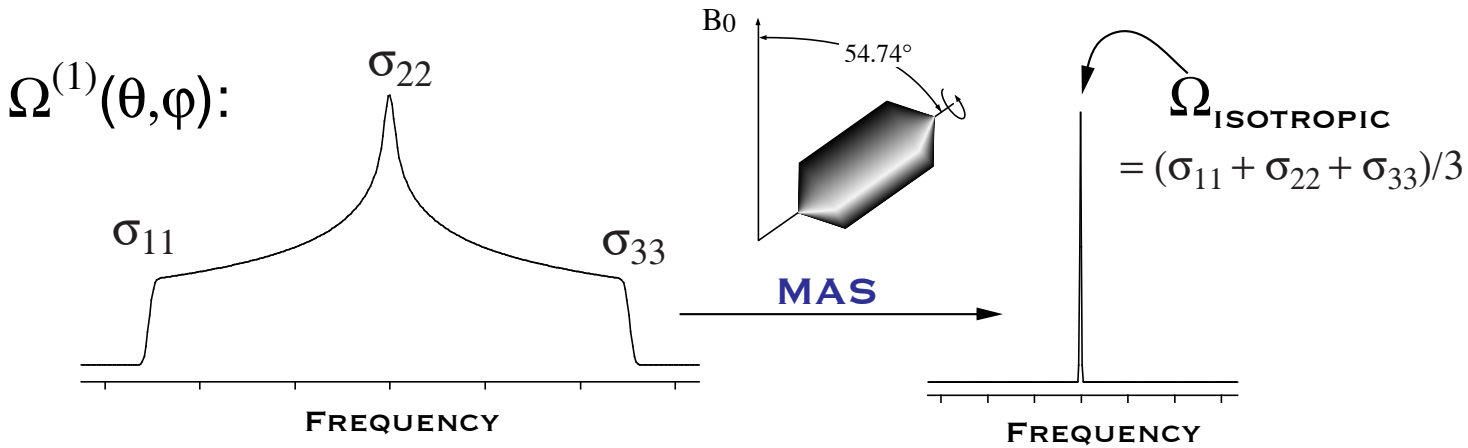

Eliminated by MAS

$$\Omega^{(1)}(\theta, \varphi) = \Omega^{(1)}_{iso} + \sum_m c^{(1)}_{2m} Y_{2m}(\theta, \varphi)$$

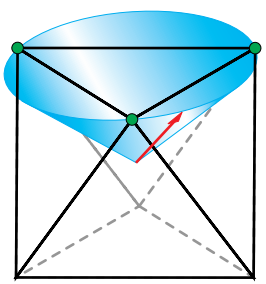

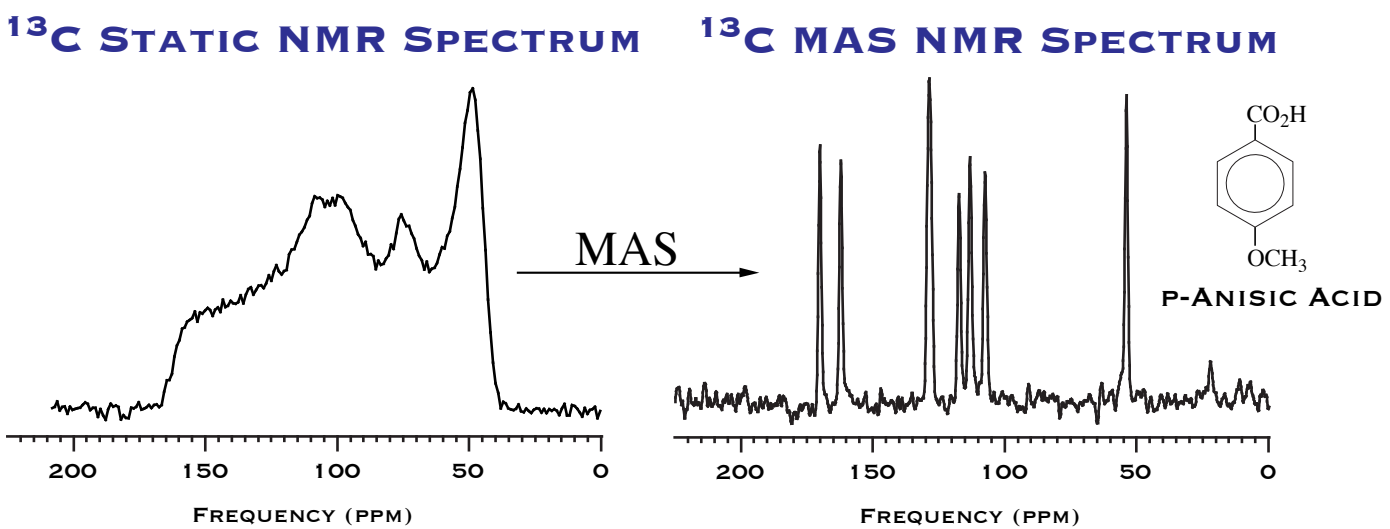

Variable Angle Spinning: Spin 1/2 Nuclei

Variable-Angle Spinning Spectra as a function of angle

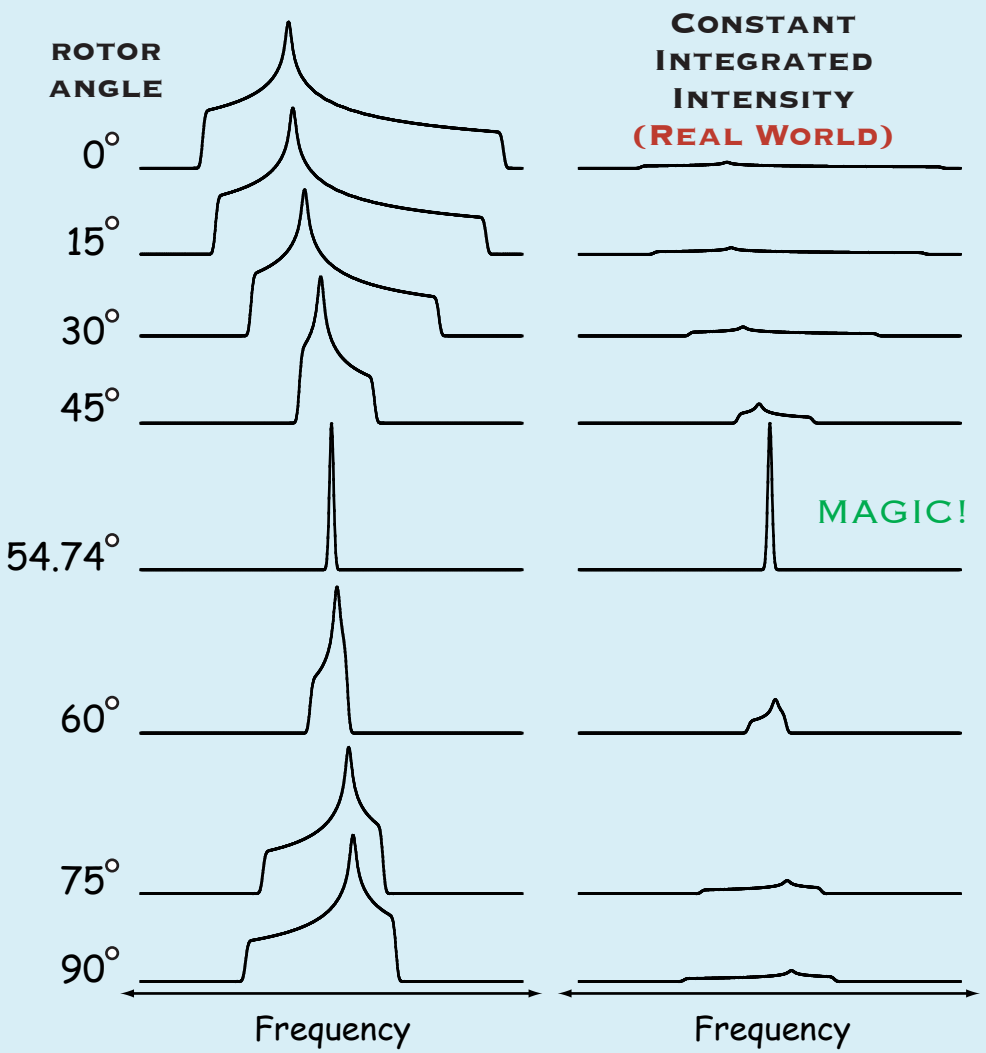

Magic-Angle Spinning Spectra as a function of spinning speed

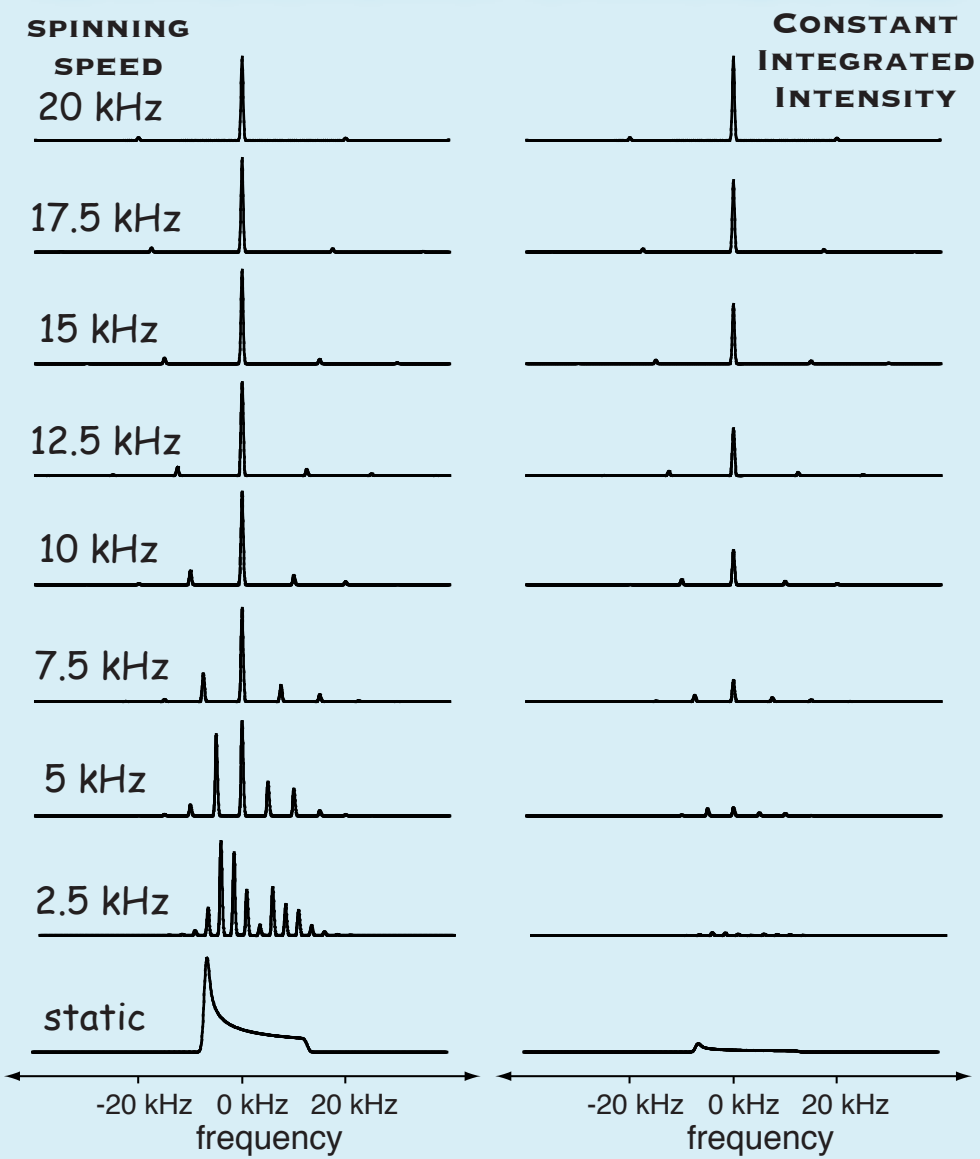

NMR of Quadrupolar Nuclei

Is there a Problem?

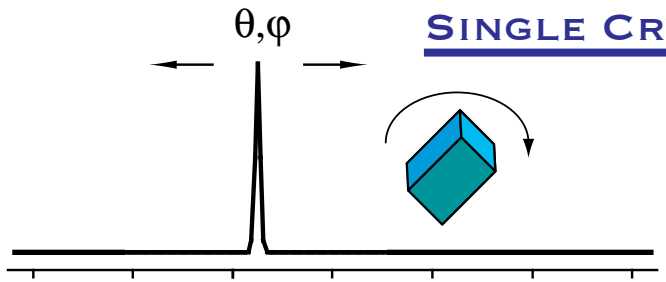

Single Crystal NMR

Polycrystalline or Frozen Samples

Distribution of θ,φ (Single Site)

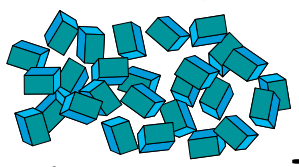

Spin 1/2

Frequency **(kHz)**

Spin > 1/2

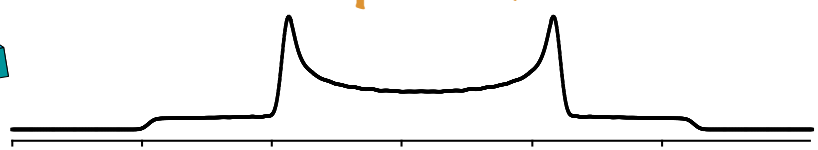

Frequency **(MHz)**

DISSOLUTION OR MELT

Spin 1/2

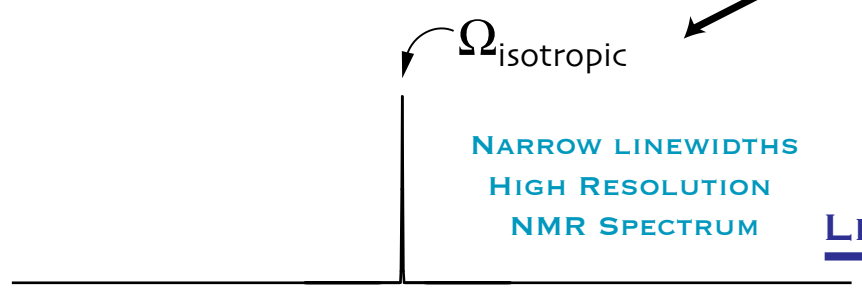

Frequency (kHz)

Narrow linewidths
High Resolution
NMR Spectrum

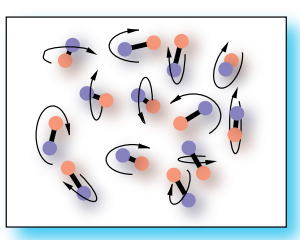

Liquid Samples

Spin > 1/2

Frequency (kHz)

Broad linewidths
Low Resolution
NMR Spectrum

Strong Quadrupolar Coupling causes short T_1 & T_2 relaxation times.

Perturbation expansion of NMR transition frequency

$$\Omega(\theta,\phi) = \underbrace{\Omega^{(0)}}_{\text{Zeeman Coupling}} + \underbrace{\Omega^{(1)}(\theta,\phi)}_{\substack{\text{Chemical Shift}\\ \text{J-Coupling}\\ \text{Dipolar Coupling}\\ \text{Quadrupolar Coupling}}} + \underbrace{\Omega^{(2)}(\theta,\phi) + \Omega^{(3)}(\theta,\phi) + \cdots}_{\text{Quadrupolar Coupling}}$$

Zeroth-Order

$$\Omega^{(0)} = \omega_0 = -\gamma B_0$$

(0 to hundreds of MHz)

First-Order Correction

$$\Omega^{(1)}(\theta,\phi) = \Omega^{(1)}_{iso}(I,m_i,m_f) + \sum_{k=-2}^{2} c^{(1)}_{2,k}(I,m_i,m_f)\; Y_{2,k}(\theta,\phi)$$

ω_q (0 to Tens of MHz)

$$\omega_q = \frac{6\pi C_q}{2I(2I-1)}$$

Second-Order Correction

$$\Omega^{(2)}(\theta,\phi) = \Omega^{(2)}_{iso}(I,m_i,m_f) + \sum_{k=-2}^{2} c^{(2)}_{2,k}(I,m_i,m_f)\; Y_{2,k}(\theta,\phi) + \sum_{k=-4}^{4} c^{(2)}_{4,k}(I,m_i,m_f)\; Y_{4,k}(\theta,\phi)$$

ω_q^2/ω_0 (0 to hundreds of kHz)

Third-Order Correction

$$\Omega^{(3)}(\theta,\phi) = \Omega^{(3)}_{iso}(I,m_i,m_f) + \sum_{k=-2}^{2} c^{(3)}_{2,k}(I,m_i,m_f)\; Y_{2,k}(\theta,\phi) + \sum_{k=-4}^{4} c^{(3)}_{4,k}(I,m_i,m_f)\; Y_{4,k}(\theta,\phi) + \sum_{k=-6}^{6} c^{(3)}_{6,k}(I,m_i,m_f)\; Y_{6,k}(\theta,\phi)$$

ω_q^3/ω_0^2 (0 to hundreds of Hz)

Higher Order Effects of Quadrupolar Nuclei on NMR

Nuclear Magnetic Dipole Moment couples to magnetic field

Nuclear Electric Quadrupole Moment couples to electric field gradient

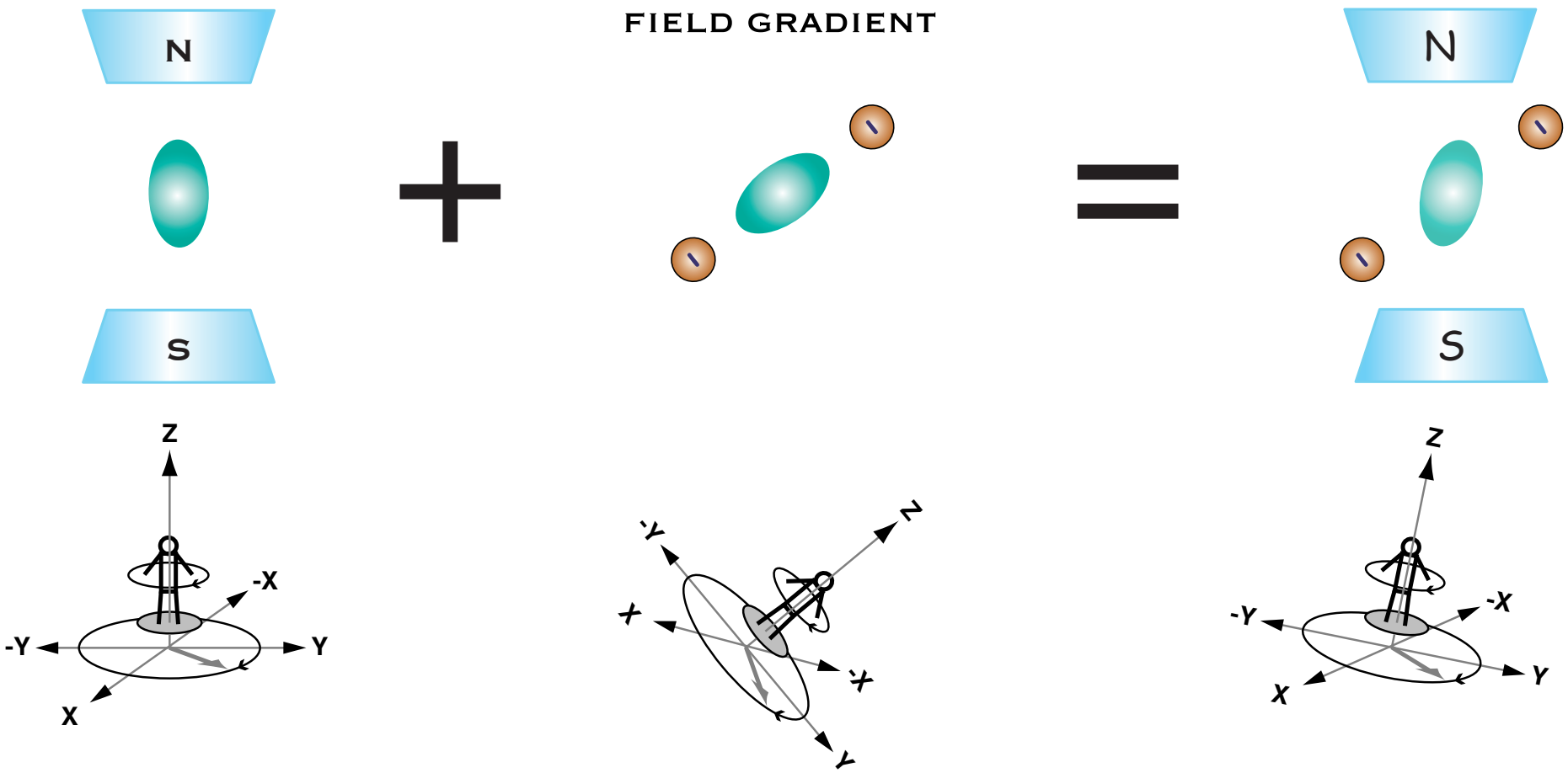

M ⟶ -M TRANSITIONS ARE UNAFFECTED BY FIRST-ORDER QUADRUPOLAR SPLITTING

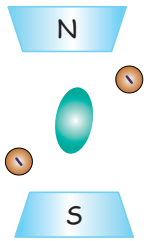

	Zeeman	Quadrupolar Interaction		
	0th	1st	2nd	3rd
Single Quantum Transitions	$\Omega_{ST_-}(\theta,\phi) = \Omega^{(0)} + \Omega^{(1)}_{ST_-}(\theta,\phi) + \Omega^{(2)}_{ST}(\theta,\phi) + \Omega^{(3)}_{ST_-}(\theta,\phi) + \cdots$			
	$\Omega_{CT}(\theta,\phi) = \Omega^{(0)} + 0 + \Omega^{(2)}_{CT}(\theta,\phi) + 0 + \cdots$			
	$\Omega_{ST_+}(\theta,\phi) = \Omega^{(0)} + \Omega^{(1)}_{ST_+}(\theta,\phi) + \Omega^{(2)}_{ST}(\theta,\phi) + \Omega^{(3)}_{ST_+}(\theta,\phi) + \cdots$			
Double Quantum Transitions	$\Omega_{2Q_-}(\theta,\phi) = 2\Omega^{(0)} + \Omega^{(1)}_{2Q_-}(\theta,\phi) + \Omega^{(2)}_{2Q_-}(\theta,\phi) + \Omega^{(3)}_{2Q_-}(\theta,\phi) + \cdots$			
	$\Omega_{2Q_+}(\theta,\phi) = 2\Omega^{(0)} + \Omega^{(1)}_{2Q_+}(\theta,\phi) + \Omega^{(2)}_{2Q_+}(\theta,\phi) + \Omega^{(3)}_{2Q_+}(\theta,\phi) + \cdots$			
Triple Quantum Transitions	$\Omega_{3Q}(\theta,\phi) = 3\Omega^{(0)} + 0 + \Omega^{(2)}_{3Q}(\theta,\phi) + 0 + \cdots$			

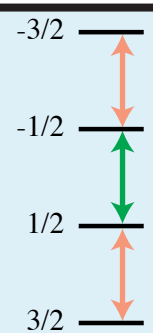

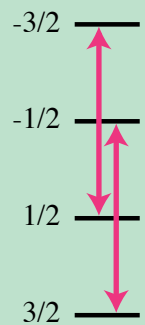

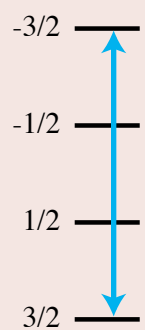

Polycrystalline Samples

Integer Spins $^{2}D(I=1)$, $^{14}N(I=1)$, $^{10}B(I=3)$, $^{6}Li(I=1)$

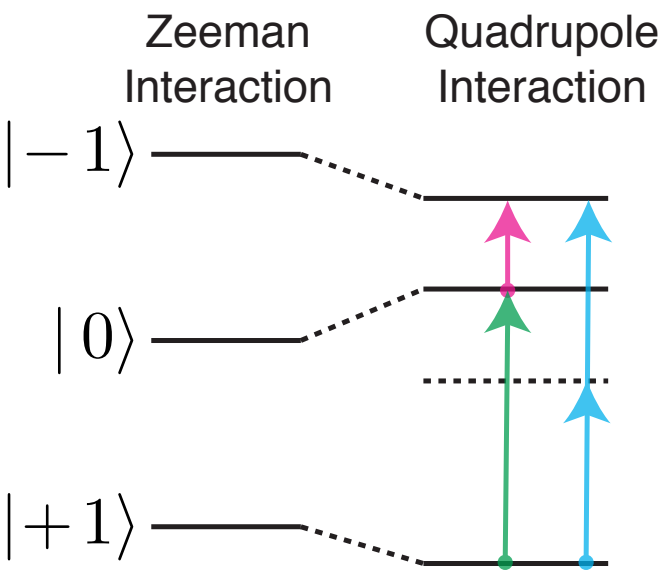

Single Quantum Transitions

$m = +1 \rightarrow 0$

$m = 0 \rightarrow -1$

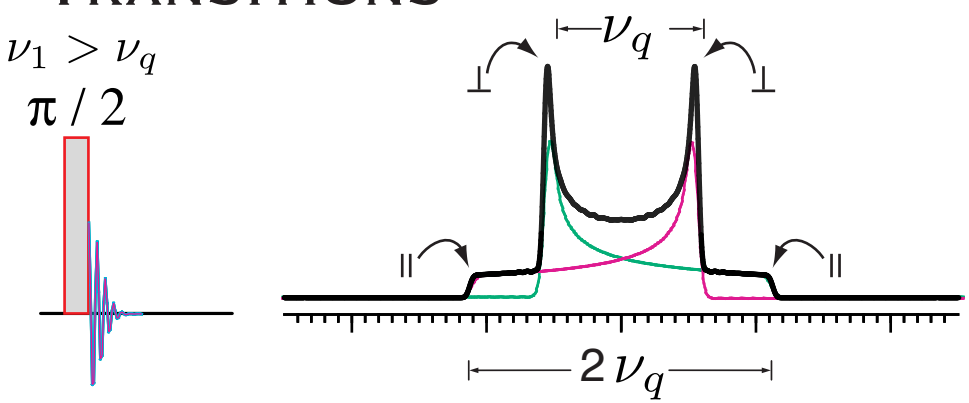

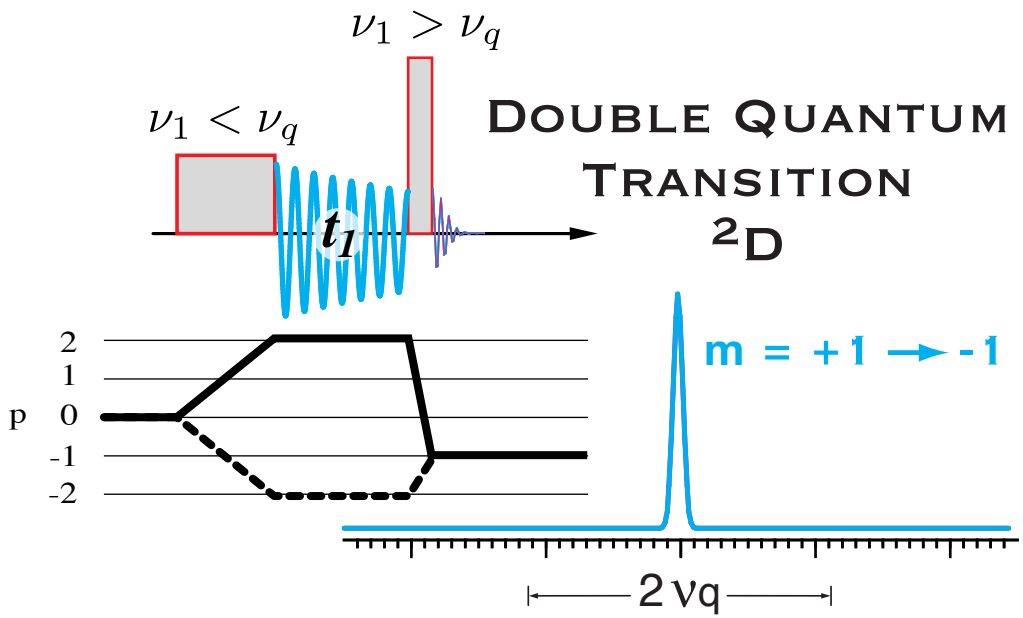

Vega, Shattuck, and Pines,
Phys. Rev. Lett., **37**, 43-46 (1976)

Half-Integer Spins: Narrow Central Transition, But MAS is Inadequate

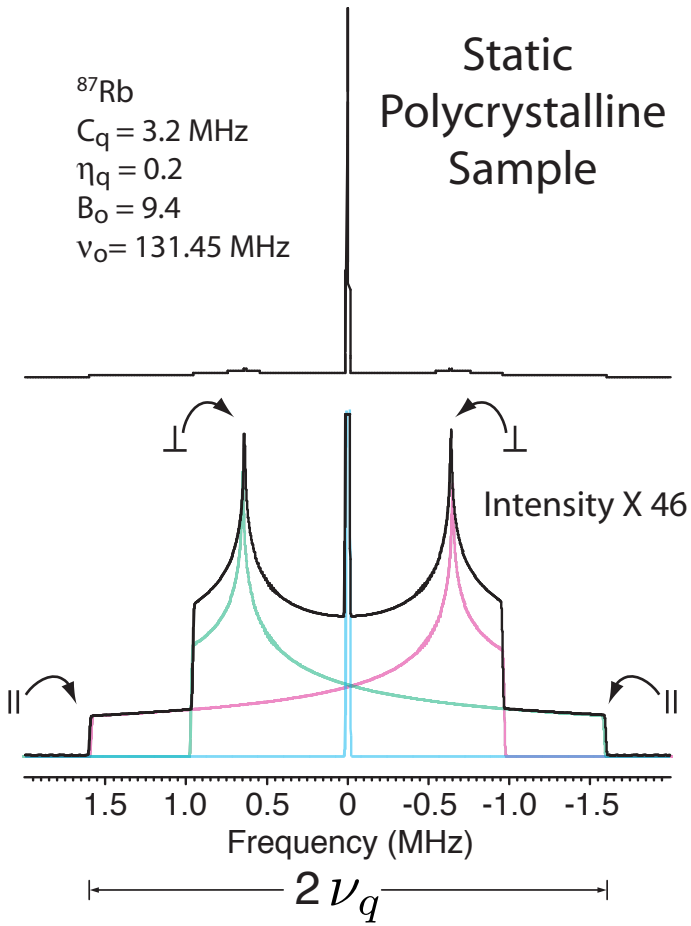

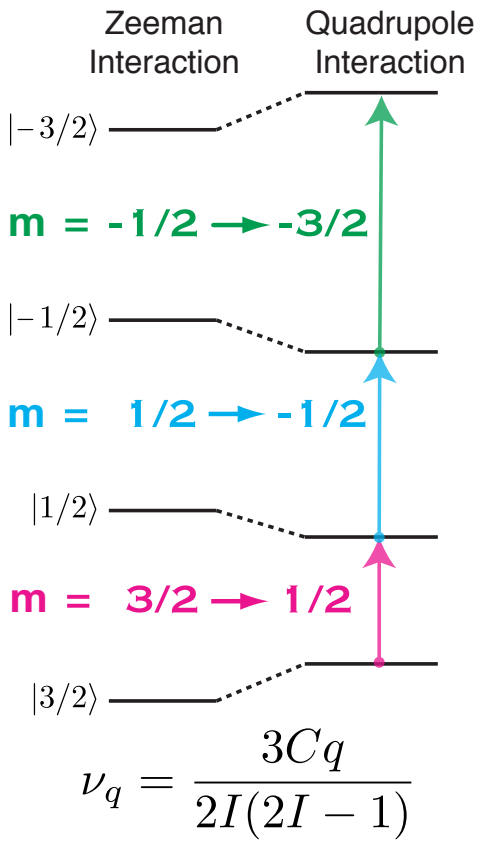

$$\nu_q = \frac{3Cq}{2I(2I-1)}$$

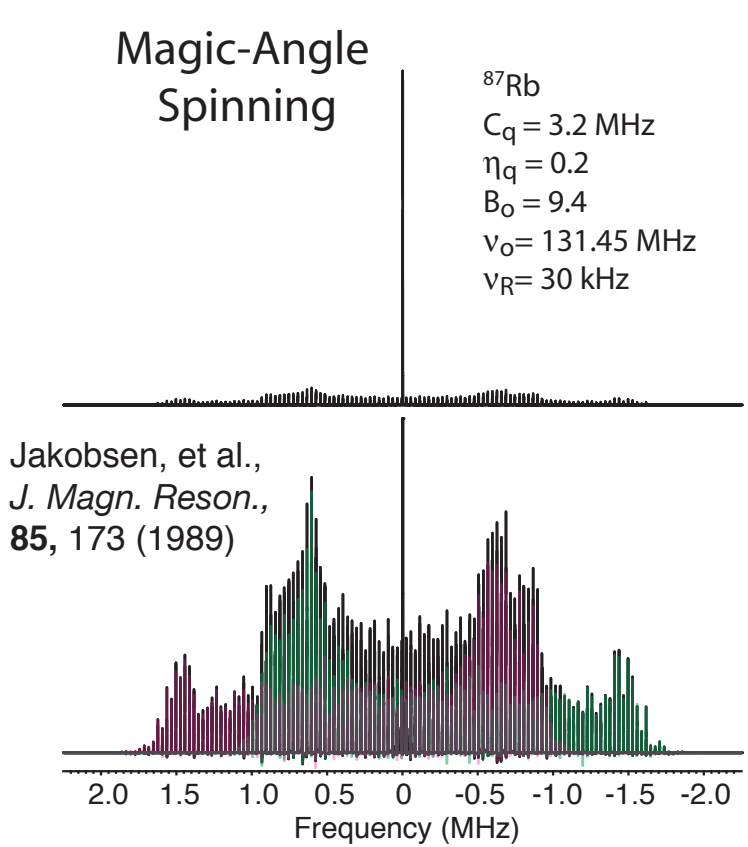

Central Transition

Unaffected by First Order Quadrupolar Splitting

m = 1/2 → -1/2

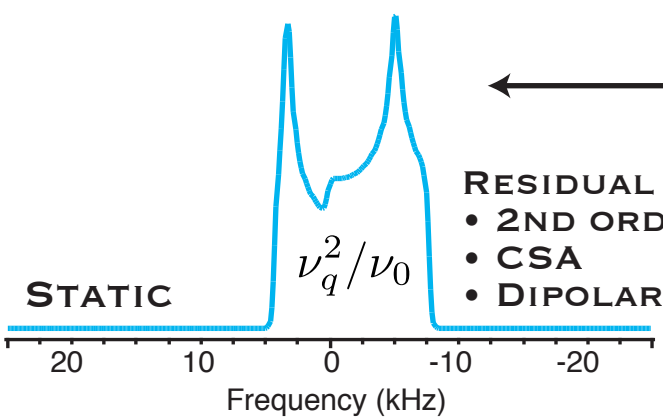

Residual Linewidth
- 2nd order Quad.
- CSA
- Dipolar Couplings

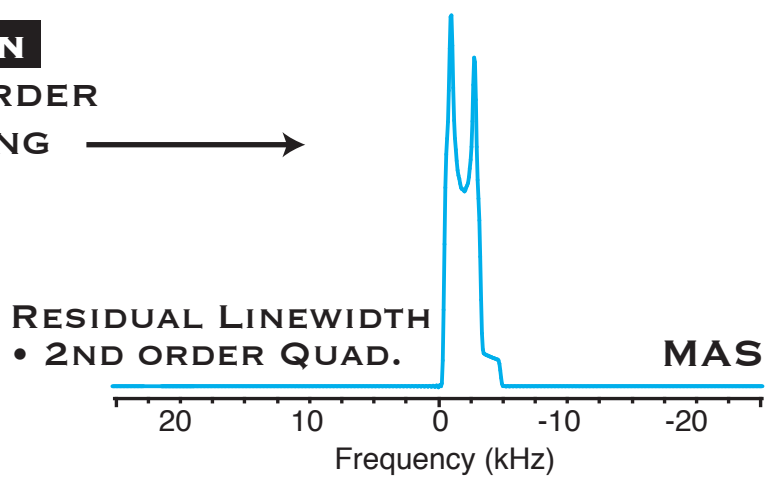

Central Transition Nutation Frequency

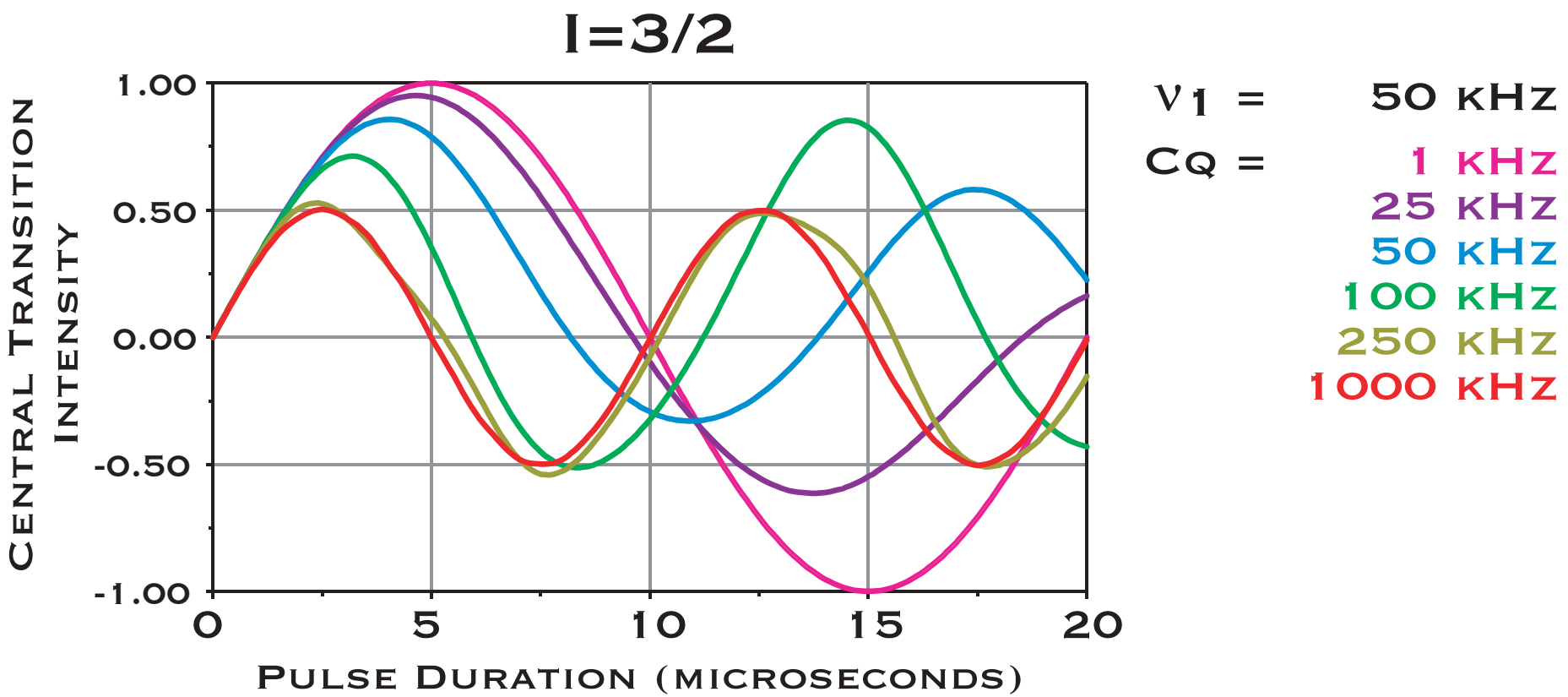

In the limit that $\omega_1 \ll \omega_q$ the effective central transition nutation frequency becomes ...

$$(I + 1/2)\ \omega_1$$

Magic-Angle Spinning:
Great for spin 1/2, but for spin >1/2?

Spin 1/2

^{13}C NMR Spectrum of p-Anisic Acid

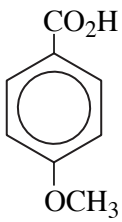

Static

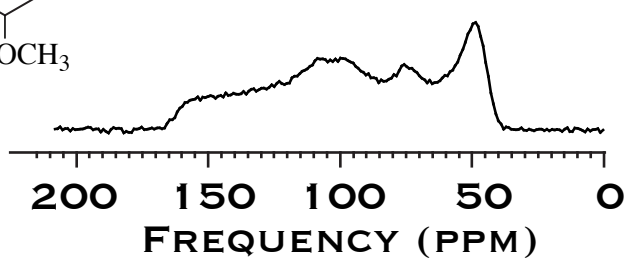

MAS

Narrow linewidths

High Resolution

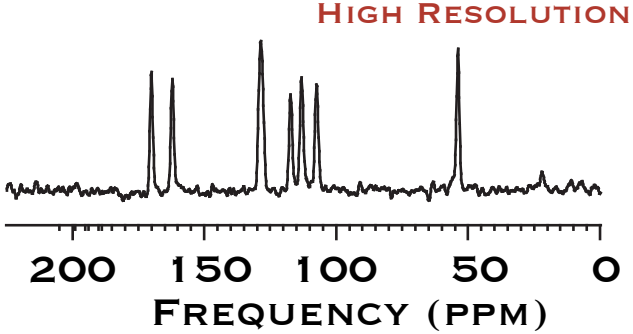

Spin 3/2

^{87}Rb NMR Central Transition Spectrum of $RbNO_3$

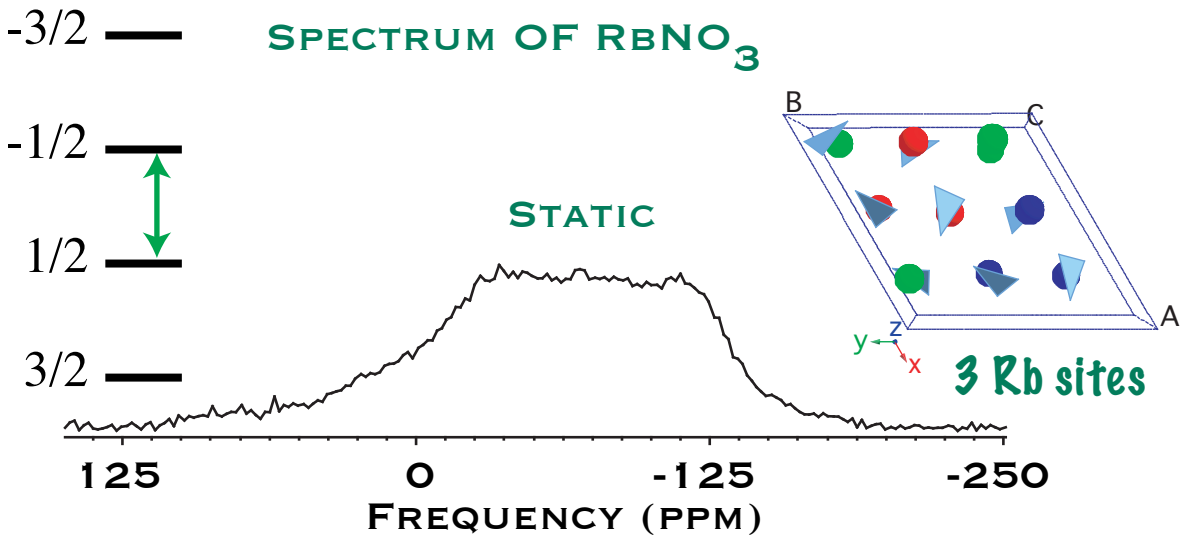

MAS

Broad linewidths

Low Resolution from residual anisotropy, not short relaxation times!

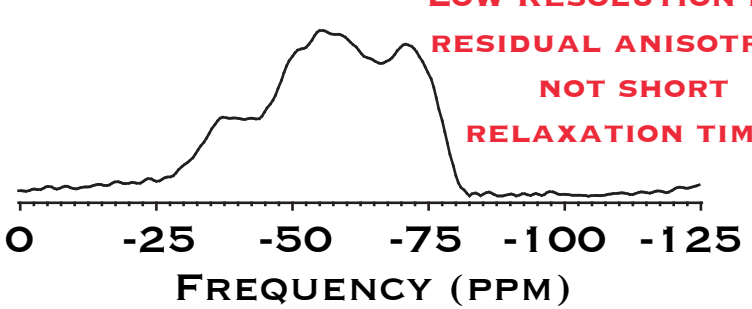

Variable Angle Spinning:
Spin > 1/2 (Quadrupolar) Nuclei

Variable-Angle Spinning As a Function of ROtor Angle and Quadrupolar Asymmetry Parameter

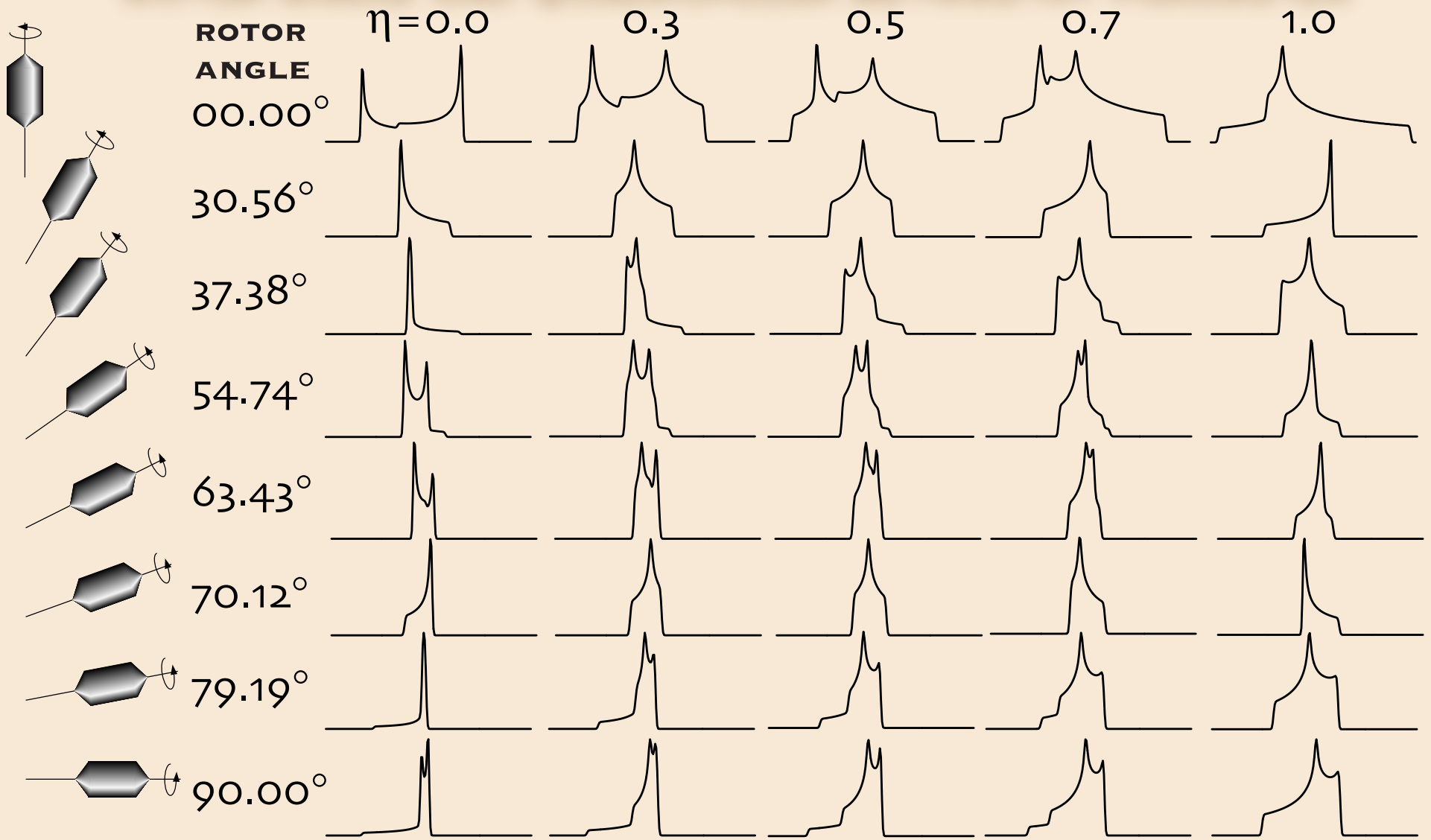

Ganapathy, Schramm, and Oldfield, *J. Chem. Phys.,1982,* 77, *4360*

One Solution:
Really High magnetic fields

2nd-order broadenings are inversely proportional to magnetic field strength

^{27}Al MAS spectra of aluminoborate $9Al_2O_3 + 2B_2O_3$ (A_9B_2) compound from 14 to 40 T.

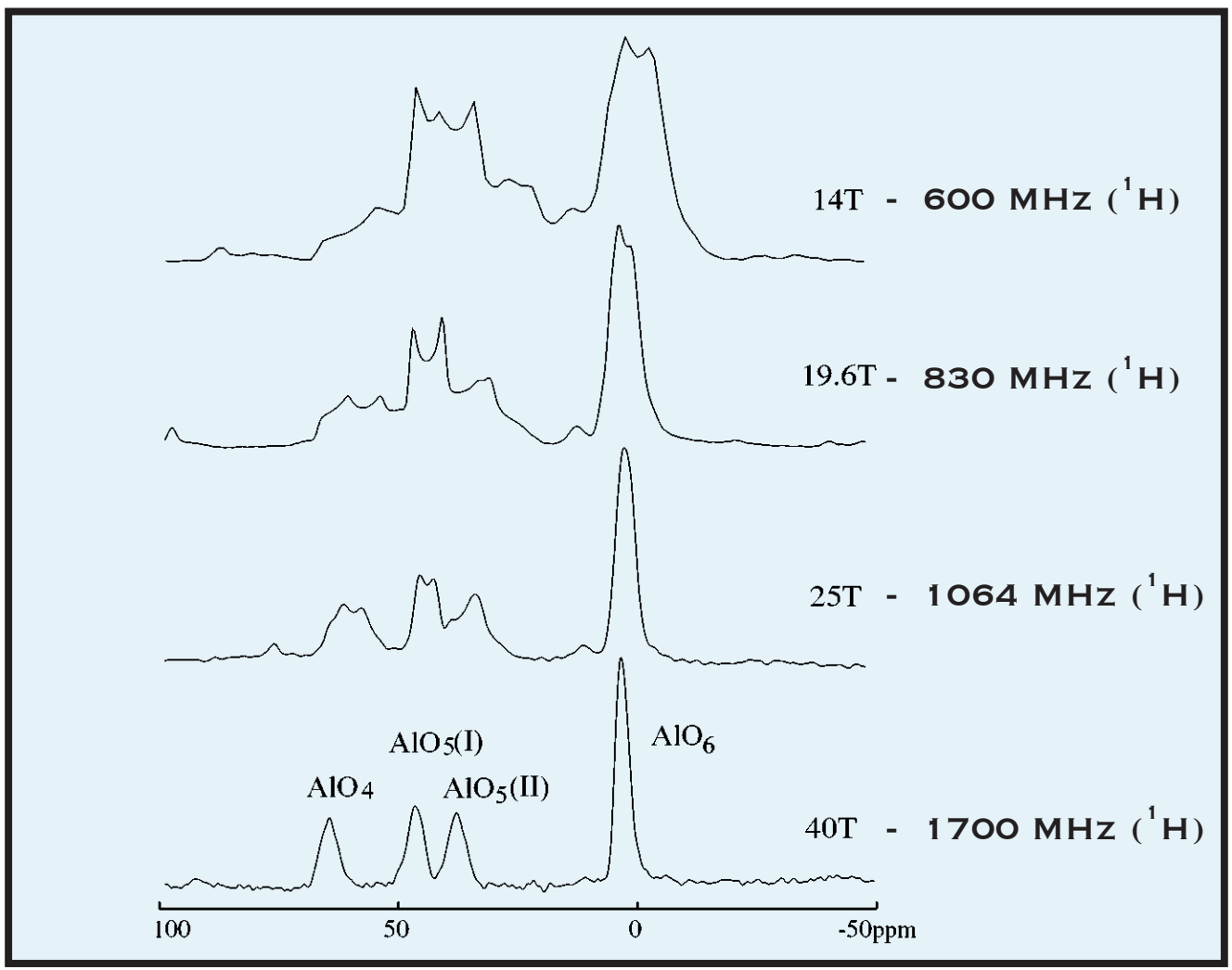

Gan,* Gor'kov, Cross, Samoson, and Massiot **J. AM. CHEM. SOC. 2002**, *124*, 5634- 5635

Another Solution: Be Clever

Averaging Anisotropy of Rank ℓ

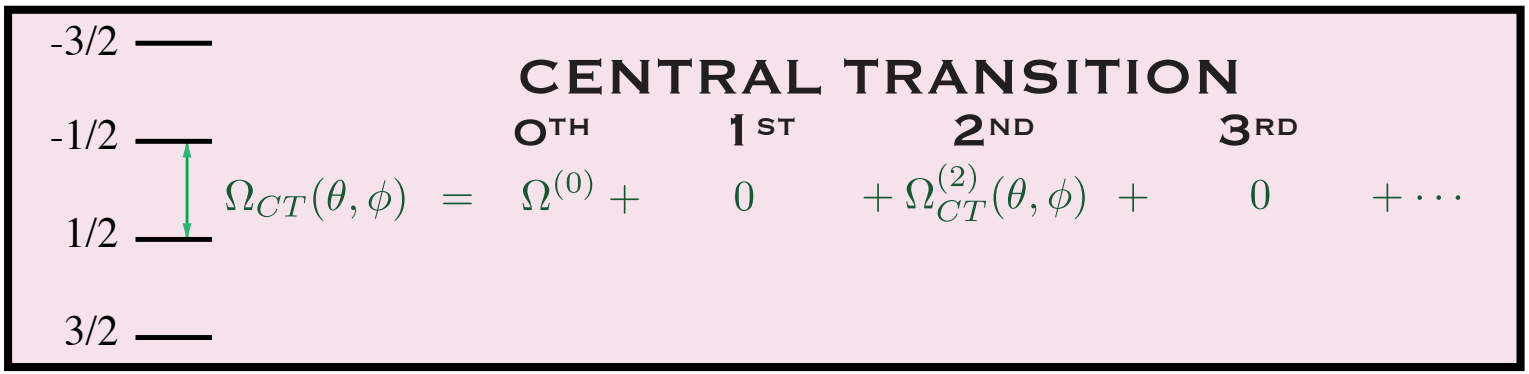

$$\Omega^{(2)}(\theta,\phi) = \Omega^{(2)}_{iso}(I,m_i,m_f) + \sum_{k=-2}^{2} c^{(2)}_{2,k}(I,m_i,m_f)\, Y_{2,k}(\theta,\phi) + \sum_{k=-4}^{4} c^{(2)}_{4,k}(I,m_i,m_f)\, Y_{4,k}(\theta,\phi)$$

Symmetry

ℓ $\langle A_{\ell,m} \rangle = 0$

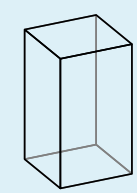

Tetragonal (D_4)

$\ell =$ 0 **1** 2 **3** 4 5 6 7 8 9 10

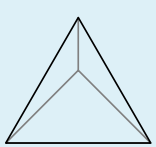

Tetrahedral (T)

$\ell =$ 0 **1** **2** 3 4 **5** 6 7 8 9 10

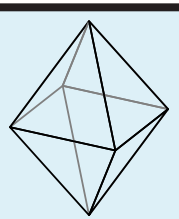

Octahedral (O) **MAS**

$\ell =$ 0 **1** 2 **3** 4 5 6 **7** 8 9 10

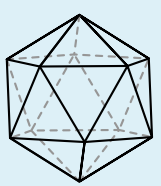

Icosahedral (I)

$\ell =$ 0 **1** 2 **3** 4 5 6 **7** 8 **9** 10

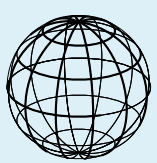

Rotation (SO(3))

$\ell =$ 0 **1** **2** **3** **4** **5** **6** **7** **8** **9** **10**

Averaging of spherical harmonics under selected proper point groups and SO(3). (Adapted by permission of Clarendon Press from A. Samoson, B. Q. Sun, and A. Pines, in *Pulsed Magnetic Resonance: NMR, ESR, and Optics - A recognition of E. L. Hahn.*)

A Solution: Double Rotation

Samoson, Lippmaa, Pines, Mol. Phys., 65, 1023(1988).

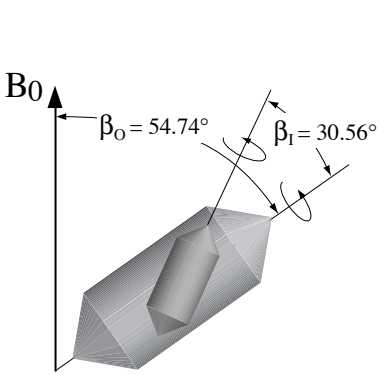

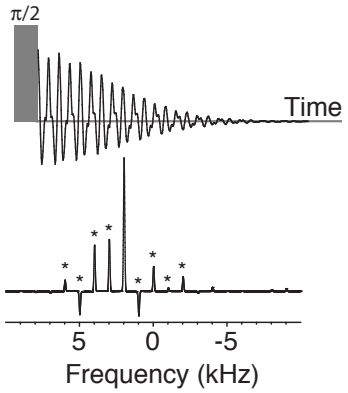

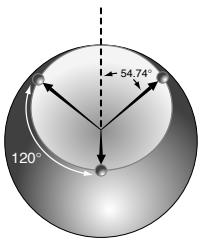

MAS Symmetry

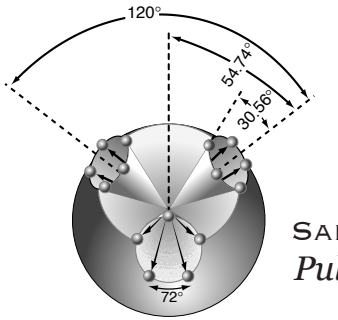

DOR Symmetry

Samoson, Sun, and Pines,
Pulsed Magnetic Resonance: NMR, ESR, and Optics

^{23}Na DOR of $Na_4P_2O_7$

Engelhardt, Kentgens, Koller, Samoson
Solid State Nuclear Magnetic Resonance **15** 1999. 171–180

Magic Angle Spinning

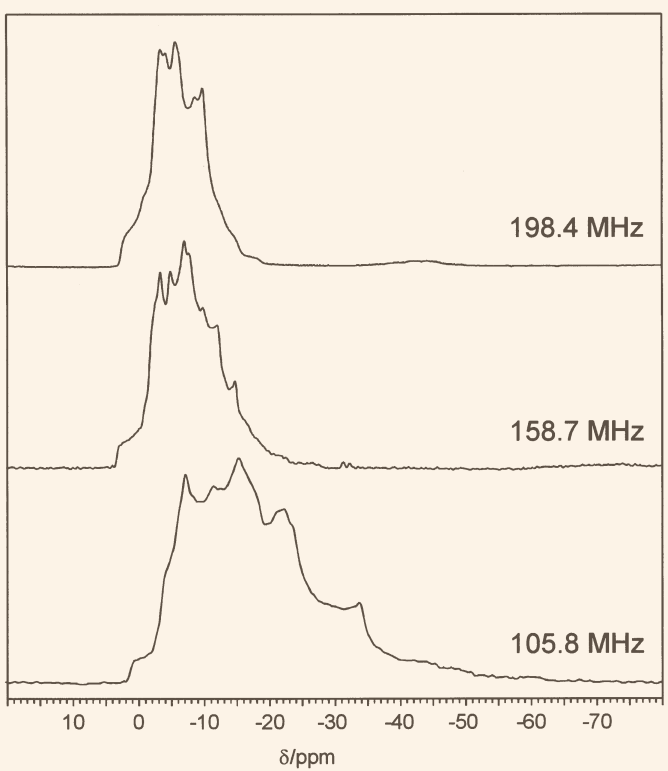

Double Rotation

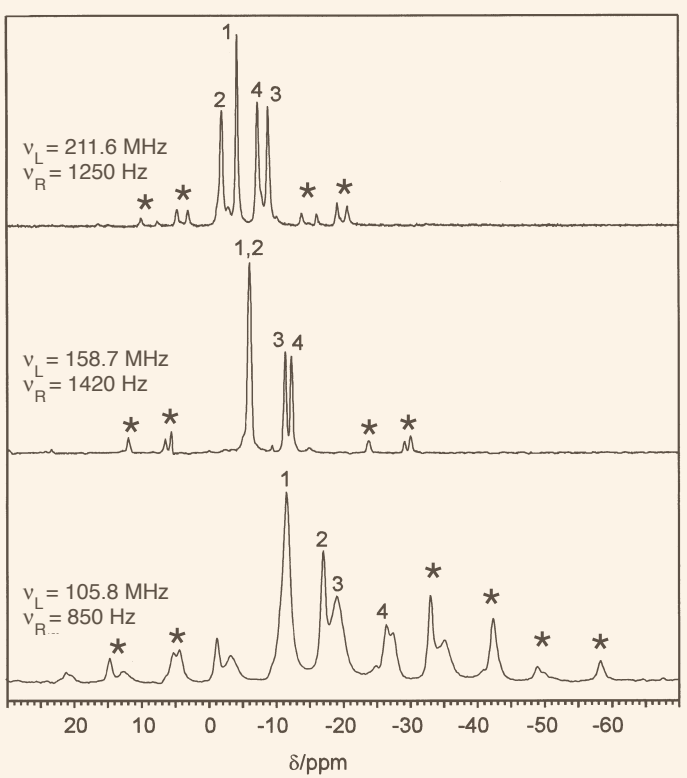

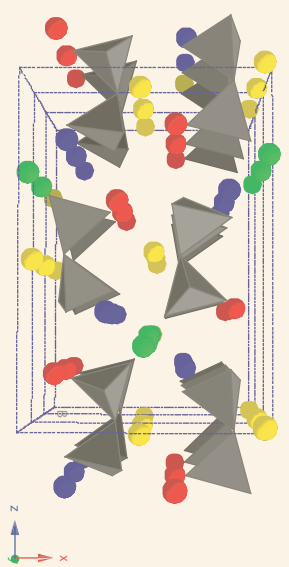

Other Solutions?
Let's make an Echo

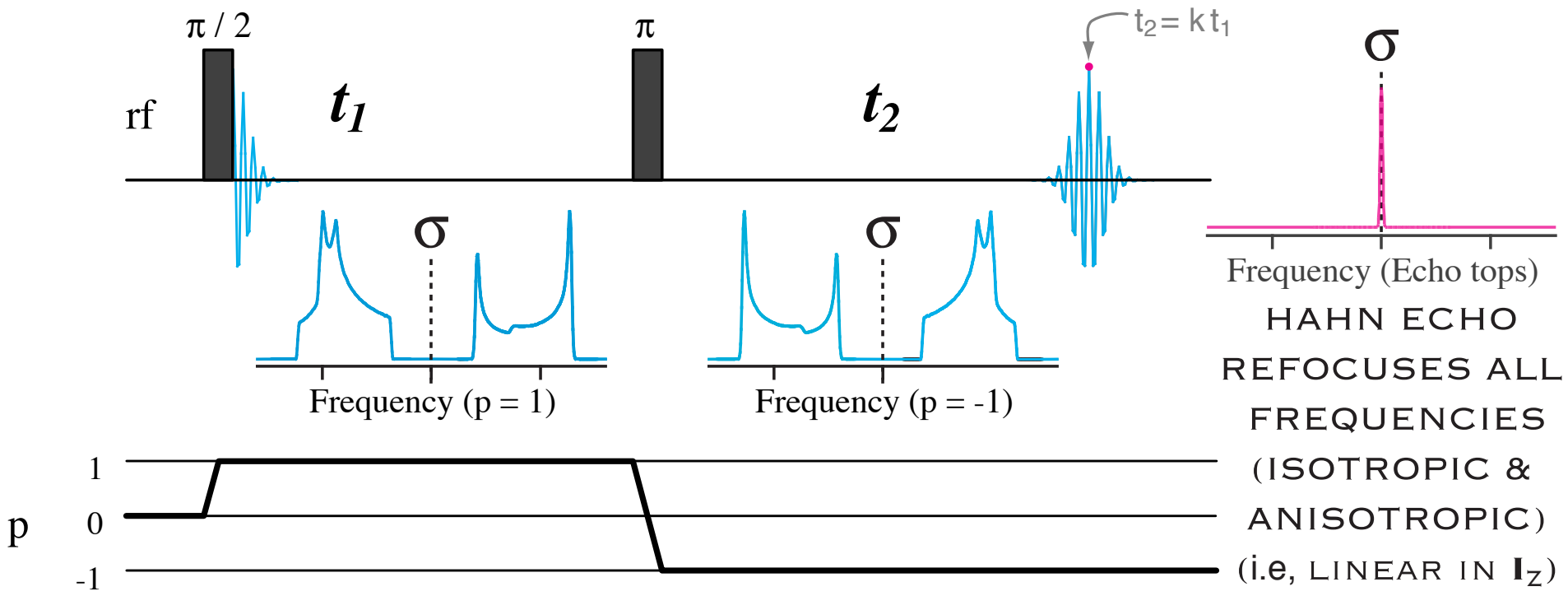

HAHN ECHO REFOCUSES ALL FREQUENCIES (ISOTROPIC & ANISOTROPIC) (i.e, LINEAR IN I_z)

Find Mirror Image Anisotropic Lineshapes

The key to understanding Dynamic-Angle Spinning

(1988: First High Resolution 2D Method for Quadrupolar Nuclei)

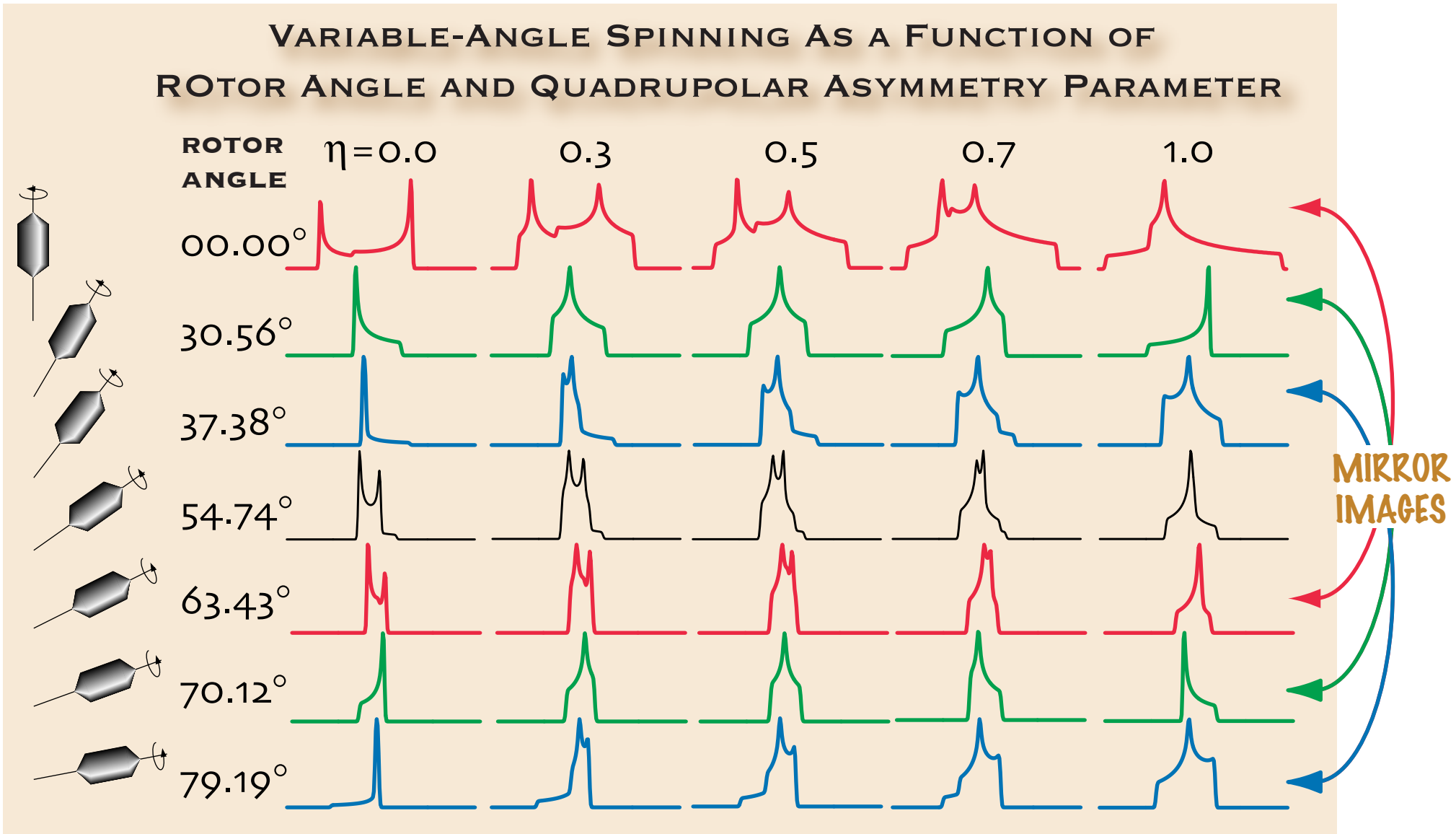

Add Another Time Dimension: Two-Dimensional NMR

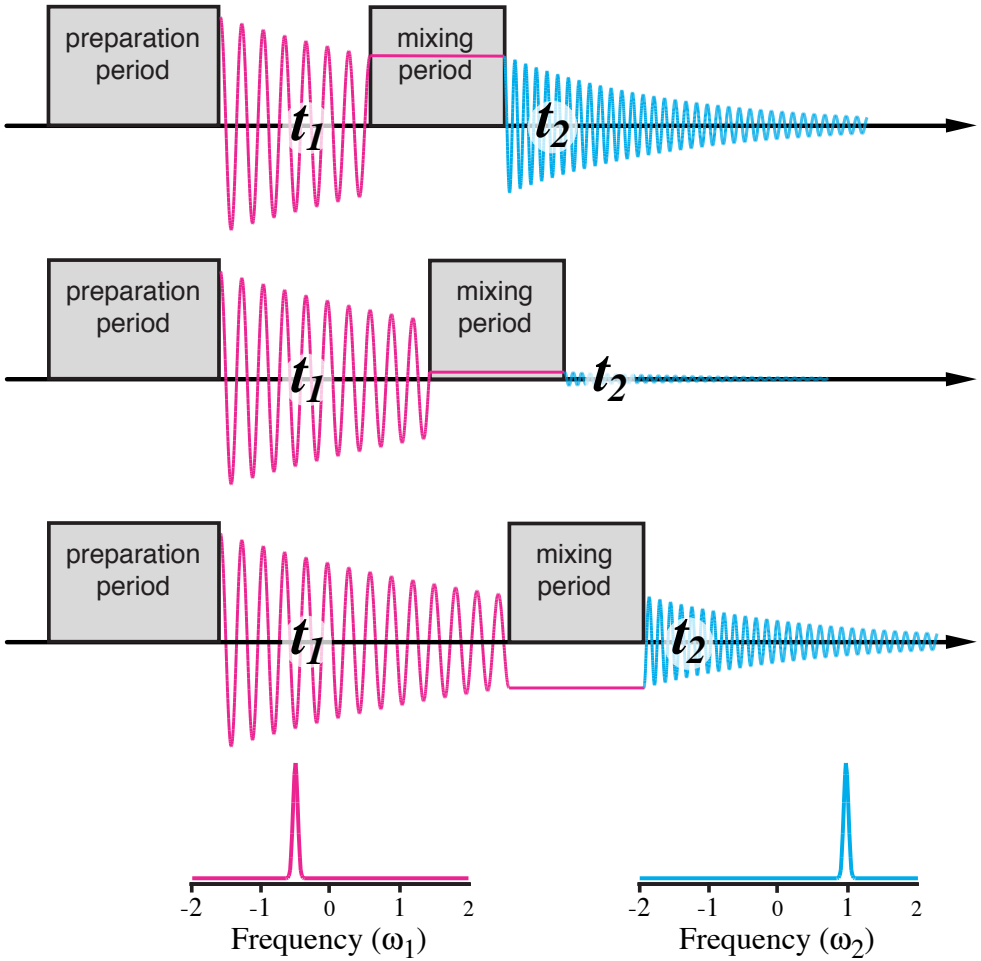

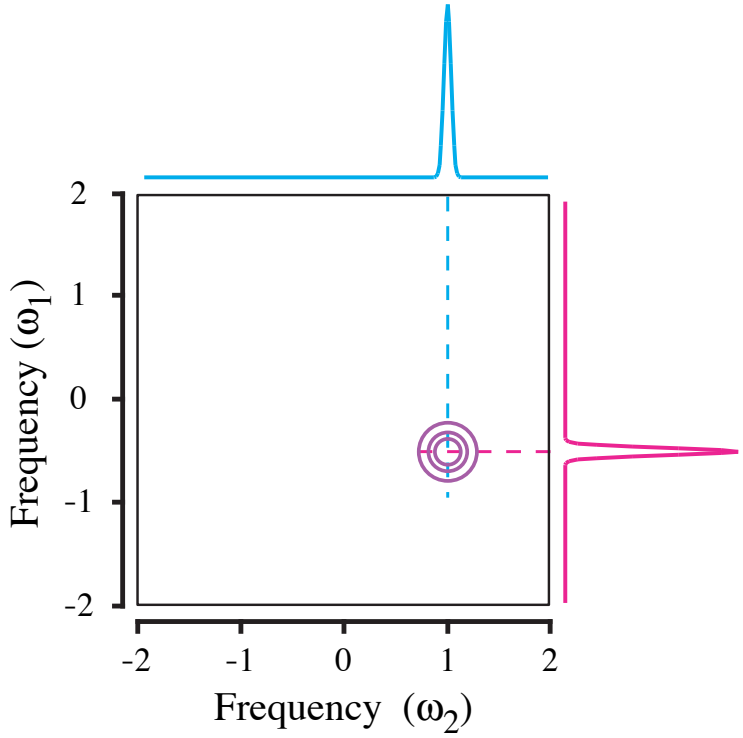

Q: How or why does the nuclear precession frequency change during the mixing period?

A: Generally, it's for the NMR Spectroscopist to decide. There are many possibilities.

examples:

(1) Change Magnetic Field Gradients during mixing period (Imaging),

(2) Allow chemical exchange or reaction during mixing time (2D Exchange Spectroscopy),

(3) Transfer magnetization between neighboring nuclei (2D Correlation Spectroscopy)

... many, Many more ...

The DAS Echo

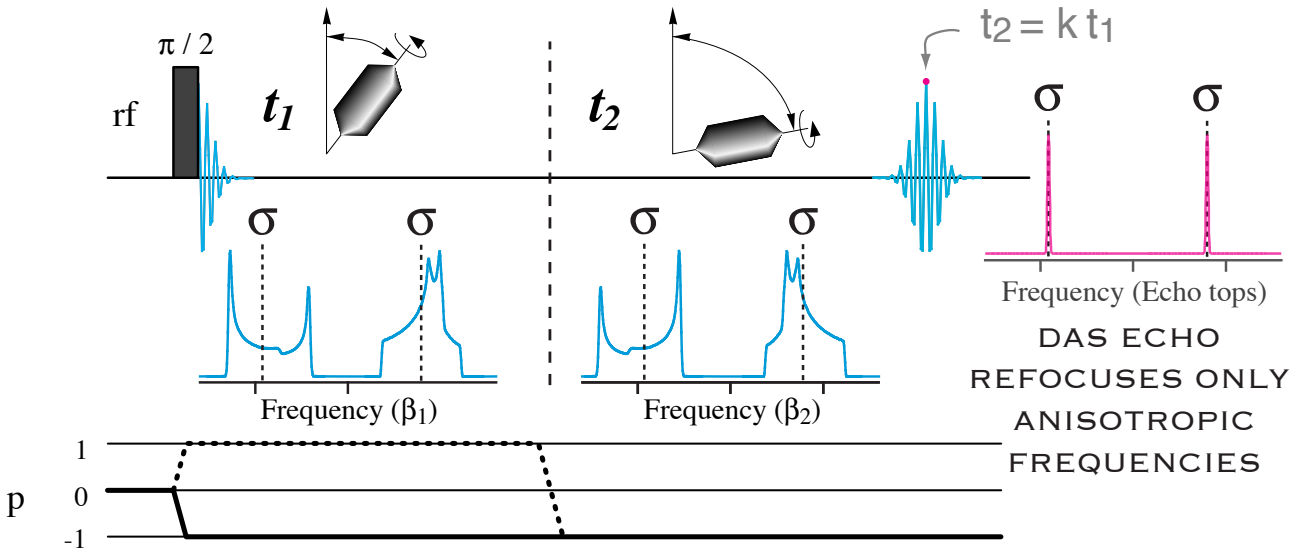

Chmelka et al.,
***Nature*, 339,** 42 (1989).
Llor and Virlet,
***Chem. Phys. Lett.*, 152,** 248 (1988).

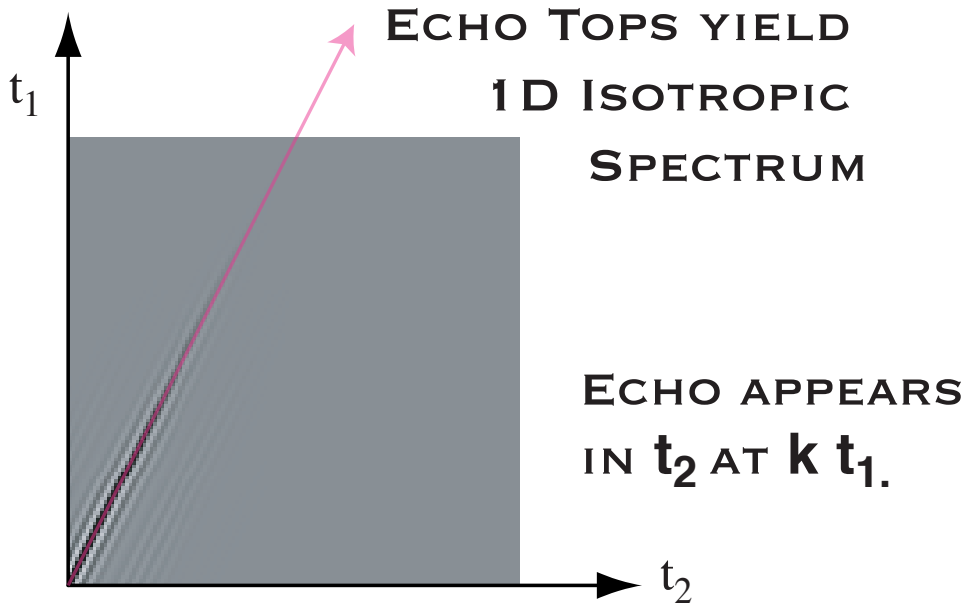

When does the echo occur in t_2?

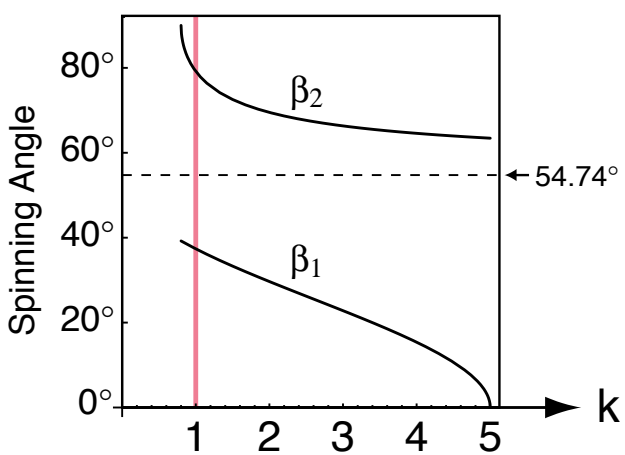

For example, with
$\beta_1 = 37.38°$, $\beta_2 = 79.19°$
we have k = 1

2D Dynamic Angle Spinning

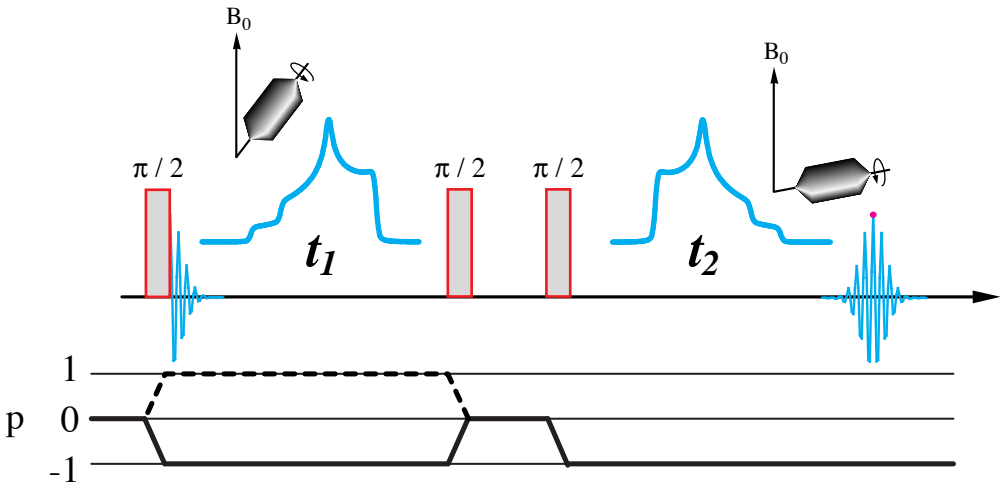

Mueller, Sun, Chingas, Zwanziger, Terao, and Pines, *J. Magn. Reson.*, **86,** 470 (1990).

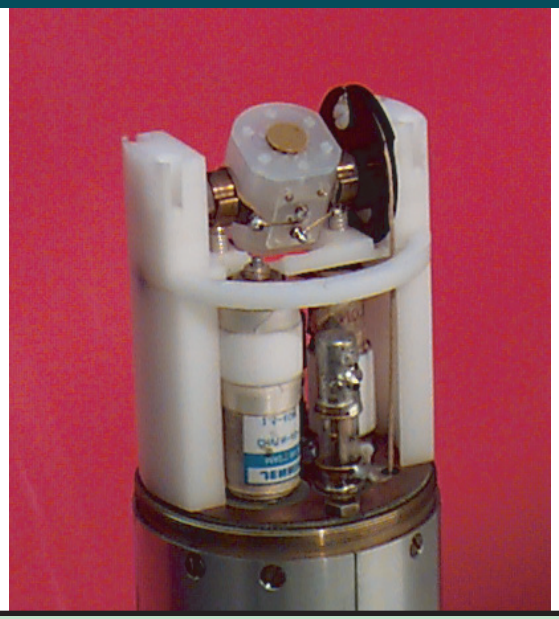

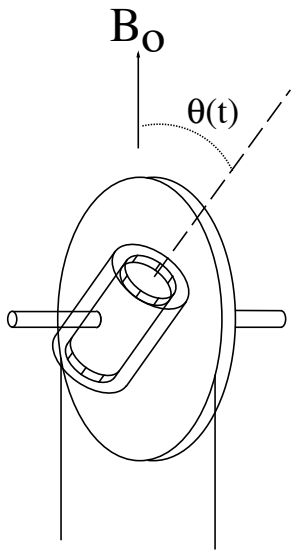

Shifted Echo Acquisition

For Pure Absorption Mode 2D Spectra in Solids

J. Magn. Reson. A, **103,** *72-81 (1993).*

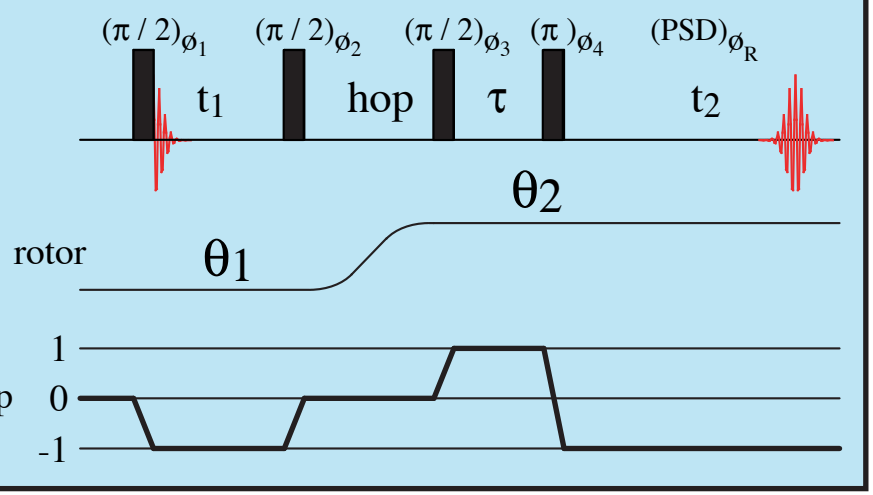

Shearing Transformation

apply t_1 dependent 1st order phase correction to ω_2 dimension

J. Magn. Reson. A, **103,** *72-81 (1993).*

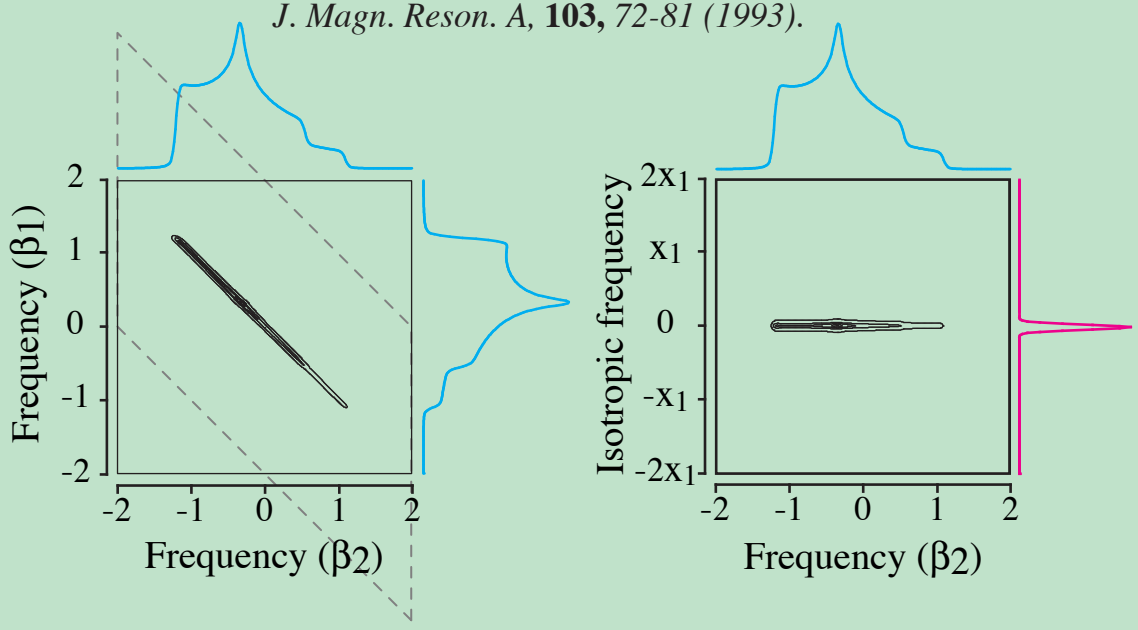

^{17}O 2D DAS of Coesite (A SiO_2 Crystalline Polymorph)

Magic-Angle Spinning

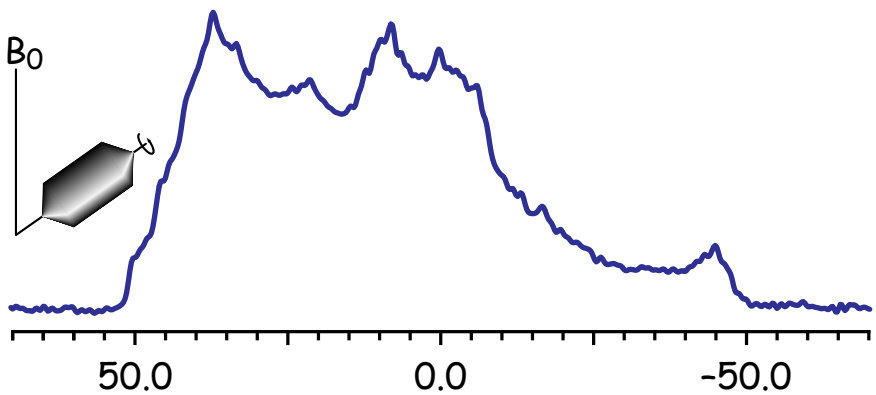

Dynamic-Angle Spinning

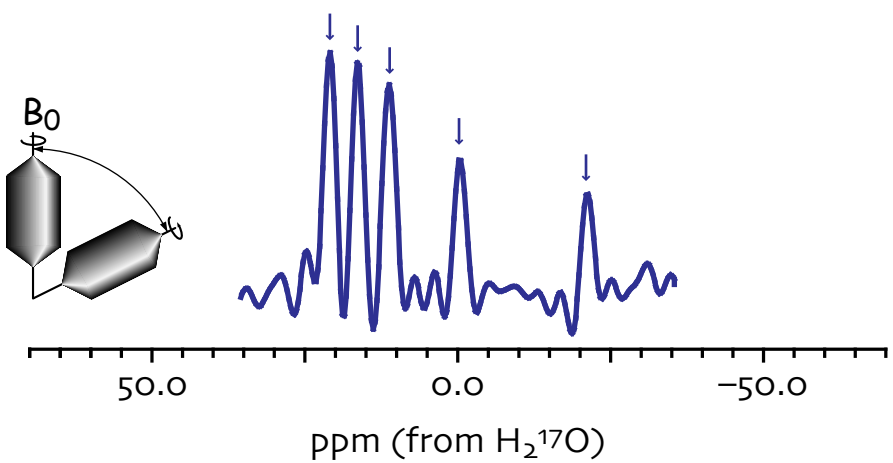

J. Phys. Chem., **99,** 12341 (1995)

Coesite Structural Fragment

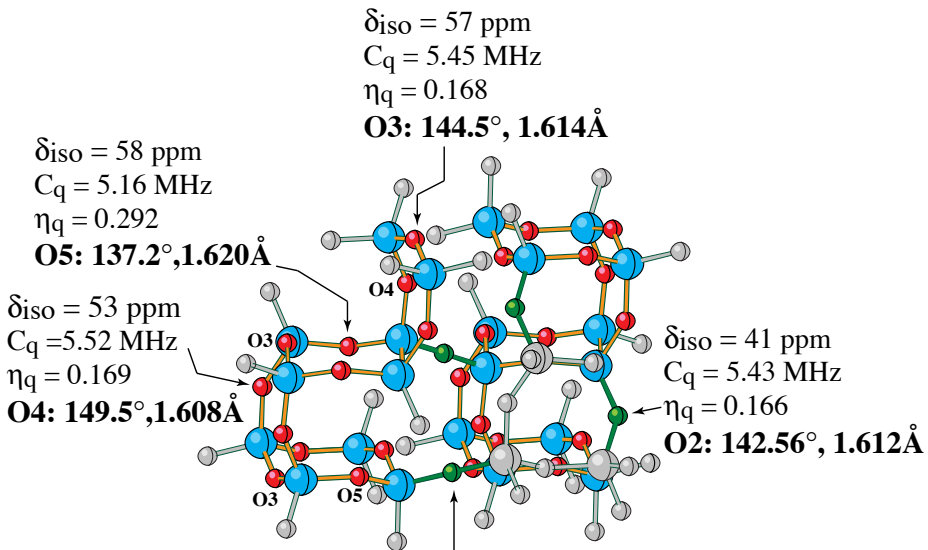

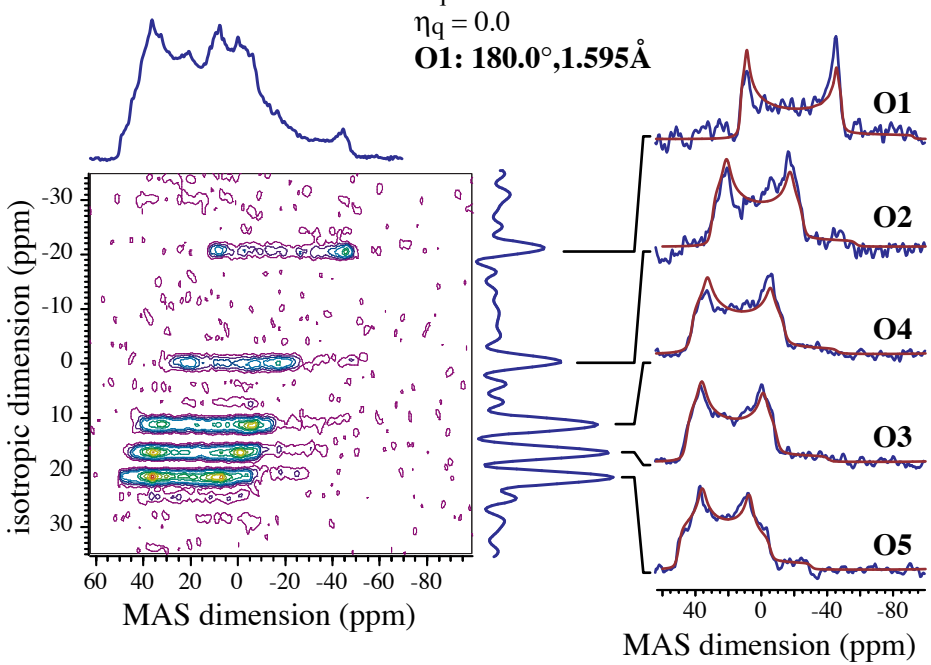

Another Solution: The MQ-MAS Echo (High Resolution for The People)

Triple quantum MAS spectrum is the mirror image of the single quantum MAS spectrum

Frydman and Harwood,
J. Am. Chem. Soc., **117,** 5367 (1995)
Medek, Harwood, and Frydman,
J. Am. Chem. Soc. **117,** *12779 (1995)*

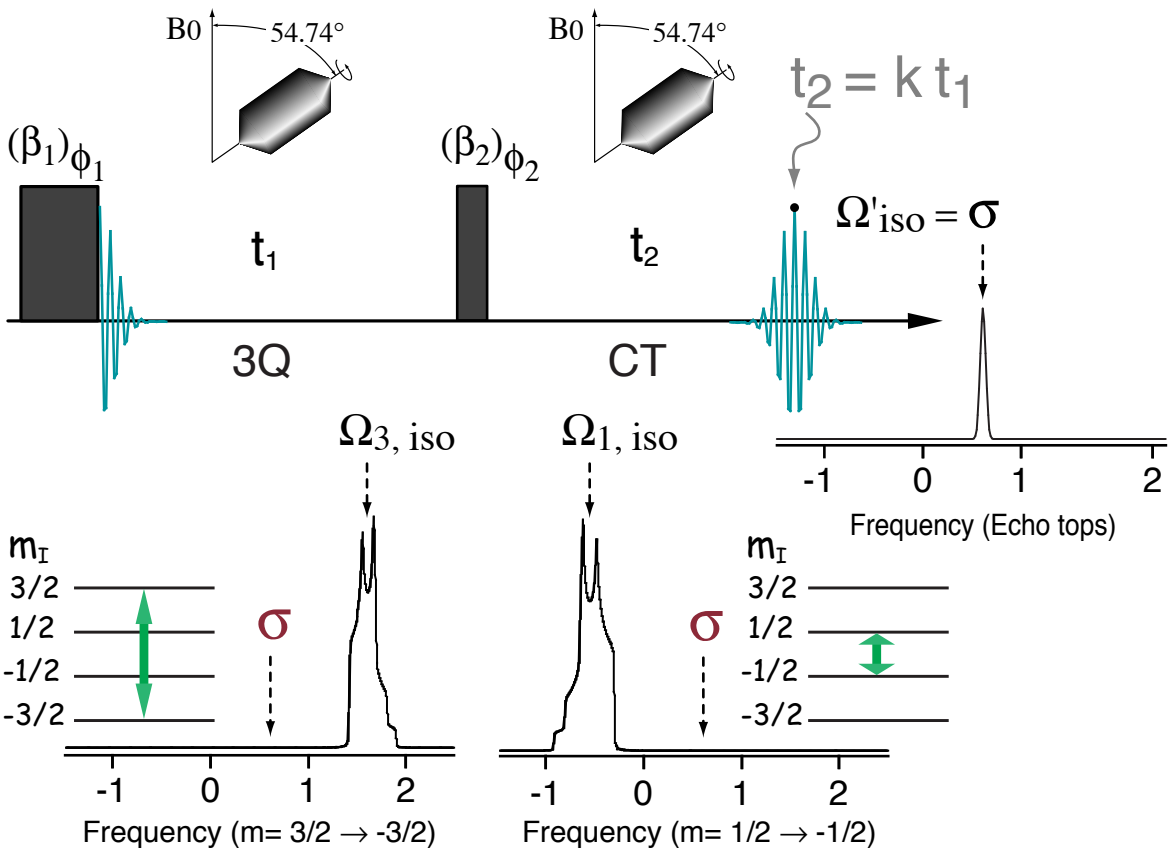

When does the echo occur in t_2?

Spin	t1 transition (m ⟶ -m)	k
3/2:	3QMAS	7/9
5/2:	3QMAS	19/12
	5QMAS	25/12
7/2:	3QMAS	101/45
	5QMAS	11/9
	7QMAS	161/45
9/2:	3QMAS	91/36
	5QMAS	95/36
	7QMAS	7/18
	9QMAS	31/6

2D Shifted-Echo MQ-MAS

Massiot et al., *SSNMR,* **6,** 73 (1996)

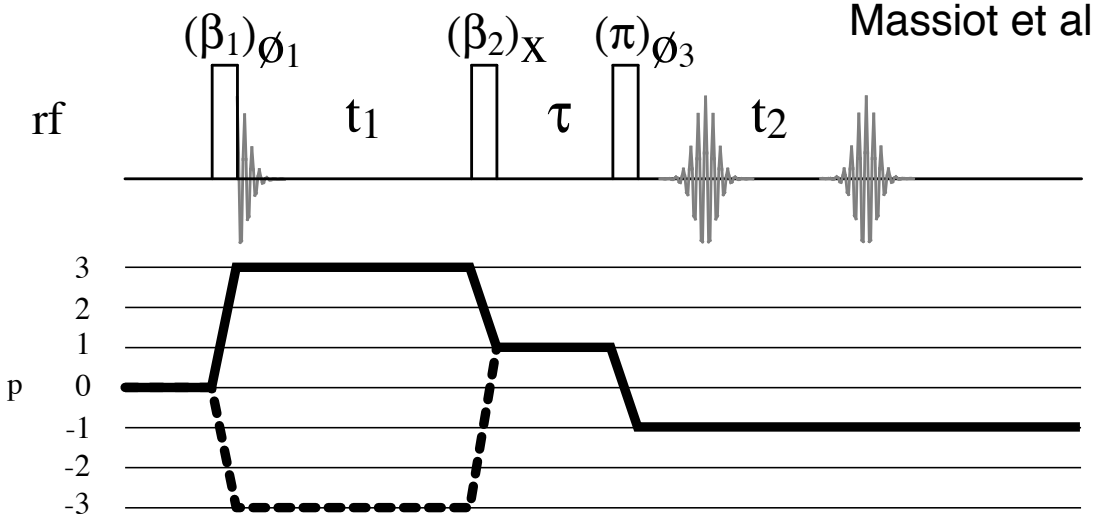

After Shearing Transformation:

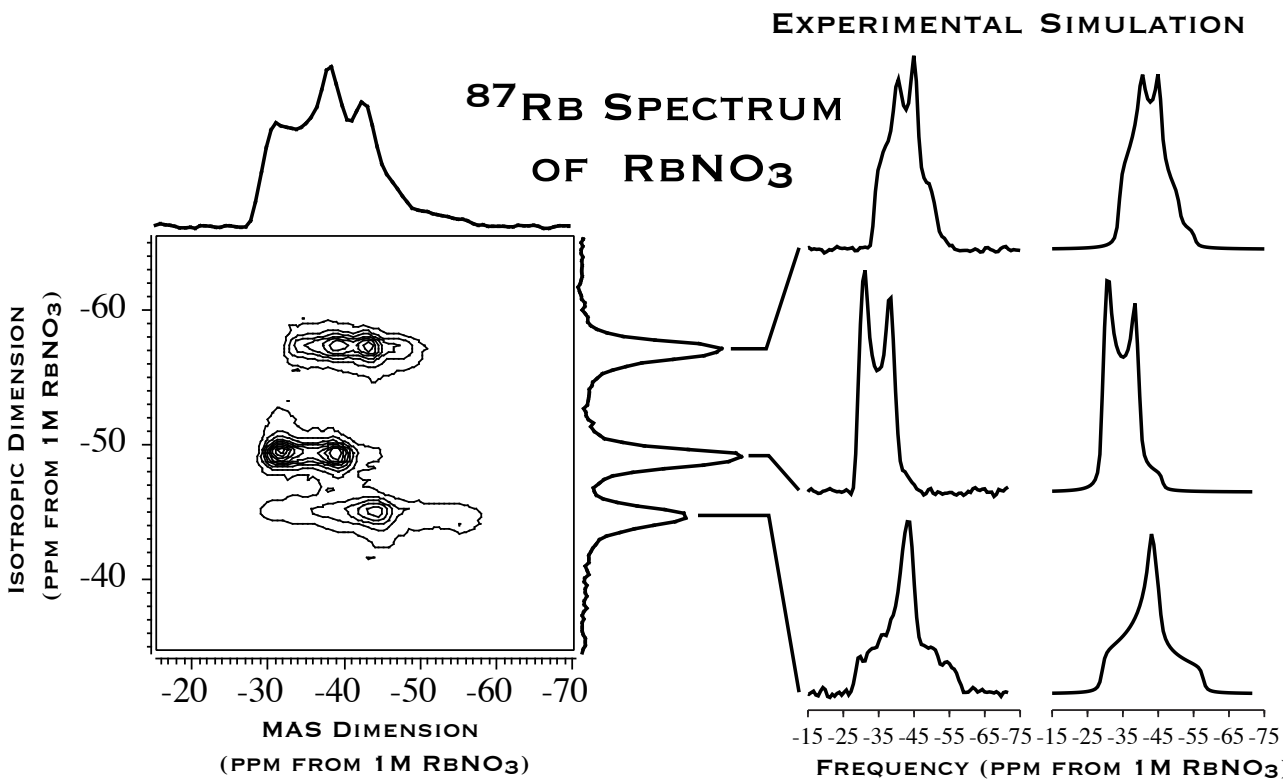

...and Another Solution: The ST-MAS Echo

The satellite transition MAS spectrum is the mirror image of the central transition MAS spectrum

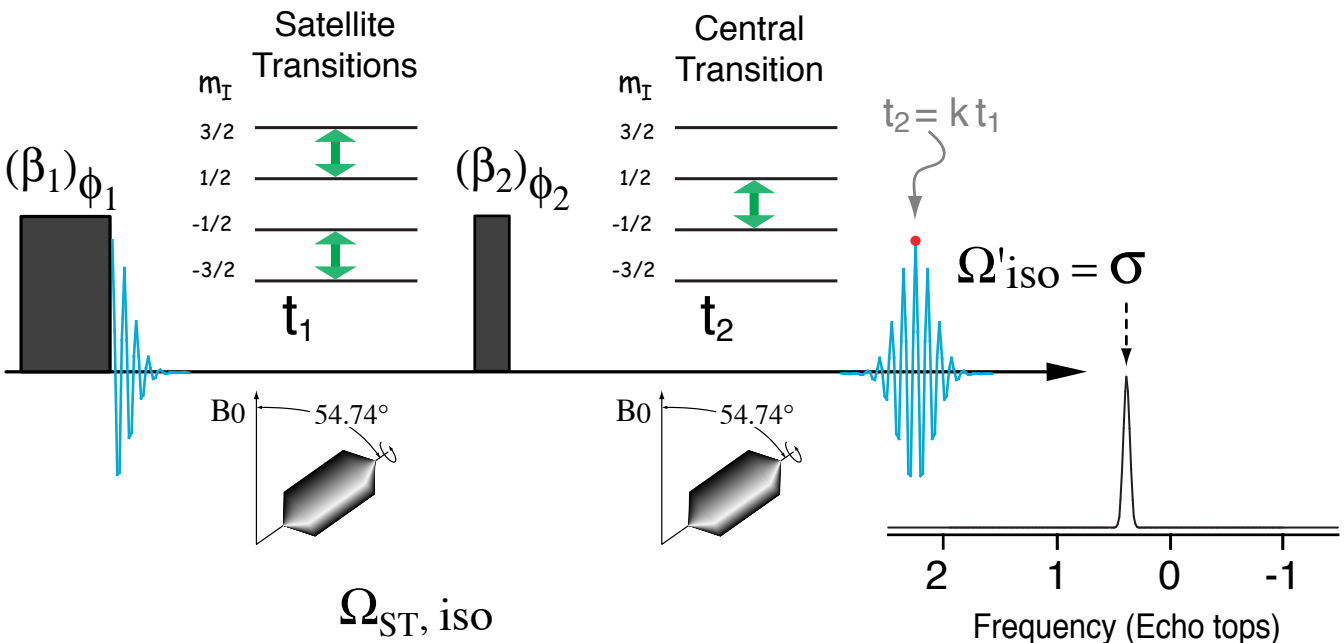

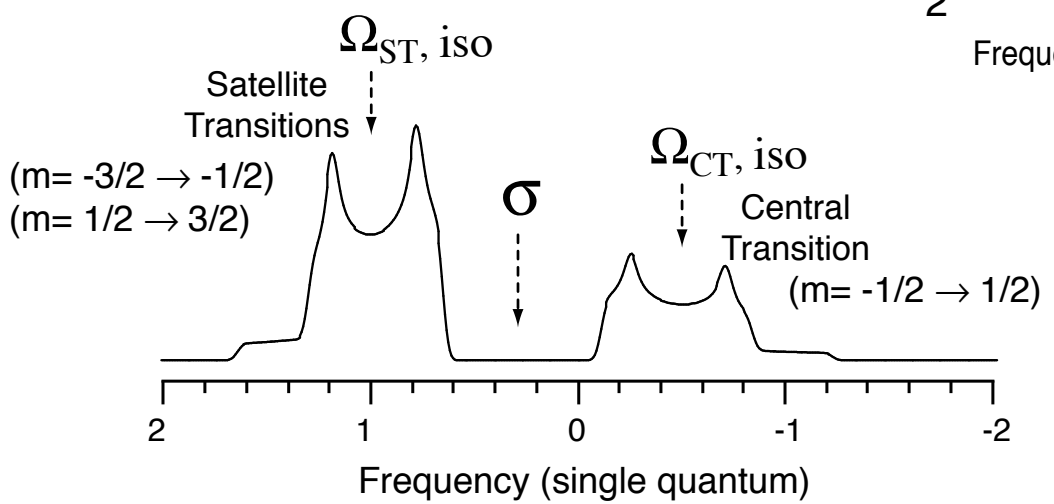

Z. Gan, *J. Am. Chem. Soc.* 2000, **122,** 3242-3243

When does the echo occur in t_2?

Spin	t_1 transition	k
3/2:	1st satellites	8/9
5/2:	1st satellites	7/24
	2nd satellites	11/6
7/2:	1st satellites	28/45
	2nd satellites	23/45
	3rd satellites	12/5
9/2:	1st satellites	55/72
	2nd satellites	1/18
	3rd satellites	9/8
	4th satellites	25/9

Use Double Quantum Filtered ST-MAS to eliminate undesired CT-CT correlation

Hyung-Tae Kwak and Zhehong Gan, *J. Magn. Reson.* **164** (2003) 369–372

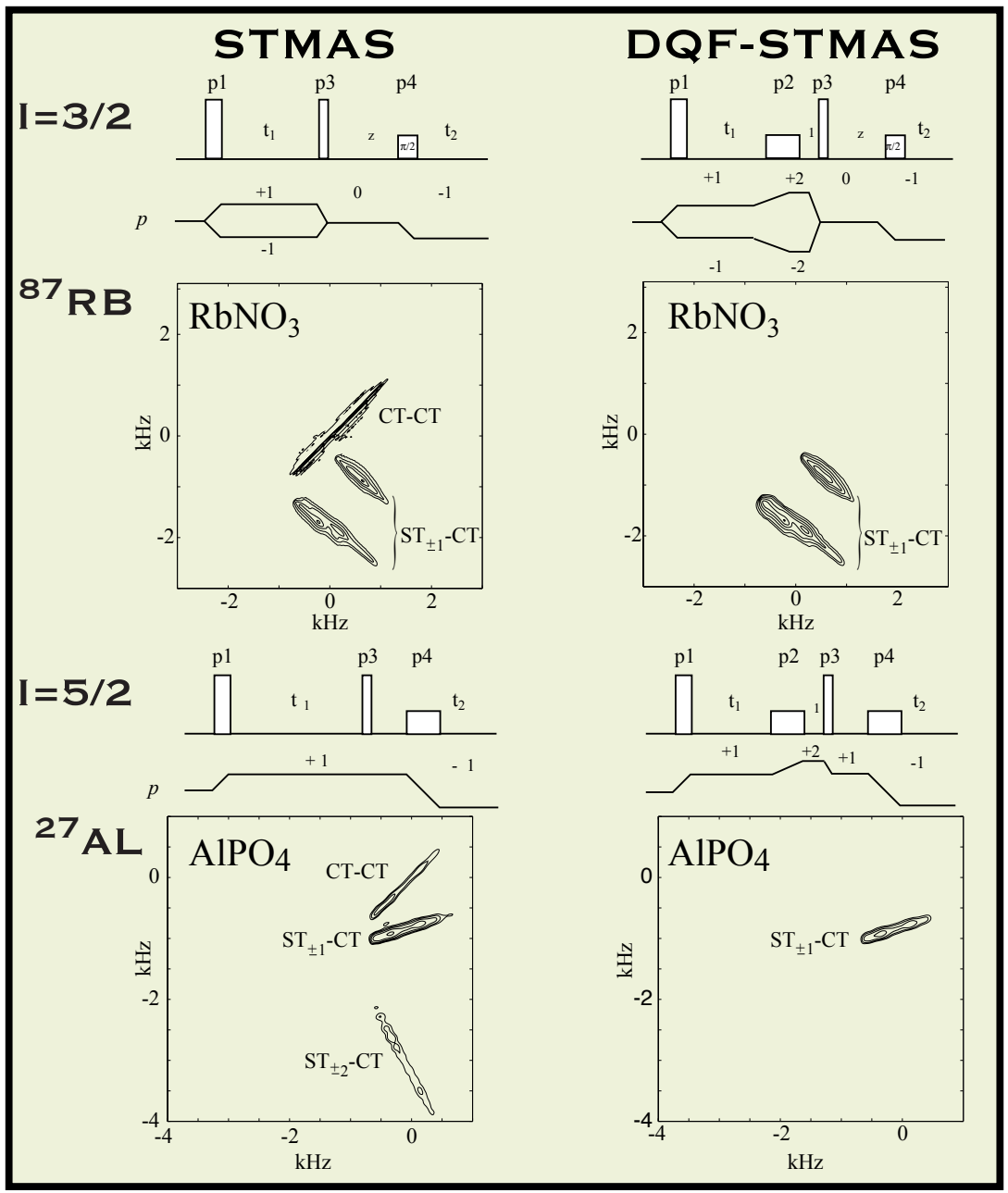

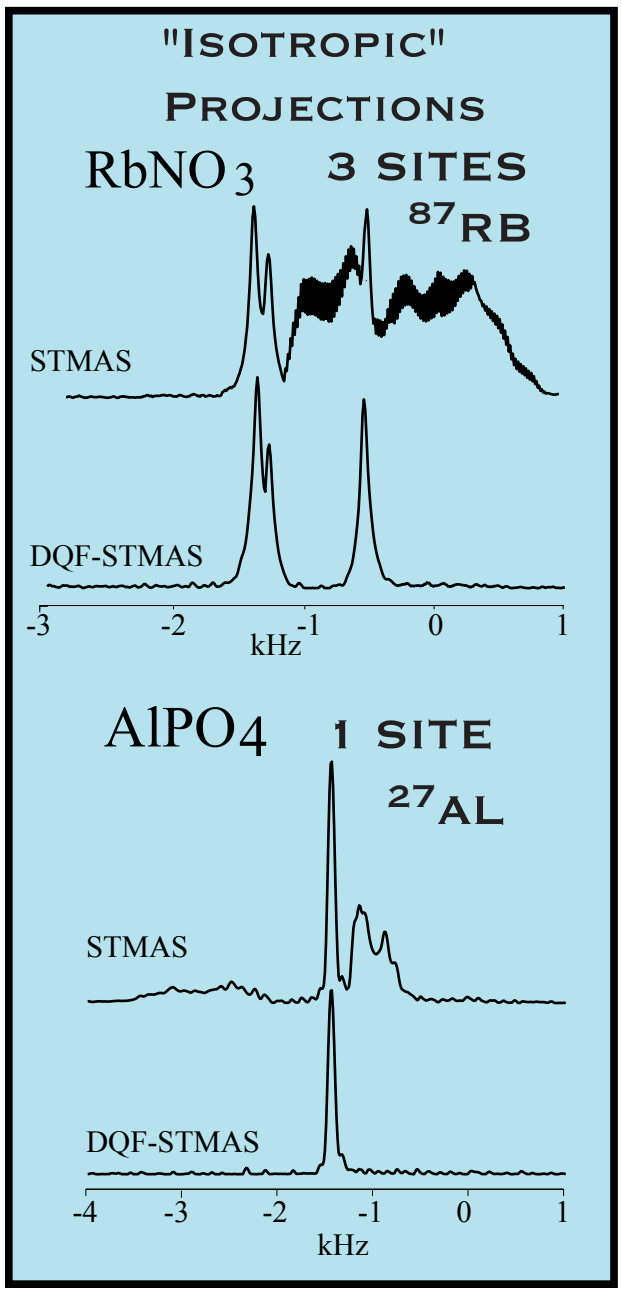

	Advantages	Disadvantages
DOR:	• Quantitative • High Sensitivity • Low rf power • One dimensional experiment - Quick experiment (In principle)	• Special Probe Required • Stable spinning requires finesse • Slow spinning speeds - (large # of sidebands) • Large coil ... low rf power - poor decoupling.
DAS:	• Quantitative • High Sensitivity, even with nuclei having large quad. couplings • Low rf power • works well for dilute quadrupolar nuclei	• Special Probe Required • Fails in presence of strong homonuclear dipolar couplings • long hop times (30 ms) limits use to samples with long longitudinal relaxation.
MQ-MAS:	• Easiest to implement (no special probe) • Works well for Abundant nuclei • Works well for nuclei with short longitudinal relaxation	• Not always quantitative • requires high rf power for excitation and mixing • Poor sensitivity for large Cq • Complex spinning sideband behavior
ST-MAS:	• Easy to implement (no special probe) • excites only single quantum transitions • Works well for Abundant nuclei • Works well for nuclei with short longitudinal relaxation	• Sensitive to magic-angle misset (< 0.01°) • stable spinning speed required. • requires high rf power for satellite excitation. • Poor sensitivity for large Cq • Not always quantitative • Complex spinning sideband behavior • fails to remove 3rd and other higher-order effects • Fails when there's motional averaging of satellite lineshapes.

Pay the Bills...

Interpreting Quadrupolar Couplings (Electric Field Gradients)

$$H_q = \sum_k (-1)^k \; R_{2k}(\Omega_q) \left[\sqrt{\frac{3}{2}}\frac{eQ_{\gamma I}}{I(2I-1)}T_{2-k}\right]$$

Electric Field Gradient at the nucleus — Nuclear Quadrupole Moment

Electric Field Gradient at the nucleus

$$R_{2,k} = \sum_{\text{all electrons}} E_{2,k}(e) + \sum_{\text{all nuclei}} N_{2,k}(n)$$

Surrounding Electrons

$$E_{2,k}(e) = -e\sqrt{\frac{4\pi}{5}}\frac{1}{r_e^3}Y_{2,k}(\theta_e,\phi_e)$$

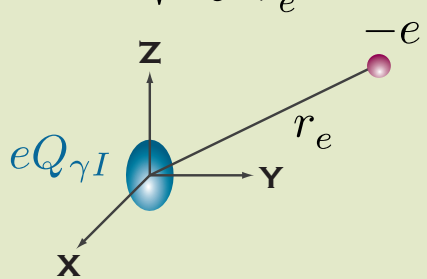

Surrounding Nuclei

$$N_{2,k}(n) = Z_n e\sqrt{\frac{4\pi}{5}}\frac{1}{r_n^3}Y_{2,k}(\theta_n,\phi_n)$$

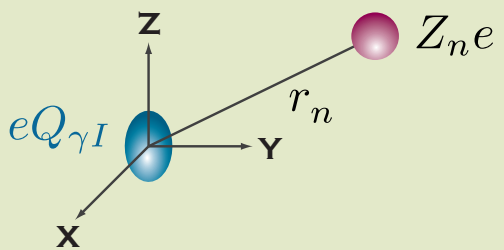

Total Electric Field Gradient at the Nucleus $\langle R_{2,k}\rangle = \langle\Psi|R_{2,k}|\Psi\rangle$

Complete Nuclear and Electronic Wavefunction

The Electric Field Gradient Tensor and its orientation

- EFG is 2nd rank traceless tensor: 5 elements, $\langle R_{2,k} \rangle$, with k = -2,-1,0,1,2.
- There exists a principal axis coordinate system (PAS) where tensor is diagonal... $\langle R^{\rm PAS}_{2,\pm1} \rangle = 0$
- Further define PAS such that $|\langle R^{\rm PAS}_{2,0} \rangle| > |\langle R^{\rm PAS}_{2,\pm2} \rangle|$

...labeling PAS components as $\langle \rho_{2,k} \rangle \equiv \langle R^{\rm PAS}_{2,k} \rangle$

For example, in a C-D bond the ^{2}D efg PAS is directed along the C-D bond axis.

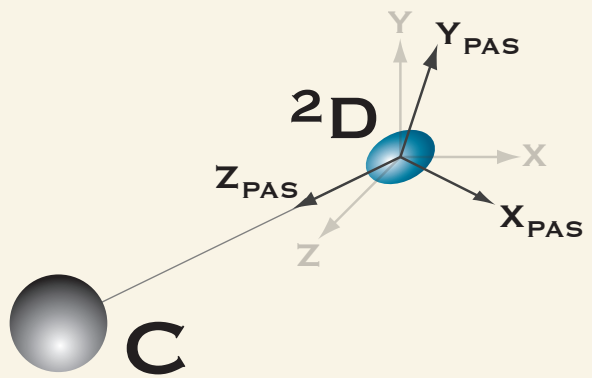

- Quadrupolar coupling Constant and Asymmetry parameters are defined ...

$$C_q = 2\,\frac{eQ}{h}\langle \rho_{2,0} \rangle \quad \text{and} \quad \eta_q C_q = 2\sqrt{6}\,\frac{eQ}{h}\langle \rho_{2,\pm2} \rangle$$

In Cartesian Coordinates... $C_q = e^2 Q \langle q_{zz} \rangle / h, \quad \text{and} \quad \eta_q = \dfrac{\langle q_{xx} \rangle - \langle q_{yy} \rangle}{\langle q_{zz} \rangle}$

Note that... $\langle q_{zz} \rangle + \langle q_{yy} \rangle + \langle q_{xx} \rangle = 0$

Point Charge Model for Predicting Electric Field Gradients

- no analytical expression for EFG exists without approximations.
- most drastic is the Point Charge Model: It's crude, but often provides a qualtitative understanding, and with calibration can sometimes be quantitative.

$$\langle R_{2,k} \rangle = \sum_{j=1}^{n} \frac{Z_j e}{d_i^3} \sqrt{\frac{4\pi}{5}} Y_{2,k}(\theta_j, \phi_j)$$

Approximate coordinating atoms as point charges and calculate sum of all coordinating atoms.

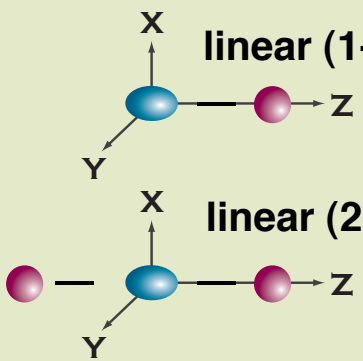

linear (1-coord.) $\theta = 0, \phi = 0$

$$\langle R_{2,0} \rangle = \frac{Ze}{d^3}, \quad \langle R_{2,\pm 1} \rangle = 0, \text{ and } \langle R_{2,\pm 2} \rangle = 0$$

linear (2-coord.) $\theta_1 = 0, \quad \phi_1 = 0$

$\theta_2 = 180°, \phi_2 = 0$

$$\langle R_{2,0} \rangle = 2\frac{Ze}{d^3}, \langle R_{2,\pm 1} \rangle = 0, \text{ and } \langle R_{2,\pm 2} \rangle = 0$$

Point Charge model predicts Cq doubles, and PAS unchanged when atom goes from one to two-coordinated linear.

Experimental ^{17}O NMR measurements in Silicates

Non-Bridging Oxygen Si-^{17}O$^-$		Bridging Oxygen Si-^{17}O-Si	
α-$Na_2Si_2O_5$	C_Q = 2.40 MHz, η = 0.20	α-$Na_2Si_2O_5$	C_Q = 5.74 MHz, η = 0.20
$Li_2Si_2O_5$	C_Q = 2.45 MHz, η = 0.10	$Li_2Si_2O_5$	C_Q = 5.60 MHz, η = 0.10

Maekawa, Florian, Massiot, Kiyono, Nakamura, *J. Phys. Chem.* 1996, **100** (17), 5525-5532.

Xue, Stebbins, Kanzaki, *Am. Miner.* 1994, **79,** 31.

Point Charge Model for Predicting Electric Field Gradients

Trigonal Planar

Place quadrupole nucleus at the origin and the z-axis perpendicular to the plane containing 3 point charges

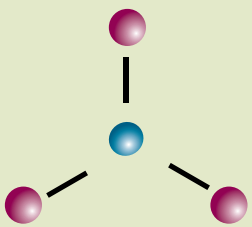

$$\theta = 90°, \phi = 0, \pm 120°$$

$$\langle R_{2,0} \rangle = -\frac{3}{2}\frac{Ze}{d^3}, \qquad \langle R_{2,\pm 1} \rangle = 0, \quad \text{and} \quad \langle R_{2,\pm 2} \rangle = 0$$

- z-axis of efg PAS is perpendicular to plane containing nucleus and coordinating charges.
- Asymmetry parameter is zero, and sign of the quadrupole coupling constant is opposite to linear cases.

Tetrahedral

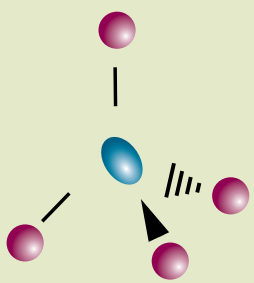

$$\langle R_{2,0} \rangle = 0, \quad \langle R_{2,\pm 1} \rangle = 0, \quad \text{and} \quad \langle R_{2,\pm 2} \rangle = 0$$

^{11}B Examples from Borosilicates...

	Cq	eta
Trigonal Planar $^{11}BO_3$ (ring)	2.65 MHz	0.20
Trigonal Planar $^{11}BO_3$ (non-Ring)	2.55 MHz	0.20
Tetrahedral $^{11}BO_4$ (1B,3Si)	0.30 MHz	0.00
Tetrahedral $^{11}BO_4$ (0B 4Si)	0.30 MHz	0.00

Lin-Shu Du and Jonathan F. Stebbins, *J. Non-Cryst. Solids* **315** (2003) 239–255

Point Charge Model for Predicting Electric Field Gradients

Bent

Place quadrupole nucleus at the origin with z-axis in plane containing atoms and perpendicular to the angle bisector

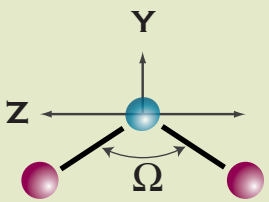

$$\langle R_{2,0}\rangle = \frac{Ze}{d^3}(3\sin^2\Omega/2 - 1), \quad \langle R_{2,\pm1}\rangle = 0, \text{ and } \quad \langle R_{2,\pm2}\rangle = \frac{Ze}{d^3}\sqrt{\frac{3}{2}}\cos^2\Omega/2$$

$$C_q = 2\frac{e^2Q}{h}\frac{Z}{d^3}(1-\cos\Omega) \text{ and } \eta = -\frac{3(\cos\Omega+1)}{3\cos\Omega - 1}$$

^{17}O quadrupolar coupling parameters in Si-^{17}O-Si linkage as a function of Si-O-Si angle

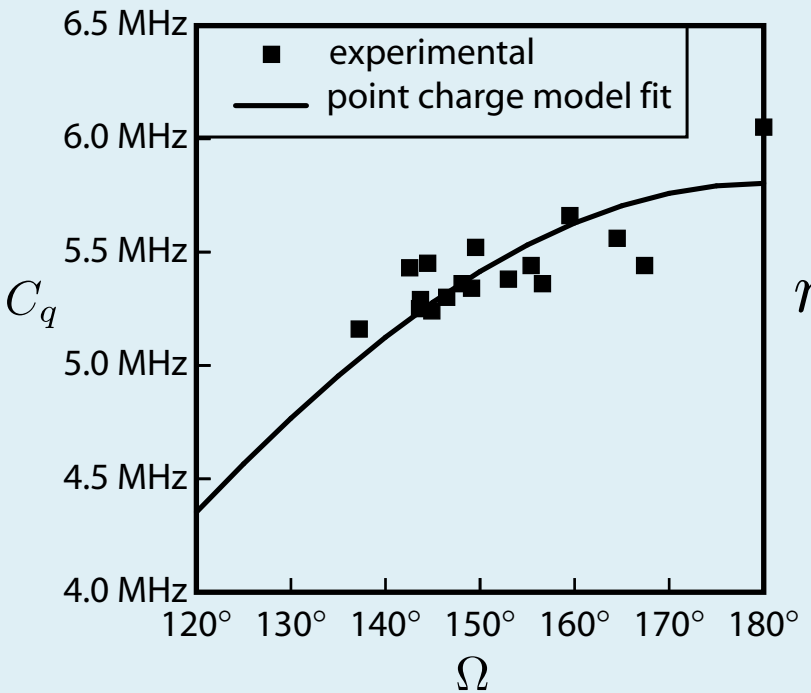

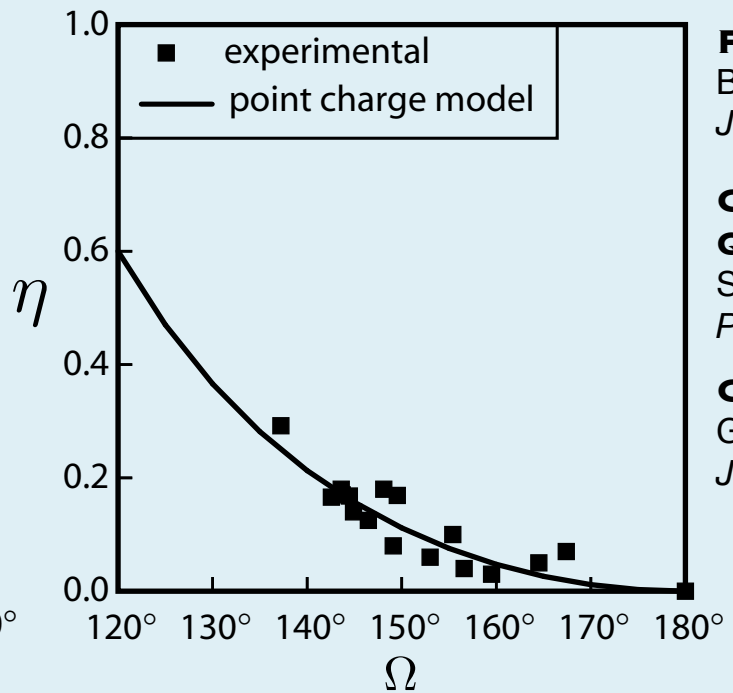

Ferrierite - 10 sites
Bull et al,
J. Am. Chem. Soc. **122** (2000) 4948

Cristobalite - 1 site
Quartz - 1 site
Spearing et al,
Phys. Chem. Min. **19** (1992) 307

Coesite - 5 sites
Grandinetti, et al,
J. Phys. Chem. **99** (1995) 12341

Rough Guide to Some Point Charge Models for EFG

Name	Structure	C_q	η_q
linear (1)	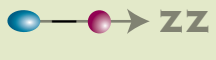	$2\frac{e^2Q}{h}\frac{Z}{d^3}$	0
linear (2)	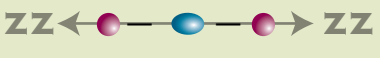	$4\frac{e^2Q}{h}\frac{Z}{d^3}$	0
bent (2)	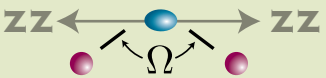	$2\frac{e^2Q}{h}\frac{Z}{d^3}(1-\cos\Omega)$	$-\frac{3(\cos\Omega+1)}{3\cos\Omega-1}$
Trigonal Planar (3)	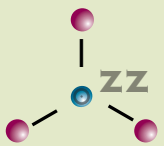	$-3\frac{e^2Q}{h}\frac{Z}{d^3}$	0
Tetrahedral (4)	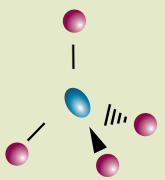	0	0
Trigonal Bipyramidal (5)	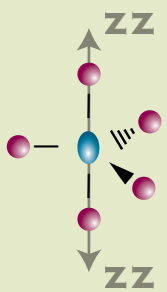	$\frac{e^2Q}{h}\frac{Z}{d^3}$	0
Octahedral (6)	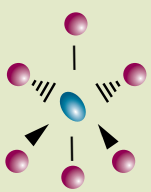	0	0

Nature of M determines ^{17}O Quadrupolar Coupling Constant in M-^{17}O-M linkage

$[(OH)_3M\text{-}O\text{-}M(OH)_3]^{2-}$ where M=B, Al, and Ga

$(OH)_3M\text{-}O\text{-}M(OH)_3$ where M=C, Si, and Ge

$(OH)_2OM\text{-}O\text{-}MO(OH)_2$ where M=P and As

$(OH)O_2M\text{-}O\text{-}MO_2(OH)$ where M=S and Se

M-O-M Angle and MO distance at optimized value

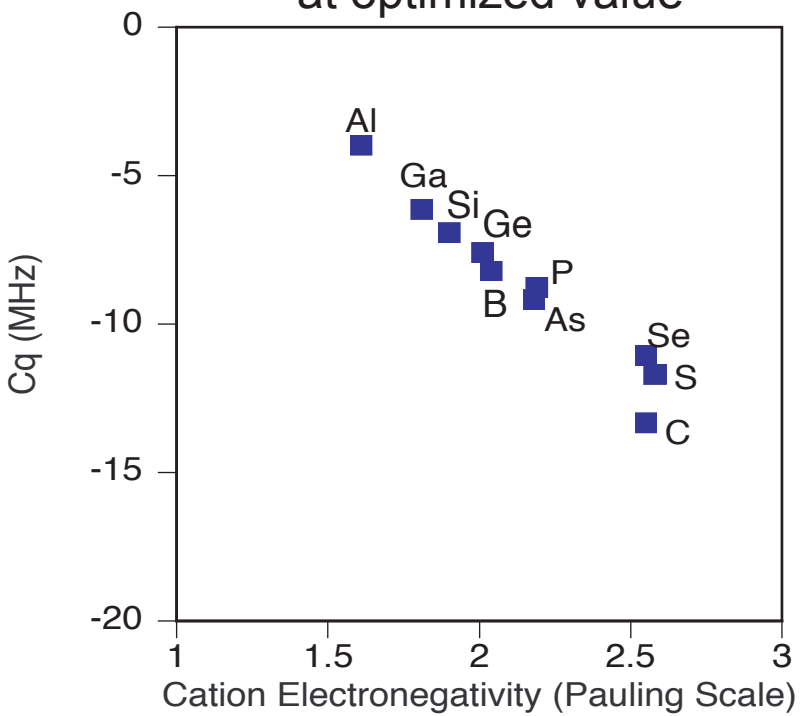

After Oldfield and Co-Workers

JACS, **106**, 2502 (1984), *JACS*, **108**, 7236 (1986)
JPC, **91**, 1054 (1987).

Identical M-O-M angles and MO distances

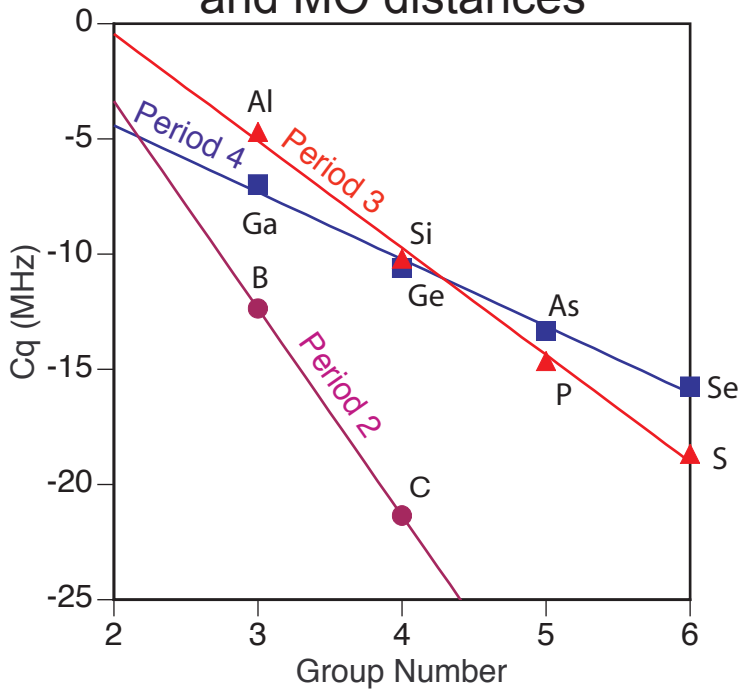

Clark and Grandinetti

SSNMR, **16**, 55 (2000).

Local Geometry is Secondary Factor

How does Local Geometry determine Bridging Oxygen EFG?

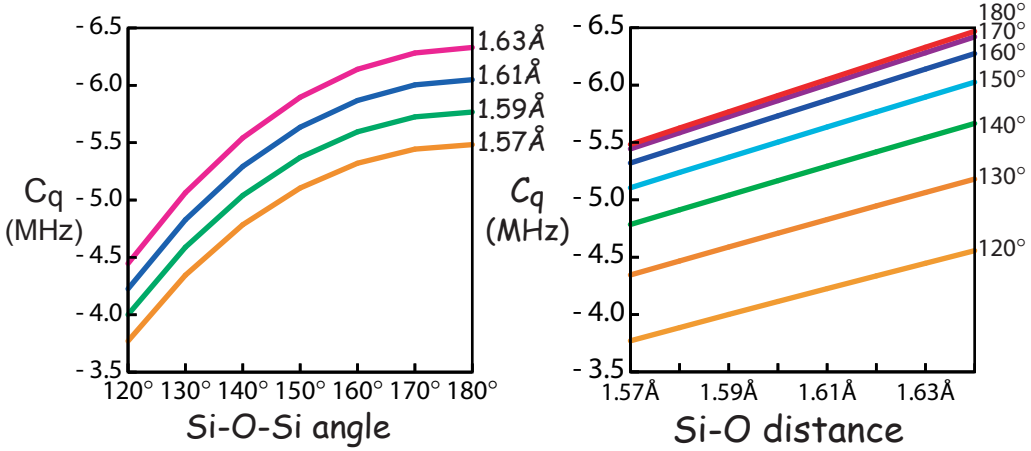

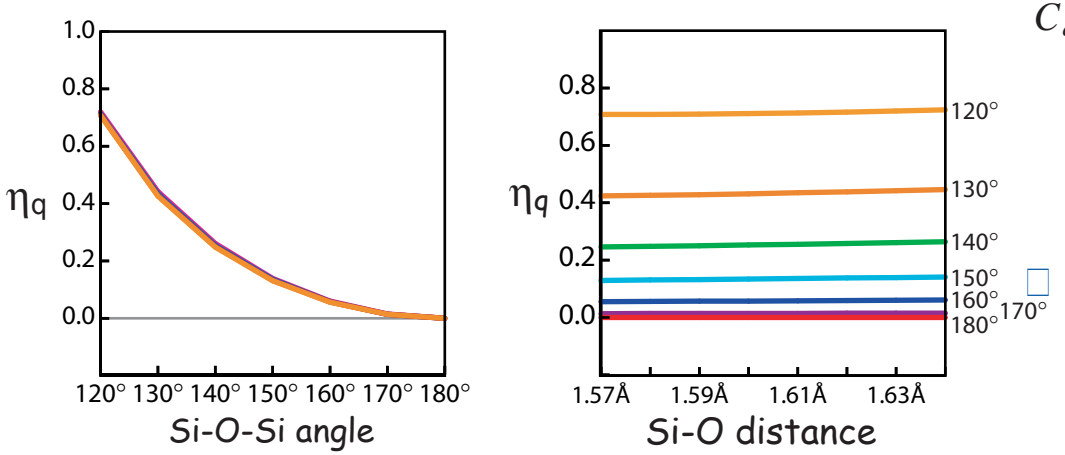

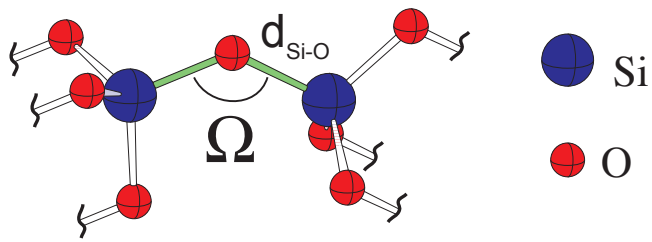

With all other factors constant ...

Bridging Oxygen |Cq| values

- decrease with decreasing Si-O-Si angle
- decrease linearly with decreasing Si-O distance

$$C_q(d_{\text{Si-O}},\Omega) = -(5.91\,\text{MHz})\left(\frac{1}{2}+\frac{\cos\Omega}{\cos\Omega - 1}\right)^{1.948} - (15\,\text{MHz/Å})(d_{\text{Si-O}} - 1.6\text{Å})$$

Bridging Oxygen η_q values

- increase with decreasing Si-O-Si angle
- are nearly independent of Si-O distance

$$\eta_q(\Omega) = 5.03\left(\frac{1}{2}-\frac{\cos\Omega}{\cos\Omega - 1}\right)^{1.09}$$

Clark and Grandinetti, *J. Phys. Condensed Matter,* **15**, S2387-S2395,(2003)

Quadrupolar Coupling Parameters can be used to measure Angles and Distances

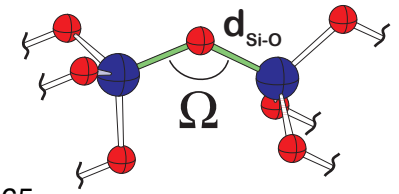

Si

O

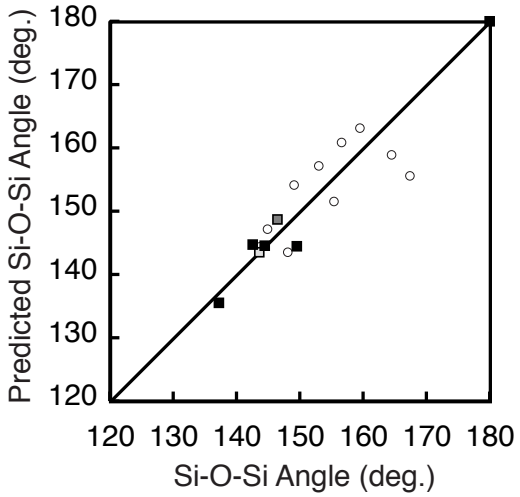

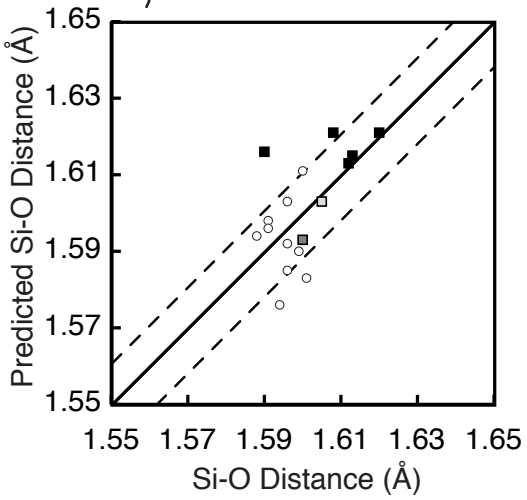

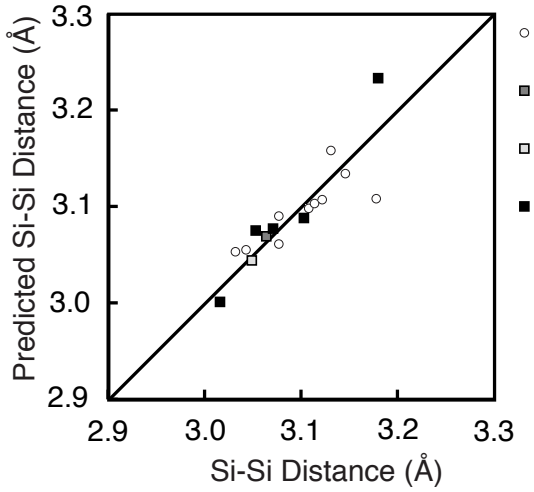

Ferrierite

Cristobalite

Quartz

Coesite

And Their Correlations

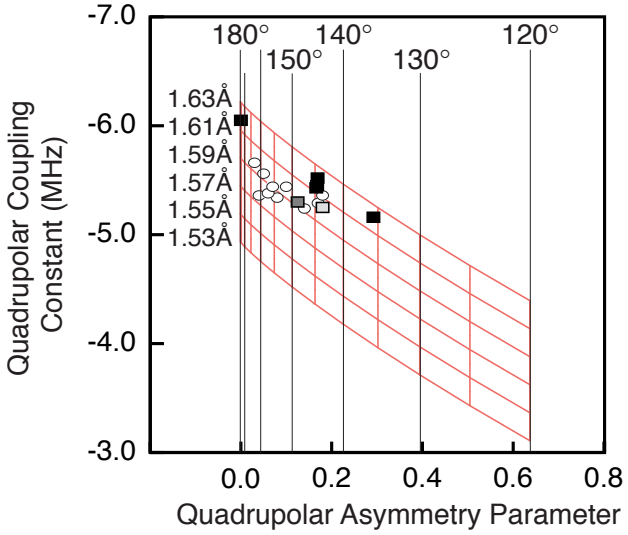

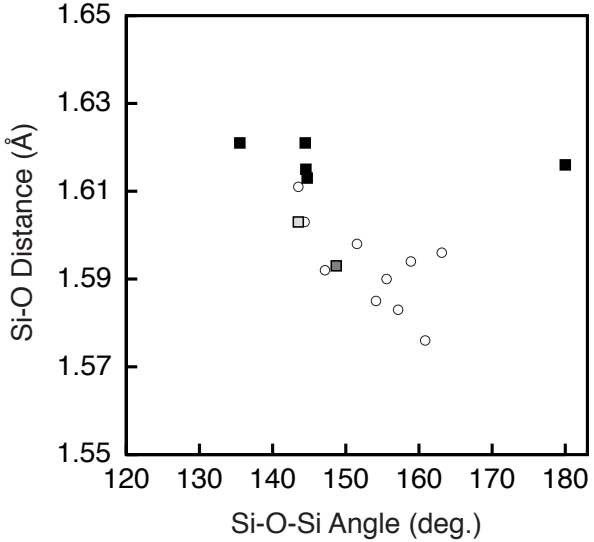

Ferrierite

Cristobalite

Quartz

Coesite

RAPT Enhanced ^{17}O DAS of SiO_2 Glass

Clark, Grandinetti, Florian, Stebbins, *Phys. Rev. B,* **70**, 064202 (2004).

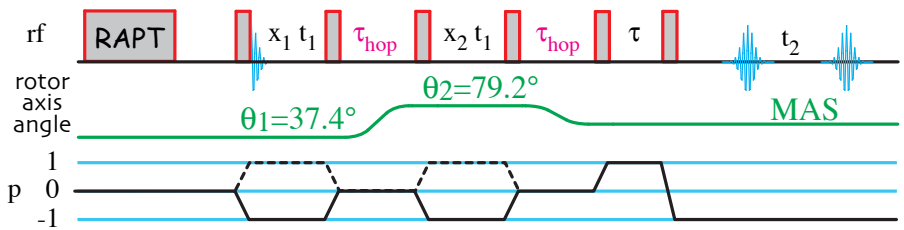

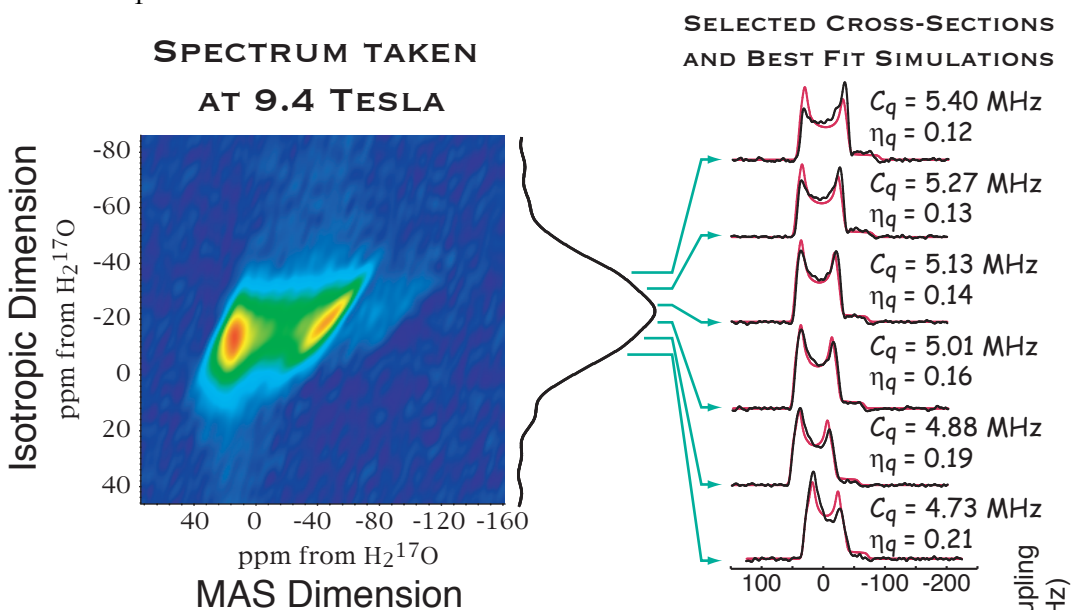

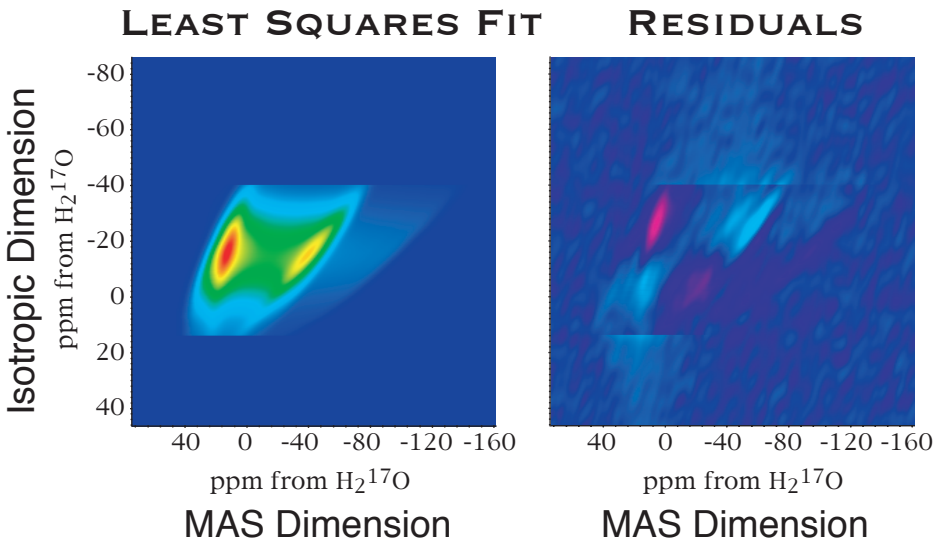

Distribution and Correlation of ^{17}O NMR Parameters in SiO_2 Glass

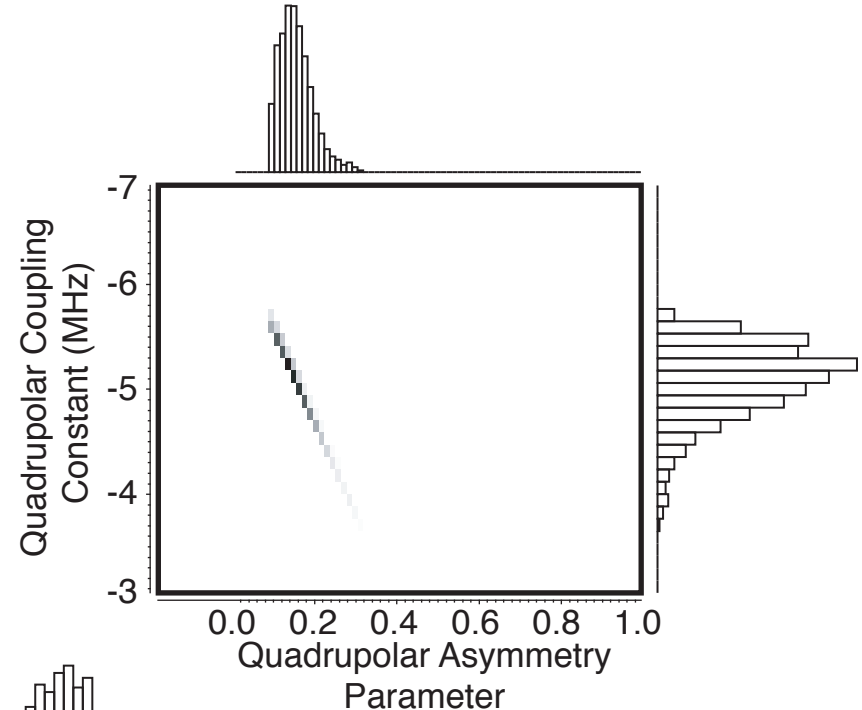

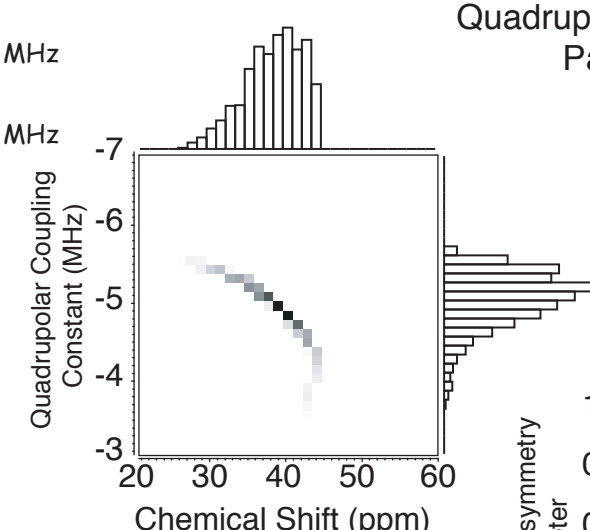

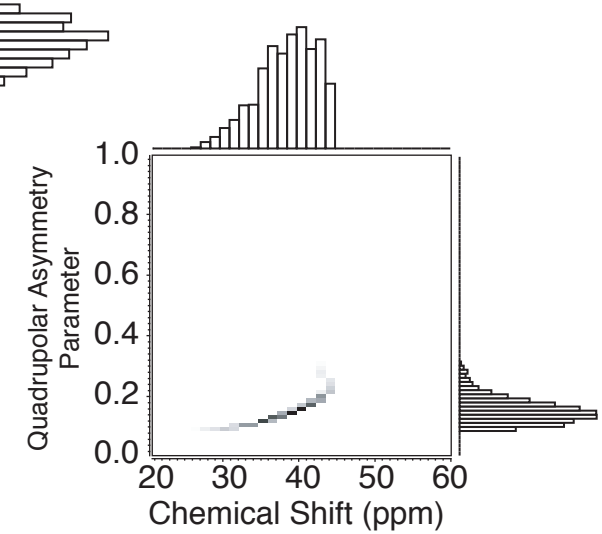

Si-O-Si Angle And Distance Distributions in Silica Glass from Cq and ηq

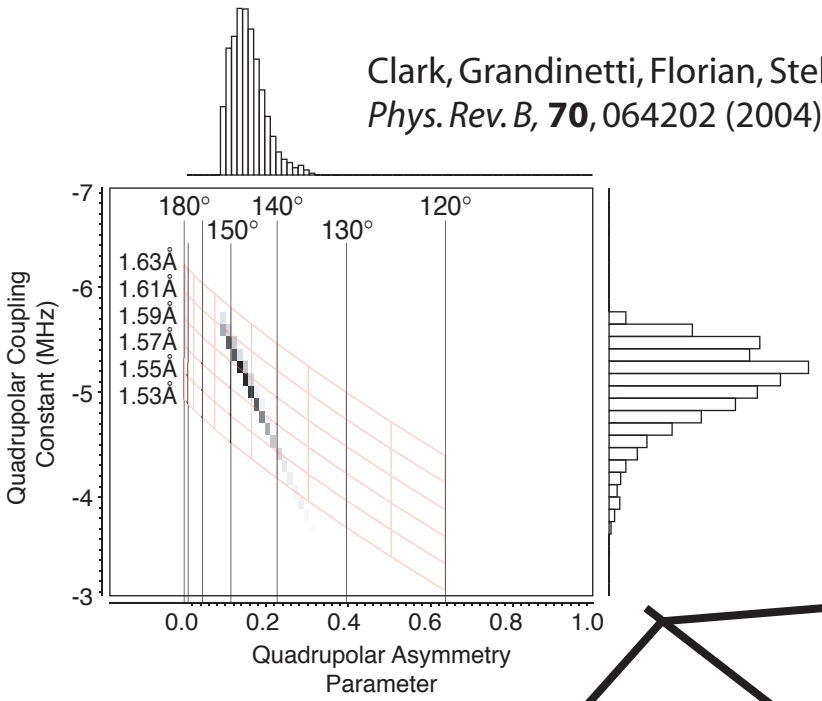

Clark, Grandinetti, Florian, Stebbins,
Phys. Rev. B, **70**, 064202 (2004).

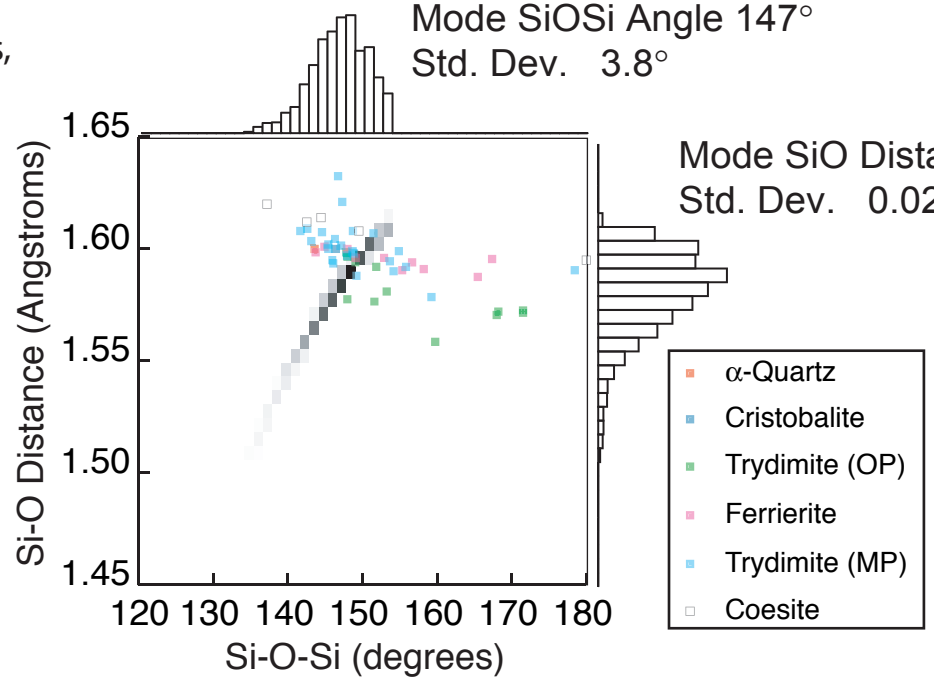

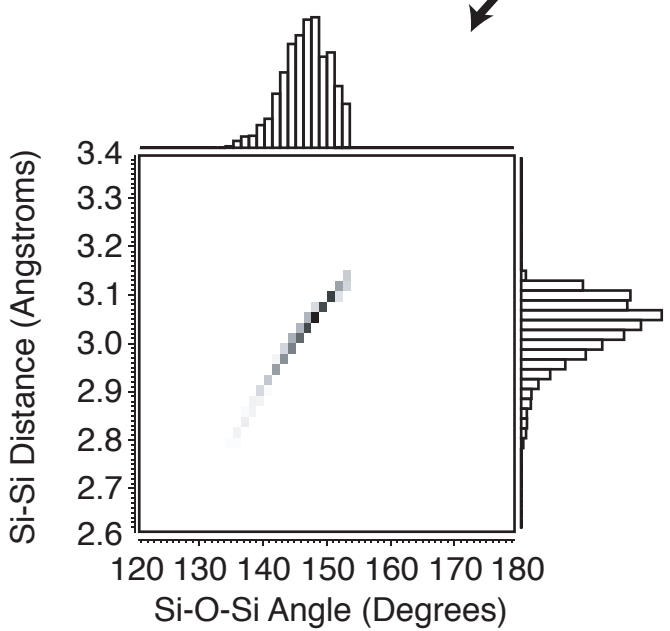

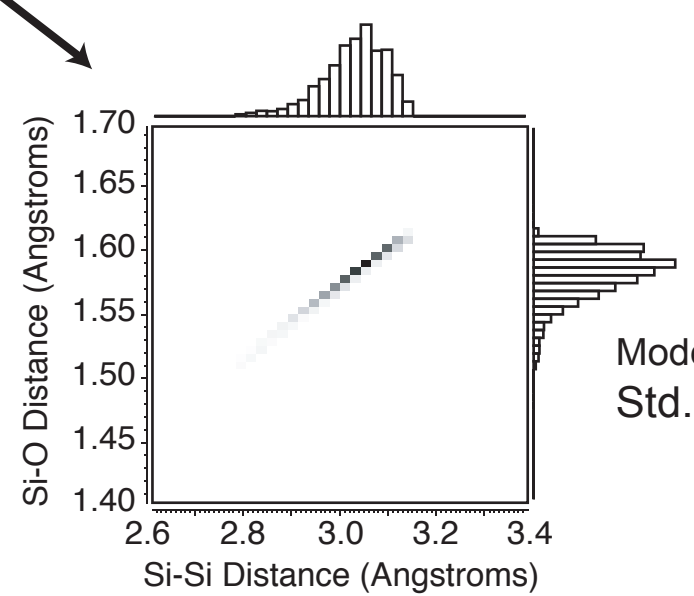

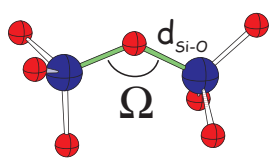

In Silica Glass
Si-O distance decreases
as Si-O-Si angle decreases !!

Mode Si-Si Distance 3.04Å
Std. Dev. 0.06Å

Comparison of Modified NMR Distance Distributions with X-ray

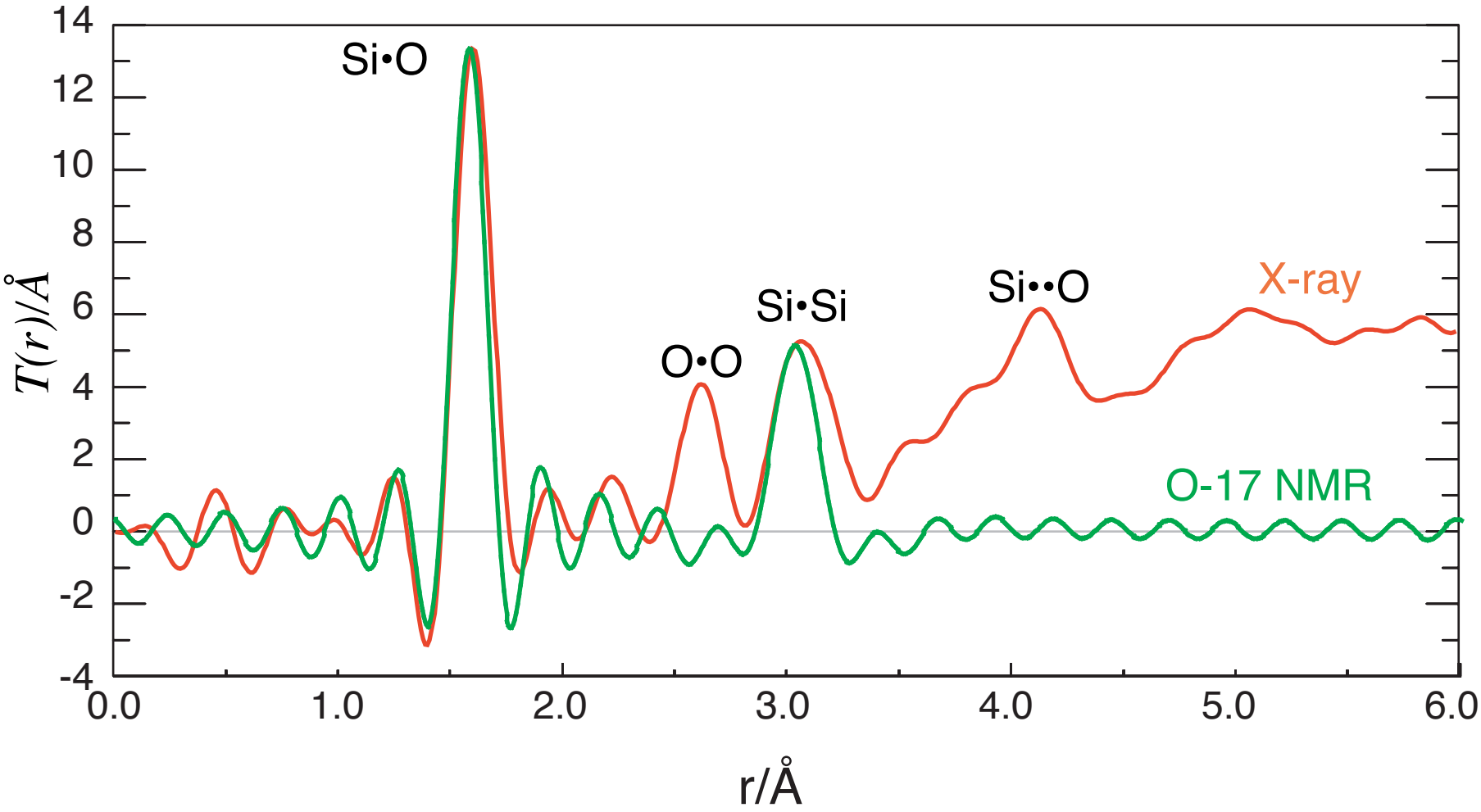

Clark, Grandinetti, Florian, Stebbins, *Phys. Rev. B,* **70**, 064202 (2004).

Acknowledgements

Current Group

Nicole Trease
Jason Ash
travis Sefzik
Krishna Kishor-Dey
Samantha Farley

Past Group Members

Pierre Florian
Alex Klymachyov
Ted Clark
Subramanian Prasad
Karl Vermillion
Ping Zhang
Zhi Yao
Hyung-Tae Kwak
Ramesh Sharma

"Quadrupole" Collaborators

Alex Pines, Jay Baltisberger, Antoine Llor, Margaret Eastman, Young Lee, Boqin Sun, Yue Wu, Jonathan Stebbins, Ian Farnan, Ulrike Werner-Zwanziger, Sheryl Gann, Josef Zwanziger, Joe Sachleben, Maurice Goldman, Zbigniew Olejniczak, Andrew Kolbert, Lucio Frydman, Gerry Chingas, Raz Jelinek, Brad Chmelka, Jacek Klinowski, Dominique Massiot, Joseph Virlet, Zhehong Gan, Thomas Vosegaard, Lyndon Emsley, Dimitri Sakellariou, Todd Lowary, Michael Deschamps, Franck Fayon, Stefan Steuernagel

The Ohio State University

National science Foundation